16.89J / ESD.352J Space Systems Engineering
Spring 2007

Project MINERVA

Establish an Enabling Space Infrastructure that will Support the Exploration of Mars

Design Report

Document Version	1.0
Document Manager	Karen Marais
Authors	Jason Andringa, Marshall Brenizer, Robert Dare, Jay M. Falker III, David Ferris, Elisabeth Lamassoure, Alexander Manka, Karen Marais, Jessica Márquez, Richard Millard, Simon Nolet, Alexander Omelchenko, Jeremy Rea, Joseph Saleh, Samuel Schweighart, Alexis Stanke, Zachary Warfield, Julie Wilhelmi
Under the Supervision of	Prof. Dan Hastings, Prof. Joyce Warmkessel, Prof. Lorraine Fesq, Prof. David Miller, Col John Keesee

Course 16.89 – Space Systems Engineering

Department of Aeronautics and Astronautics

Massachusetts Institute of Technology

Acknowledgements

Throughout the course of this class, there were numerous people who have been instrumental in our understanding of the project. We would like to specifically thank:

For instructing the class and having always been available to provide additional insight: Prof Dan Hastings, Prof. Joyce Warmkessel, Prof. Lorraine Fesq, Prof. David Miller Col John Keesee, and Prof. Walter Hollister.

For their interesting lectures about space systems engineering and additional information in their fields of expertise: Dr. James Lesh, Dr. Robert Shisko, Dr. Fred Culick, Dr. Joel Sercel, Dr. Charles Elachi, Dr. Chad Edwards, Dr. Vincent Chan, Dr. Ray Sedwick, Dr. Raymond Leopold, Prof. Thomas Herring, Dr Jane Hansen , Mr Cyrus Jilla.

For their time invested in facilitating the organization of the class while also participating as class members: Mr Simon Nolet, Mr Joe Saleh

For contributions outside of the class: Charles Hoskinson, Joshua Hopkins, James Do, and Chuck Solomon.

And finally, for generously allowing the use of their facilities: the MIT Space Systems Laboratory.

Contents

List of Figures

List of Tables

Abbreviations/Acronym List

ADCS	Attitude Determination and Control System
BER	Bit Error Rate
BPSK	Binary Phase Shift Keying
CDR	Critical Design Review
COTS	Commercial-Off-The-Shelf
DOD	Depth of Discharge
DOP	Dilution of Precision
DSN	Deep Space Network
DTE	Direct to Earth
EDAC	Error Detection and Correction
EELV	Evolved Expendable Launch Vehicle
EEPROM	Electrically Erasable PROM
EGS	Earth Ground Station
EIRP	Effective Isotropic Radiated Power
FSK	Frequency Shift Keying
GINA	Generalized Information Network Analysis
GPS	Global Positioning System
GRS	Gamma Ray Spectrometer
I/O Handler	Input/Output Handler (computer)
ICE	Integrated Concurrent Engineering
IMU	Inertial Measurement Unit
IOC	Initial Operating Capability
JPL	Jet Propulsion Laboratory

LEO	Low Earth Orbit
LGA	Low Gain Antenna
LMRE	Lander Mounted Rover Equipment
LV	Launch Vehicle
MARIE	Mars Radiation Environment Experiment
MGS	Mars Global Surveyor
MIT	Massachusetts Institute of Technology
MOI	Mars Orbital Insertion
MOLA	Mars Orbiter Laser Altimeter
MSE	Mars Surface Element
MMH	Mono-methyl hydrazine
NASA	National Aeronautics and Space Administration
NTO	Nitrogen tetra-oxide
O/S	Operating System
PDR	Preliminary Design Review
PROM	Programmable Read Only Memory
PRN	Pseudo-Random Noise
QPSK	Quadriphased Phase Shift Keying
RAF	Royal Air Force
RAM	Random Access Memory
RTG	Radio-isotope Thermal Generator
SEU	Single Event Upset
SLOC	Source Lines of Code
SMAD	Space Mission Analysis and Design
SRT	Sardinia Radio Telescope

SSME	Space Shuttle Main Engines
TARR	Trade Analysis and Requirements Review
TCM	Trajectory Correction Maneuvers
TDRSS	Tracking and Data Relay Satellite System
THEMIS	Thermal Emission Imaging System
UHF	Ultra-High Frequency
USAF	US Air Force
USO	Ultra Stable Oscillator

1 Executive Summary[1]

The MINERVA mission will revolutionize the future of Mars exploration by providing on-orbit relay of communications to and from Earth as well as the capability for position determination on the surface of the red planet. The MINERVA infrastructure improves the extent, reliability, capacity and uniformity of Mars coverage. From the Mars mission designer's point of view, MINERVA simplifies the design process since future missions will be able to achieve large transfer rates (10 Gb/sol divided among users) for science data without carrying their own high power communications systems. Also, these missions will have a greater probability of mission success given MINERVA's ability to determine their position on the surface with hundred-meter accuracy. Designers will be able to focus their efforts on science collection to a much greater degree than had previously been possible. MINERVA's return on investment will be in the form of a vast increase in science data collection for the taxpayer's dollar.

The MINERVA mission design evolved during the course of three distinct phases. The initial phase leading up to the Trade Analysis and Requirements Review (TARR) involved evaluation and comparison of three candidate architectures: a Mars ground-based architecture, an Earth-based architecture, and a Mars orbiting architecture. The class looked at the ability of the architectures to perform the communication and positioning missions, and assigned a rating in the areas of risk, reliability, robustness, and cost. In the final analysis, the Mars orbiting architecture was the clear winner. A rough order of magnitude (ROM) cost analysis made it clear that the program's $300 million cost cap would be a major driver in the preliminary design phase.

The second phase, leading up to the Preliminary Design Review (PDR), narrowed the trade space from a family of Mars orbiting architectures to a single viable design solution. In the process, several design features, including heliocentric orbits, use of the Martian moons, and Mars airplanes were eliminated due to complexity and cost. By the PDR, the requirements for the system were defined in greater detail and analysis indicated that the MINERVA system would be able to meet all requirements within the cost cap. The payload design team defined the technical approach for performing the communication and position determination missions. Characteristics for the communications system include cross-link capability between satellites, a high gain antenna for Earth communications and a UHF link for communication with users on the surface of Mars. The positioning system uses two-way ranging and two-way Doppler shift techniques, employing the same frequency band as the communication link with Mars. The bus team evaluated performance of all required subsystems, including an option for electric propulsion. Finally, the systems group completed a risk management strategy, a program schedule, functional and data flows, and a methodology for getting to CDR.

[1] RED

In the critical design phase, the class optimized the MINERVA design using concurrent engineering sessions in the design lab. Each group performed extensive design trades and analysis of performance levels to ensure all requirements were met. These efforts established the detailed system and subsystem designs. Launch analysis led to selection of a Mars transfer injection using a Delta III launch vehicle. The class defined in detail the payload and bus components, and determined software functions and spacecraft autonomy levels. The class determined that chemical propulsion would be more cost effective than electrical propulsion given excess launch vehicle performance. The orbits group, working with payloads, defined the optimal constellation altitude and inclination, to maximize performance within cost constraints. Payloads selected parabolic dishes for interplanetary and cross link communications, and a helix antenna for the MINERVA-Mars link. The systems/operations group finalized the description of system functions, evaluated system reliability, and used a design-based Cost Estimating Relationship (CER) methodology to quantify development and operations costs. While this method has limited accuracy, results indicated the system could be delivered under the cost cap.

The final MINERVA design consists of a 4 spacecraft Walker constellation around Mars at an altitude of 2000 km and an inclination of 27º. Each spacecraft has a wet mass of 470 kg and employs a chemical propulsion system for Mars capture, with no aerobraking requirement. The maximum spacecraft revisit time for the required coverage band is less than 30 minutes. MINERVA provides a reduced level of coverage up to 65º North and South of the equator. The system achieves 100-meter accuracy for position determination within 6 hours at 15 degrees latitude and within 90 minutes at the equator. In the worst case scenario (maximum planetary separation) MINERVA's communication throughput meets or exceeds 10 Gb/sol.

The class learned several valuable lessons through working on the MINERVA design project. Our efforts to retain design flexibility allowed innovative thinking, but the team reached a point where a significant reduction of the trade space was essential in order to meet design review milestones. The biggest challenge, especially given the large class size, was maintaining communication between the different groups. The class instituted the practice of frequent integration meetings, in which the systems group met with group representatives to discuss technical issues and status. The class observed that the transitions between phases of design work were potential stumbling blocks if they were not handled crisply. Recognition of this phenomenon led to a much more rapid and effective transition after the PDR than had taken place after the TARR. The class found concurrent engineering to be a useful practice for rapid characterization of a multitude of design options. It was essential to continue the detailed design analysis work in between sessions to clarify which options should be evaluated in concurrent engineering.

Most of all, the class learned about the challenges of doing systems engineering for a major design project in a large group setting. Tools, theory, and methodology were important, but so was the dynamic of human interaction. In the end, the people are what determine the level of project success.

2 Mission Statement[2]

US leadership in space exploration has inspired a generation of Americans and people throughout the world. Looking to the future, US space policy calls for a "strong commitment to space science" and tasks NASA to "undertake a sustained program to support a robotic presence on the surface of Mars." To facilitate future Mars exploration, NASA must put in place an infrastructure to support communication, position determination and Mars observation functions. NASA's implementation of this infrastructure must be innovative, flexible and robust to maximize the benefit obtained for the taxpayer's dollars.

The Mars infrastructure will enhance the capabilities of future robotic missions while significantly reducing their cost. This magnification of capability will provide improved opportunities for international cooperation as well as increasing public awareness and involvement in Mars exploration. Ultimately, the Mars infrastructure will be a key enabler for establishing a human presence on Mars.

[2] RED

3 Mission Overview[3]

The goal of the MINERVA mission is to establish an infrastructure to support future missions to Mars. The system we have developed, to meet the specified requirements within cost and schedule constraints, consists of four satellites. Distributed evenly around Mars in two orbital planes, these satellites will facilitate communication and navigation for surface explorers over much of the planet.

There are three main phases of the MINERVA mission: setup, on-orbit operations, and disposal. This section provides a brief overview of each phase.

3.1 Set-up

The MINERVA system is scheduled to lift-off on August 18, 2007, on a Delta III launch vehicle. It will cruise briefly around the Earth before boosted into a hyperbolic, trans-Mars orbit. The transit phase will last for 283 days. During this phase, the MINERVA spacecraft will deploy their solar panels and some antennas, and perform partial system checkouts. Mars capture will take place on May 29, 2008, and each spacecraft will assume its position in the MINERVA constellation. Finally, full system checkouts will be completed, enabling Initial Operating Capability (IOC) by July 9, 2008.

3.2 On-Orbit Operations

The MINERVA constellation will provide coverage for all MSEs within 60° latitude of the Mars equator, for at least five years. Within 15° of the equator, a satellite will come into view every twenty minutes on average, and it will remain in view for about fifty minutes per pass. As long as at least one satellite is in view, any MSE will be able to send and receive communication data, and take positioning measurements.

The two satellites in view of Earth will communicate with it through the Deep Space Network (DSN). Meanwhile, all four satellites will be able to communicate with Mars surface explorers and with each other. Any satellites not in view of Earth can relay communications to Earth by cross-linking. To perform these functions, MINERVA will operate according to a user table, which lists all the MSE locations, communication codes, and action schedules. Thus the table tells each satellite which MSEs should be in view at any given time, how to contact them, and whether or not they need communication or positioning services. Principal Investigators on Earth can modify the user table entries pertaining to their MSEs at any time.

3.3 Disposal

As each MINERVA satellite's on-orbit operations phase is concluded, it has the capability to be boosted into a disposal orbit with an altitude of 2150 km, to avoid cluttering the working orbit.

---

[3] JMF

4 MINERVA Mission Requirements[4]

4.1 Overview

System design requires substantial consideration of both program and performance requirements. The objective of the requirements analysis is to translate user needs into a quantifiable set of performance requirements that can be used to derive design requirements.

The MINERVA requirement flow-down portrays a logical and coherent picture of the system's functional architecture.

The requirement hierarchy was developed by deriving specific requirements from both user needs and the system design, and ordering these requirements in such a way that the entire system could be accepted by validation and verification of the sub-elements. The requirement flow down is shown in **Error! Reference source not found.**.

The MINERVA system is composed of elements orbiting Mars, elements on Mars, and elements on Earth. The elements orbiting Mars can be separated into payload and bus.

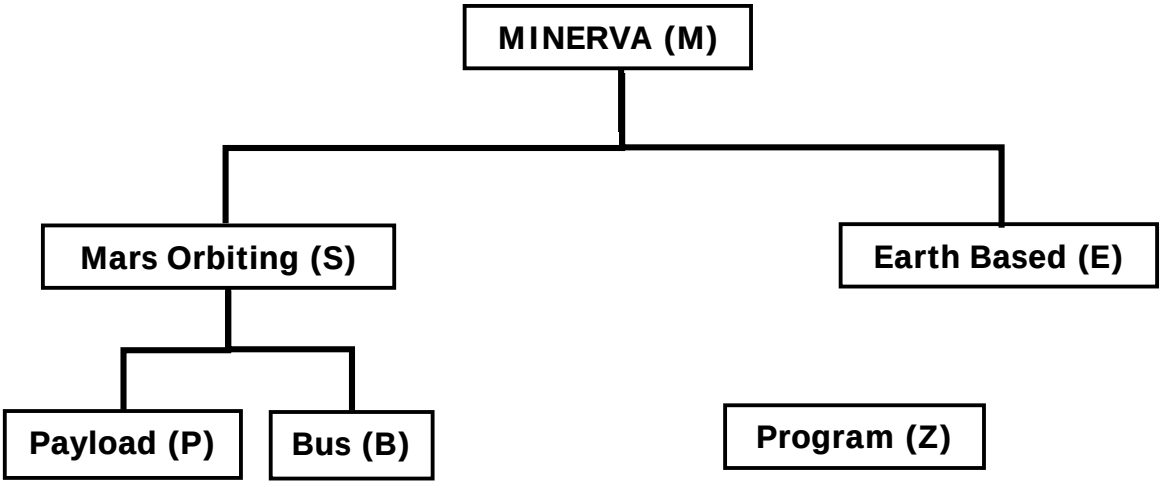

Figure 4.1: MINERVA Requirements Hierarchy

[4] AKS, JS

4.2 Objectives

The MINERVA mission is to provide an enabling infrastructure for Mars exploration.

The primary mission objective is to provide an infrastructure that enables data transmission between Earth and Mars and position determination for Mars surface explorers.

Secondary mission objectives, not required of the current design, are to provide an observational capability to permit collection of weather and surface detail data and to expand the position determination capability to airborne and orbiting craft.

4.3 User Needs

The following user needs statement has been developed from the mission statement of the MINERVA design team.

> *"The MINERVA system shall provide an enabling infrastructure to support the exploration of Mars. Specifically, the system shall provide Mars Surface Elements (MSEs) with communication services between the Mars surface and Earth Ground Stations (EGSs), and with their position on the surface of Mars, without imposing additional design constraints on the MSEs."*

4.4 Specified Requirements

Part of the challenge of creating meaningful requirements for the MINERVA system was the small number of specified requirements. Although an enabling factor in exploring a wide trade space, it was at times difficult to derive and write detailed requirements from the few requirements given. The minimum requirements as specified in the Program Plan are as follows:

- The MINERVA system shall provide position determination solutions to 100 m accuracy for users on the surface of Mars in the ± 15° latitude band.
- The MINERVA system shall provide communication relay between Earth and Mars Surface Explorers (MSEs) in the ±15° latitude band that will allow the download of at least 10 Gb of data from the Mars surface per sol.
- The MINERVA system shall provide these services by 2010.
- The MINERVA system shall have a minimum design life of five years.
- The cost to IOC (initial operating capability) shall not exceed $300 Million.

The observation requirement is secondary. Since the primary requirement is to provide an enabling infrastructure for Mars and the Mars weather in general does not endanger Mars missions [Sheehan], it has been decided not to perform observation. Furthermore, observation is too expensive.

4.5 Requirements Document

The requirements document in its entirety can be found in Appendix A. Included in the document is a description of terminology and definitions used, as well as a statement of the assumptions made. The requirements and their intent are listed.

4.6 References

Sheehan, W. The Planet Mars: A History of Observation and Discovery. The University of Arizona Press, Tucson, 1996.

5 Character of Mars Missions[5]

"This quest for life, this realization that we might not be alone in the universe, is a primary force driving our Mars missions"

Dan Goldin

Over the next ten years the National Aeronautics and Space Administration and its European partners plan to send at least four orbiters and four landers to the Martian surface, culminating in a mission that will use highly sophisticated rovers to collect samples of rock and soil that will be delivered to Earth by 2008. The agenda holds out the possibility of seven or so additional trips to the Red Planet, including several relatively inexpensive "micromissions" and a second series of flights that would return dozens more samples between 2008 and 2012. This ambitious series of probes is in addition to the Mars Global Surveyor spacecraft, which has been orbiting the planet since 1997, and a Japanese orbiter called Planet-B, launched in 1998 on a two-year mission to study Mars's atmosphere and ionosphere.

The upcoming Mars missions are designed to pursue a couple of relatively well defined goals: expanding what is known about Mars's climate, geology and hydrology, both past and present, particularly in relation to the question of whether life has ever existed on the planet, and laying the groundwork for future human exploration of the planet, possibly as soon as 2020. Robotic vehicles will roam several kilometers, taking scores of samples as part of the most extensive search yet for signs that microbial life persists in the soil below the surface of the red world or that organic matter exists in its rocks or soil.

Human exploration and settlement of Mars is not beyond our reach. Indeed, all the technologies needed for sending humans to Mars are available today. The first piloted mission to Mars could reach the planet within a decade.

5.1 MARSNET

The Mars Network (MARSNET) is a project being studied by Jet Propulsion Laboratory (JPL). Its goals are to develop communication capability to provide a substantial increase in data rates and connectivity from Mars to Earth; and to develop an in situ navigation capability to enable more precise targeting and location information on approach to and at Mars. The mission objective is to support Mars global reconnaissance, surface exploration, sample return missions, robotic outposts, and eventual human exploration.

JPL enumerates in its study of MARSNET several benefits to creating a Mars infrastructure. The availability of MARSNET will:

[5] AO, JJM

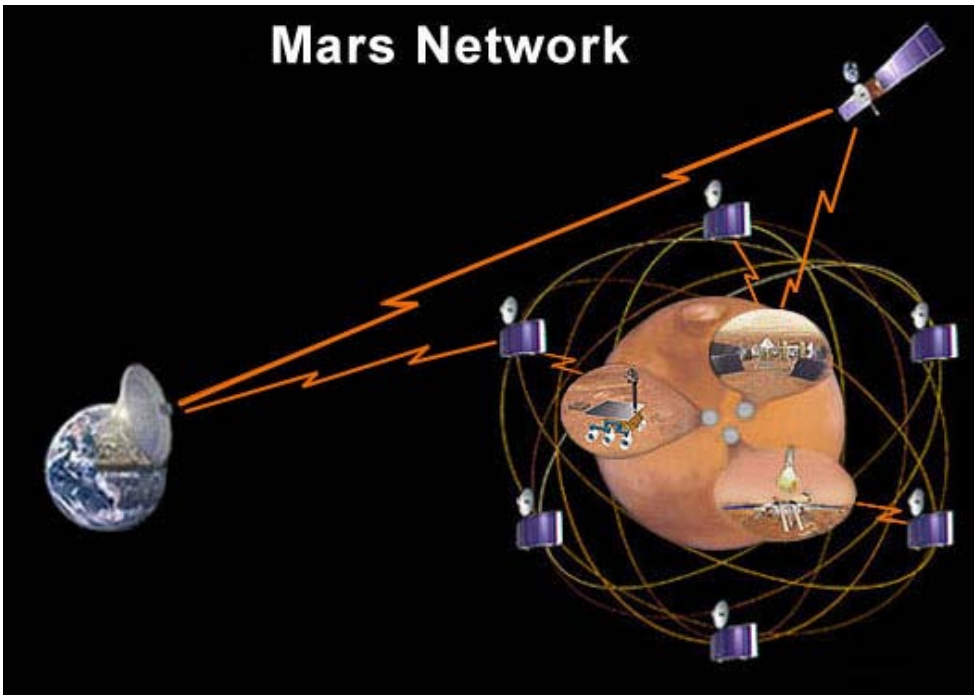

Figure 5.1: Mars Network

- Reduce communication-related power, volume, and mass requirements on future Mars exploration elements,

- Enhance connectivity and bandwidth for increased communication rate and/or contact time with surface robotic elements,

- Improve targeting and location information (in situ navigation).

In addition, by providing increased data rates and connectivity, MARSNET would enable greater information flow to the public for the purpose of engaging them in the Mars exploration adventure. In essence, MARSNET would be building a publicly accessible "gateway" to Mars.

The MARSNET architecture consists of a constellation of microsatellites and one or more relatively large Mars ariastationary relay satellites. The microsatellites are intended to serve both as communication relays between Mars exploration elements and the Earth and as position determination aids for the exploration elements. The relay satellites are similar to very high-bandwidth geostationary communication satellites currently orbiting Earth.

Communication with the Mars exploration elements would occur using an Internet protocol similar to that used by Earth's Internet.

A possible scenario for MARSNET is to launch a first microsatellite in 2003 that will orbit Mars around its equator. Two additional microsatellites would be launched during the subsequent Martian launch windows, one of these having a polar orbit. In this scenario, MARSNET would have in situ navigation-capabilities with a three-satellite constellation by late 2005. In 2007, one of the two large Mars ariastationary satellites would be launched. A fully operational six-satellite constellation in this scenario would occur in late 2009. Mars Network would be on a path to providing "a quantum leap in communication capability for exploration elements planning to capture near-continuous video."

Reference: http://marsnet.jpl.nasa.gov

5.2 Mars Global Surveyor

Figure 5.2: Artist's Conception of Mars Global Surveyor spacecraft

The Mars Global Surveyor (MGS) is part of the Mars Surveyor Program, whose main goal is to explore the red planet. The program consists of orbiters and landers to be launched at every launch opportunity between 1997 and 2006. The 1996 launch to Mars included the Mars Pathfinder and MGS. While Pathfinder's mission has been completed, MGS continues to orbit the red planet.

The MGS mission objectives are threefold. The first is to perform scientific measurements. The second is to provide at least three years of service as an on-orbit communication relay for Mars landers and atmospheric vehicles. The third is to support planning for future Mars missions through data acquisition with special emphasis on those measurements that could influence landing site selection. Among its scientific objectives are to build comprehensive data sets for the shape and composition of the planet's surface, the structure of the atmosphere, and Mars' magnetic properties.

Mars Global Surveyor is providing high resolution imaging of the Martian surface, which has revealed the following:

- Clear evidence of previously flowing water
- Ubiquitous dust and sand dunes
- Water-ice clouds and dust storm observations
- Extremely smooth northern hemisphere suggests ancient ocean
- Intense magnetic stripes

Some of the data collected for MGS will be invaluable to the creation of MINERVA. The Mars Orbiter Laser Altimeter (MOLA) is bouncing infrared laser pulses off of the surface to determine range of the MGS spacecraft to the Martian surface. The range measurements are used to construct a precise topographic map of Mars that has many applications to studies in geophysics, geology and atmospheric circulation.

With one year of global mapping of the Mars Global Surveyor mission completed, the MOLA dataset has achieved excellent spatial and vertical resolution. Surface maps have been produced from the altimetric observations collected during MOLA's first year of global mapping and provide a variety of regional topographic views of the Martian surface. The best spatial resolution (for selected sites) is approximately 1/16° by 1/32° (where 1° on Mars is about 59 km) and the vertical accuracy is approximately 1 m.

This data set will be part of MINERVA's position determination system. Information on Martian atmosphere and weather patterns also proved helpful in planning the MINERVA mission.

Aside from the scientific information about Mars that MGS has provided, the MGS mission has been a guide in designing MINERVA. MGS's second mission objective is similar to one of MINERVA's: to provide support for future landers by relaying data from the Martian surface back to the Earth. While MGS is only one satellite and not a constellation, the mission provides a source of comparison. For example, MGS uses DSN to transmit its data back to Earth, much like the MINERVA constellation.

Finally, there are lessons learned from the MGS mission that have aided in the MINERVA design. MGS's biggest problem was aerobraking. The aerobraking procedure had to be suspended because air pressure from the atmosphere caused one of Surveyor's two solar panels to bend backward by a slight amount. It was determined that aerobraking is still feasible but at a gentler, slower pace than first intended. MGS's mishap highlighted the risk involved with using aerobraking. In order to avoid high risk, MINERVA elected to use an orbit insertion about Mars without the use of aerobraking.

See also: http://mars.jpl.nasa.gov/mgs/

5.3 Mars Surveyor 2001 – 2003[6]

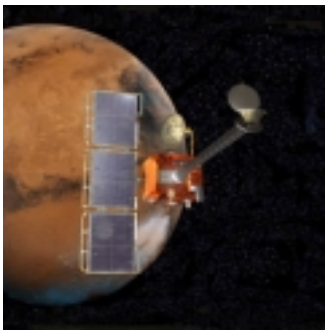

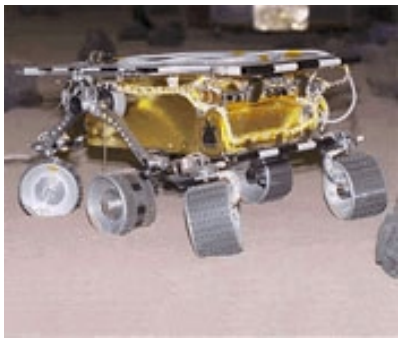

Figure 5.3: 2001 Orbiter, 2003 Lander and 2003 Rover

The Mars Surveyor 2001 Orbiter is scheduled for launch on April 7, 2001 and should arrive at Mars on Oct. 20, 2001. After a propulsive maneuver into a 25-hour capture orbit, aerobraking will be used over the next 76 days to achieve the two-hour science orbit. Aerobraking was used on the Mars Global Surveyor mission. The Orbiter will carry three science instruments: the Thermal Emission Imaging System (THEMIS), the Gamma Ray Spectrometer (GRS), and the Mars Radiation Environment Experiment (MARIE). THEMIS will map the mineralogy and morphology of the Martian surface using a high-resolution camera and a thermal infrared imaging spectrometer. The GRS will achieve global mapping of the elemental composition of the surface and determine the abundance of hydrogen in the shallow subsurface. The GRS is a rebuild of the instrument lost with the Mars Observer mission. The MARIE will characterize aspects of the near-space radiation environment as related to the radiation risk to human explorers. It will be used in conjunction with a similar instrument on the '03 Lander to determine and model the effects of the atmosphere on the radiation-induced hazard on the surface.

Launch of the Mars Surveyor 2003 lander, if approved, would occur between May 27, 2003 and June 16, 2003. The 2003 Lander will carry an imager to take pictures of the surrounding terrain during its rocket-assisted descent to the surface. The descent imaging camera will provide images of the landing site for geologic analyses, and will aid planning for initial operations and traverses by the rover. The 2003 Lander will also be a platform for instruments and technology experiments designed to provide key insights to decisions regarding successful and cost-effective human missions to Mars. Hardware on the Lander will be used for an in-situ demonstration test of rocket propellant production using gases in the Martian atmosphere. Other equipment will characterize the Martian soil properties and surface radiation environment.

[6] AO

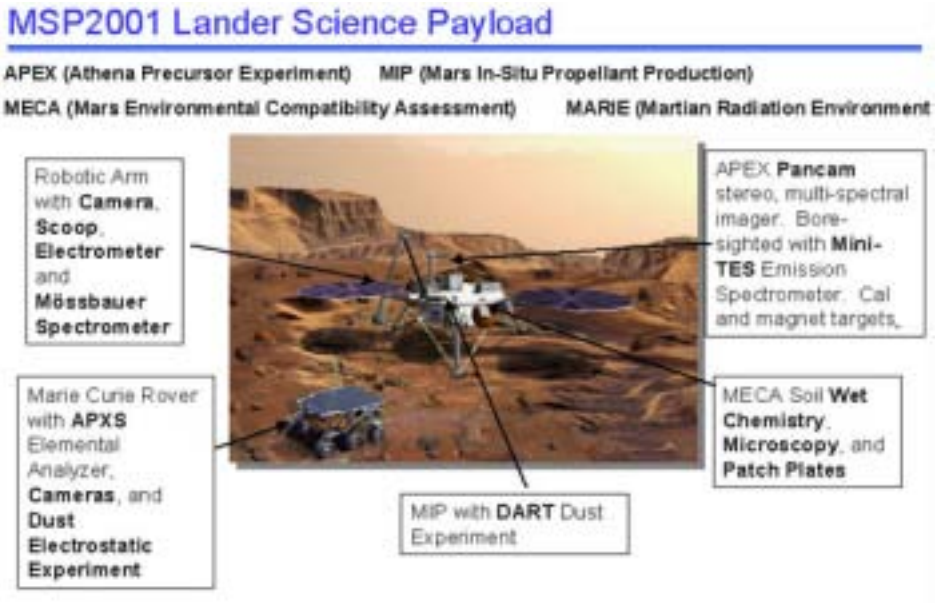

Figure 5.4: Mars Surveyor 2003 Lander

See also: http://mars.jpl.nasa.gov/

6 Design Concept

The design of the MINERVA systems was derived through several down-selection iterations. The first down-selection eliminated families of architectures that could not meet the minimum mission requirements. The next down-selection eliminated those aspects of the chosen orbital architectures that did not improve the cost-per-function of the mission. The final round involved integrated concurrent engineering, where the trade space of the driving parameters associated with the payload performance were explored. The following sections detail the design process as it evolved during the project.

6.1 Architectural Design Trades[7]

During the Trade Analysis and Requirements Review (TARR) phase of the project, several different architectures that could meet the requirements were suggested.

The candidate architectures were grouped into three families, namely Mars ground-based, Earth based, and Mars orbiting.

Preliminary investigations of each architecture family were conducted to establish their relative suitability. The most promising family of architectures, the Mars orbiting architecture, was selected for more detailed design work including trades such as those related to satellite size versus orbit, and laser versus radio communication.

More detailed analyses were performed to define a single system from which the detailed design of the specific elements could be rendered.

6.1.1 Description of Criteria Used in Architecture Down-selection

The three architecture families were evaluated based on their ability to meet the performance and cost requirements as well as their performance relative to the R^3 criteria:

Communication

- What is the best data rate that can be achieved? (Gb/sol)
- What is the maximum size of the coverage area? (° Latitude)
- What are the availability characteristics of the system? (%)

Position Determination

- What is the best possible resolution, both surface and vertical? (m)

  User specification is 100 m accuracy for MSEs.

[7] DMB

- What is the maximum size of the coverage area? (° latitude)

  User Specification is minimum of ± 15° latitude.

Cost

- Due to budgetary pressures, the total cost cannot exceed two Discovery class missions (~$150 million each).

  Therefore, the total cost to Initial Operating Capability (IOC) shall not exceed $300 million.

R^3

- Risk: What are the technological, development, and deployment risks?
- Reliability: How reliable is the system (as a whole) in performing its primary objectives?
- Robustness: Is the system able to adjust to and perform in a dynamic environment?

The following factors were also taken into account when comparing architecture families:

- What potential does MINERVA have to perform Mars observation?
- Expandability: Is the system able to support a wide range of potential missions beyond its initial mission design?

6.1.2 Mars Surface-Based Architectures

Several possible Mars surface architectures for position determination and communication were examined, based on Earth-like counterparts. The following sections describe these options [Hobbs, 1990].

6.1.2.1 Loran-C Based Navigation System

The Loran-C system relies on the propagation of ground waves. It broadcasts a pulsed waveform at a frequency between 90 and 100 kHz with a transmission power on the order of 1500 kW.

The baseline between stations is 1600 to 2400 km with an accuracy of 200 to 600 m. Differential techniques can be used to increase the accuracy (see below).

Assuming that ground waves on Mars propagate as they do on Earth, and with a baseline of 2000 km between stations, a Mars Loran system would require eleven stations along

the equator. This chain would provide navigation to latitudes up to 30°, with the highest accuracy at the equator (~200 m) and the lowest accuracy at 30^o latitude (~600 m).

While it is technically feasible to build a Loran-C based navigation system on Mars, the associated risks and costs are high. For example, a Mars-based Loran system would require a self-deploying antenna structure, as well as a large source of electric power such as a solar array farm or nuclear power.

6.1.2.2 Omega Based Navigation System

The Omega system uses a Very Low Frequency (VLF) between 10 to 14 kHz at a transmit power on the order of 10 kW. On Earth, the surface and the bottom of the ionosphere act as a waveguide to carry the waves long distances over the horizon.

The baseline between stations is 8000 to 9600 km with an accuracy of 1.6 to 3.2 km. Differential techniques can be used to increase the accuracy (see below).

Assuming that the ionosphere and surface on Mars propagate VLF waves as they do on Earth, five stations could provide global position determination for Mars with an accuracy of 1 to 2 km. Two of the stations could be at the poles, with 3 stations equally spaced along the equator. The range from the pole stations to the equator would be 5300 km, while the distance between equatorial stations would be 7100 km.

Although it is technically feasible to build an Omega based system on Mars, it would be very risky and cost prohibitive. The antenna structure of an Omega system is highly complex and requires an antenna roughly 400 m in diameter. Furthermore, the system would require an accurate model of the Martian ionosphere; none is available at this time. The risks and costs associated with this system are similar to those for the Loran type system.

6.1.2.3 Differential Radio Navigation Techniques

In this method, a reference receiver is placed at an accurately known position. Then, the reference position given by the navigation system is compared to the actual position. The difference between the actual position and the measured position is then broadcast as a correction. This method can produce accuracies on the order of 1 to 2 m. It is limited by how far the correction data can be broadcast, and by how accurately the reference position is known.

Differential techniques are complementary to an existing navigation system and require the installation of ground references. The position of the ground references would have to be determined using DSN, which has an accuracy on the order of 100 km for objects on the surface of Mars.

Therefore differential techniques cannot be used for the primary position determination system.

6.1.2.4 Communication Array

The primary problem with ground-based communication systems is the coverage. Without communication relay satellites, future missions would have to be deployed within line-of-sight of a Mars-to-Earth communication antenna. To meet the coverage requirements, a large number of ground-based antennas would be required.

A ground-based communication system could meet the data rate requirements, but a large number of ground stations would be necessary to meet the coverage requirements.

6.1.2.5 Location of Mars Ground Stations

The following figure describes the layout of some potential Mars ground-based position determination and communication systems. For the Loran-C type navigation system, eleven ground stations are needed. For the Omega-type navigation system, five stations are needed. These stations are equidistantly spaced around the equator, and at the poles for total coverage.

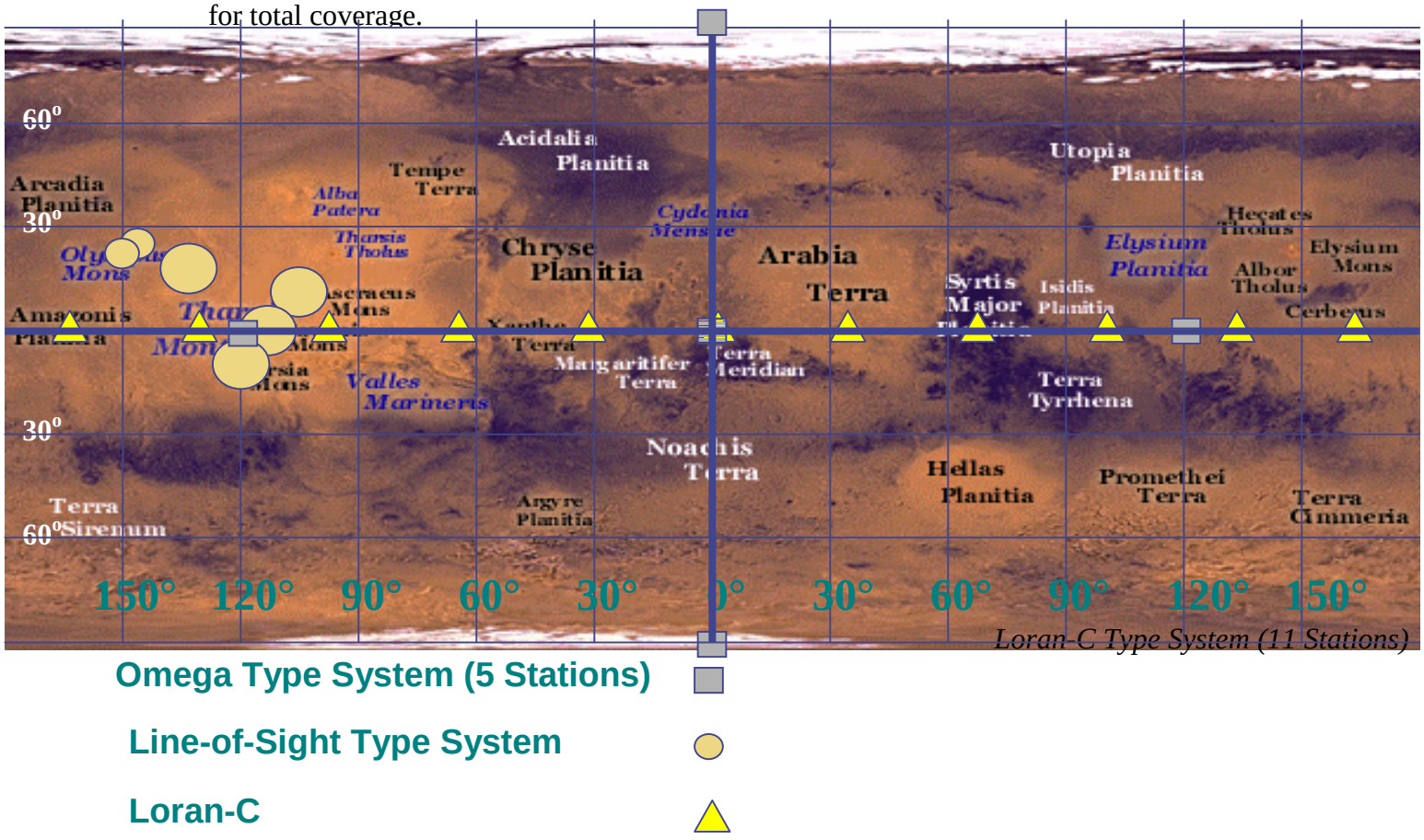

Figure 6.1: Location of Martian Ground Stations.

For communication, it is possible to build large antennas to receive and transmit high power signals between Earth and Mars. The key issue is how to get MSE data to and from the stations. While it may be possible to transmit low data rate commands through the navigation beacons to an MSE, it would be difficult for a power and mass limited MSE to transmit a high data rate stream through the navigation beacons to a transmitter station. This means that a large number of communication relays would be required. Six line-of-sight communication beacons could be located at the tops of the high volcanoes listed in Table 6.1.

Table 6.1: Communication Beacons

Name	Height	Position
Iecates Tholes	10 km	22° N 150° W
Elysium Mons	10 km	25° N 146° W
Olympus Mons	27 km	18° N 133° W
Arsia Mons	27 km	10° S 120° W
Pavonis Mons	27 km	0° N 113° W
Ascraeus Mons	27 km	11° N 105° W

At a height of 10 km, the line-of-sight range is 260 km. At a height of 27 km, the line-of-sight range is 426 km. While ground waves could extend to this range over the horizon, the real issue is with the transmit range of an MSE. It would require over fifty 27-km high ground stations to cover just the equator with line-of-sight coverage.

6.1.3 Earth-Based Architectures

The second family of architectures involves Earth-based systems only. The primary system we would expect to use is the Deep Space Network (DSN), an international network of antennas used to support space missions and astronomy.

The DSN is managed by the Telecommunication and Missions Operations Directorate (TMOD) of NASA's Jet Propulsion Laboratory (JPL). It is used to provide two-way communication links for space mission guidance, control, and data reception. On recent Mars missions, lander targeting accuracies of 500 km (at 77° S latitude) and 100 km (at 15° S latitude) were achieved with DSN support.

DSN complexes are located at three main locations: Canberra, Australia; Madrid, Spain; and Goldstone, CA, USA. Each complex is equipped with 70 m, 34 m, 26 m, and 11 m antennas. The 70 m antennas have 400 kW transmitters. DSN systems use long wave radio, short wave radio, and microwave frequencies. Most deep space mission operations use X-band microwave frequencies (8 to 12.5 GHz).

Pictured in Figure 6.2 are the ground-based Very Large Array in New Mexico, and a conceptual representation of a space-based very large baseline interferometer (SVLBI). The Japanese VLBI Space Observatory Program (VSOP) is an example of an SVLBI already in orbit. The US plans to launch the Advanced Radio Interferometry between Space and Earth (ARISE) mission in 2008, in which an orbiting 25 m inflatable antenna will enable an angular resolution of about ten micro-arcseconds.

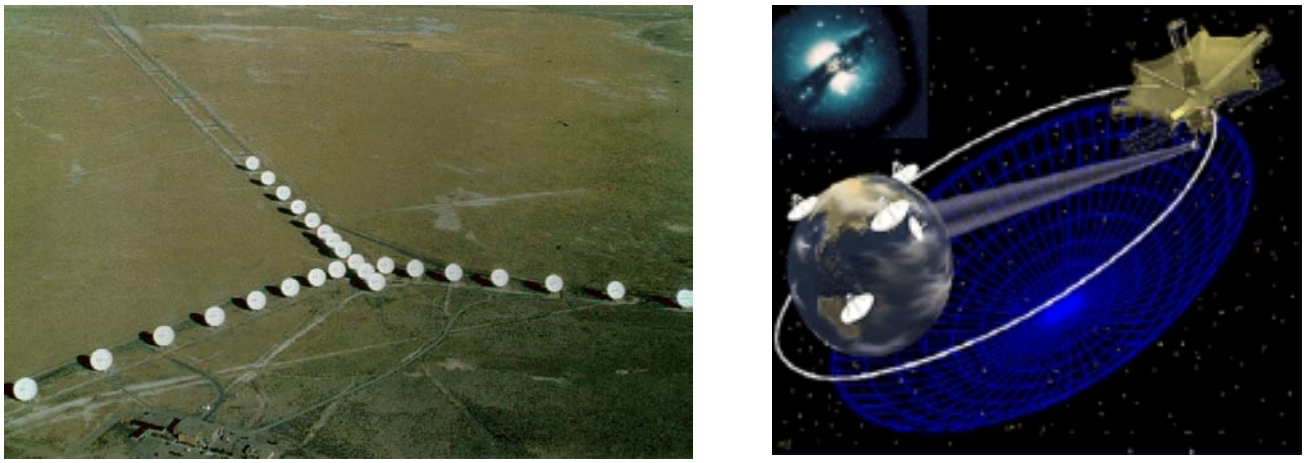

Figure 6.2: Possible Earth-Based Systems

The analysis performed on this Earth-based architecture was broken down into communication and position determination.

A communication system using only DSN, without an intermediate relay, would require high-power MSE communication subsystems. This implies that MSEs would have to be larger, more complex and therefore more costly.

For position determination, angular resolution calculations were performed assuming X-band frequencies for DSN and existing ground VLBI. The angular resolutions for the 70 m DSN antenna and an 8600 km ground VLBI array were found to be approximately 125 and 0.8 arcseconds, respectively. For space-based VLBI, the slightly shorter wavelength ARISE target specifications were used, resulting in an angular resolution of 1e-5 arcseconds. The latter angular resolution corresponds to surface resolution on Mars over 100 m. This does not meet the system requirements.

Therefore an existing Earth-end architecture could not be used to meet the position determination requirements.

6.1.4 Mars Orbiting Architecture

The third architecture family consists of systems containing at least one Mars-orbiting satellite. The use of additional assets to augment the capability of the single Mars-orbiting satellite was left as a design element subject to trade.

In an attempt to bound the problem, the following three variables with significant impact on the overall constellation design were identified:

- Altitude

  The altitude of most Mars constellations would fall somewhere between a low 800 km orbit and the ariastationary orbit at 17,030 km.

- Number of satellites
- Number of orbital planes

Preliminary analysis showed the clear superiority of this architecture family over the other families. The detailed analysis is exposed in the rest of this document.

6.1.5 Architectural Down-Selection

A discrimination matrix was used to identify the best candidate architecture. The traditional stoplight approach was used to classify the ability of each architecture to meet or exceed the design specifications:

- Red indicates that the architecture does not meet the required specification
- Yellow indicates that the architecture meets the specification but presents significant challenges
- Green indicates that the architecture meets or exceeds the specification with acceptable difficulties

Figure 6.3 shows the matrix for all three architectures, as described in the preceding sections.

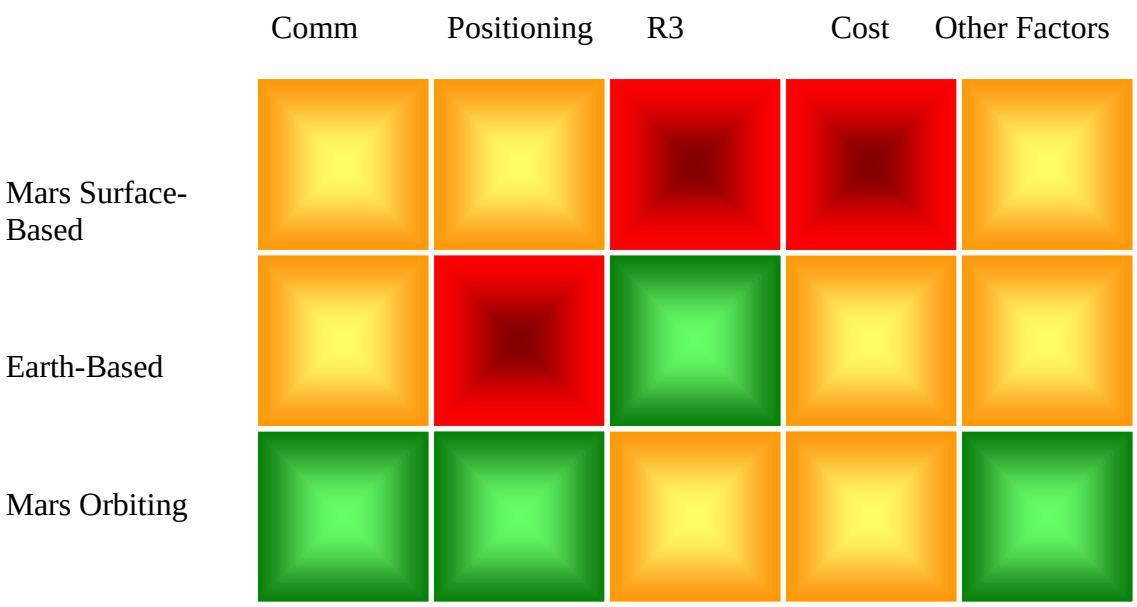

Figure 6.3: Downselection Discrimination Matrix

Results of the analysis showed that the Mars Ground Based and the Earth Based architectures were not able to meet the required system specifications. Thus, both were eliminated from the trade space.

The Mars orbit based architecture family was able to meet all the requirements and was accordingly selected.

6.2 Further Down-Selection[8]

Several areas considered in the original trade space were subsequently eliminated. This section briefly describes the elimination process.

For example, there are significant advantages to using a laser communication system, including reduction of size, mass and power, and increased data rates. However, the primary disadvantage of optical communication links is the need for precision pointing of the optical beam. Stringent pointing requirements increase the complexity and cost of the attitude determination and control system (ADCS) and onboard computing systems. Consequently, laser communication was not considered.

[8] DMB

Another option was to use the Martian moons as a communication relay base. The advantage of using a Martian moon is the ability to station a relatively large relay antenna on the surface. An interesting property of the Martian moons is that the orbital period equals the rotational period for both moons, which means that one side of the moon is constantly in view of the Mars surface. However, the risks and costs associated with this type of design were prohibitive.

Two Lagrange points, one between Mars and the Sun, and the other on the opposite side of Mars, located approximately 1,000,000 km from Mars, were considered as locations for communication relays. However, existing antenna technology proved capable of communicating with the Earth without the need for additional satellites at the Lagrange points.

Finally, using atmospheric vehicles, such as balloons, dirigibles, and airplanes on Mars could provide added benefits. However, the risk associated with using those objects, as well as the positional uncertainty due to atmospheric effects rendering them incapable of meeting the position determination requirement eliminates this as a possible option.

Therefore, the remaining trade space contains satellites of variable number, size, altitude, phase, and inclination. These variables were altered to explore the remaining trade space.

6.3 Final Top-Level Design Trades: an Overview[9]

This section summarizes the initial design process from mission requirements to the top-level design trades that led to the choice of number of satellites, altitude and orbital inclination. Further details can be found in the subsequent sections.

To minimize development and infrastructure costs, we decided to use DSN as a communication link with the Earth.

A DSN pass is defined as a ten-hour continuous period during which DSN is available for tracking, commanding, telemetry and data return. DSN currently provides Mars Global Surveyor with one such pass per day. One DSN pass per day is also assumed to be available for MINERVA.

Implementing a near real-time communication link with MSEs enhances the value of the MINERVA system. Opportunities for near real-time communication occur during each DSN pass. Implementing satellite cross-links ensures maximum use of near real-time opportunities. Satellite cross-links also increase the failure tolerance of the system (see section 10.1) and the accuracy of orbit determination (see section 10.2). We therefore decided to implement satellite cross-links.

On the basis of the above decisions, the top-level requirements were separated into a cost constraint, three types of communication links (MINERVA-Earth, cross-links, and

[9] EL, KM

MINERVA-Mars), and the position determination requirement. For each type of link, the parameters possibly affecting performance and cost are frequency, data rate, bit error rate, antenna gain and RF output power.

1. Cost constraint

   The first main requirement is a cost constraint, specifying that the mission cost to initial operating capability (IOC) should not exceed $300M.

2. MINERVA-Earth link

   To avoid single point failures in the system, more than one MINERVA satellite must have the capability to communicate with the Earth. Since the cost constraint does not allow MINERVA to afford more than a few satellites, it was decided that all satellites would have an Earth link.

   The Earth-link antenna power-aperture product is the dominating factor for payload cost and mass.

   The possible frequencies for this link are limited to those with which DSN can interface. The top-level requirement sets the total data transfer from all MSEs to the Earth to at least 10 Gb/sol, whatever the Earth-Mars distance. This requirement and the choice to use one DSN pass per day sets the minimum total effective data rate from MINERVA to Earth (see 10.1).

   Data from the Earth to Mars, be it for MINERVA or for MSEs, can be divided into two main types. The first is command type data, which is typically small, but requires high accuracy and minimum delivery delay. The second is mission reconfiguration data, which is larger, also requires high accuracy, but for which longer delivery delays are acceptable. The uplink from the Earth to Mars therefore requires a low data rate and BER and is not a limiting factor for the MINERVA-Earth link design.

   The constellation altitude and inclination have no effect on the required Earth antenna gain.

   Therefore the only parameter affecting this link is the number of satellites. The required antenna power-aperture product decreases as the number of satellites increases, because the total data return rate is split among several satellites among those that simultaneously see the Earth.

3. Cross-links

   The data rate for the cross-links is also driven by the requirement on data return to the Earth. In the worst case, all MSEs communicate with MINERVA through a single satellite on the dark side of Mars. Since a main factor in implementing the cross-links was to provide near real-time communication, the availability requirement on this link is high. This ensures that 90% of near real-time opportunities can be made use of.

The antenna aperture-power product for this link is determined according to the maximum distance between two satellites, which is a function of the number of satellites and their altitude. However, the variations in size and cost of cross-links are small with respect to the other two links.

The main influence of cross-links in the top-level design trades was therefore to set the minimum altitude for a given number of satellites.

4. MINERVA-Mars link

   The top-level coverage requirement is that each MSE in the ±15° latitude band should see a satellite with a maximum of three hours revisit time, and 50% availability. Availability is defined as the total time in view per sol and is the limiting factor in this case (see 6.5).

   The number of satellites, altitude and orbital inclination are all main drivers for meeting the coverage requirements. Increasing the altitude or decreasing the inclination decreases the minimum number of satellites for the required coverage (see 6.5). Thus, the coverage requirement sets the relation between orbital altitude and inclination and minimum number of satellites.

   The MINERVA-Mars link design makes minimum assumptions about MINERVA users. Firstly, most MSEs should carry omni-directional antennas at UHF, with an RF output power on the order of 10 W. Secondly, building a whole constellation would not be worthwhile if less than two such MSEs where present on Mars.

   Given the small gain of the user's antenna, the limiting factor for the MINERVA-MSE link is the uplink from MSEs. The requirement for 10 Gb/sol of data return to the Earth places a lower bound on the total data rate from all MSEs to MINERVA. The type of data being transmitted (mostly scientific data) sets the required bit error rate.

   The orbital altitude sets the minimum receiving antenna gain to meet these data rate and BER requirements. The gain affects the antenna size and therefore its cost. (see 10.1).

   As the antenna gain increases, the antenna half-power beamwidth decreases. When the beamwidth becomes smaller than the planet's angular diameter, the coverage performance decreases.

5. Position Determination

   The top-level position determination requirement is to gather sufficient information to determine the position of MSEs in the ±15° latitude band with an accuracy of 100 m (1σ).

   The position determination requirements are more easily met using distinct inclined orbital planes. Placing satellites into distinct planes at Mars is no more costly or

technically difficult than placing satellites into the same plane. MINERVA satellites will therefore be into distinct inclined orbits.To minimize payload requirements, it is desirable to use the communication hardware for positioning. Therefore active position determination using RF signals is preferable. MINERVA will use the existing two-way communication link between satellites and MSEs for positioning (see 10.2).

The decision to perform positioning using both two-way ranging and Doppler shift measurement makes positioning performance largely independent of altitude.

The only parameter directly affecting position determination is orbital inclination. Positioning accuracy requirements are more easily met at higher inclinations.

Positioning performance is also indirectly linked to altitude and number of satellites through coverage performance, since increasing the time in view of an MSE increases the number of measurements.

These trades are summarized in Table 6.2. The table indicates the relations between three main top-level design parameters and the main requirements. References indicate the section of the report that describes each relation in more details.

This trade process resulted in the choice of four satellites in two orbital planes at 2000 km altitude and 27° inclination.

Table 6.2: Summary of Top-Level Design Trades

	Number of Satellites	Altitude	Inclination
MINERVA-Earth Performance	The data return requirement and number of satellites set the minimum transmitting data rate per satellite (10.1.3).	-	-
MINERVA-Earth cost	The transmitting data rate per satellite sets the minimum power aperture product for a given BER (10.1.3).	-	-
MINERVA-Mars Performance	Coverage requirements set the relation between minimum number of satellites, altitude and inclination (0). Coverage slightly degrades when the maximum half-power beamwidth gets below Mars' angular diameter.		
MINERVA-Mars Cost	The data return requirement and the total time in view of an MSE set the minimum data rate (10.1.3).	Receiving data rate and BER set the relation between altitude and antenna gain. To a minimum gain corresponds a maximum half-power beamwidth	-
Cross-Links Performance	The need for cross-links sets the minimum altitude for a given number of satellites (6.5.1.2).		-
Cross-Links Cost	The minimum antenna gain decreases when the number of satellite is increased.	The minimum required gain increases as the altitude increases (10.1.3).	The minimum required gain slightly increases as the inclination increases.
Positioning Performance	Positioning performance improves as time in view of an MSE improves (10.2.4).		Positioning performance improves as inclination increases (10.2.4).
Positioning Cost	No direct influence since the communication hardware will be used for position determination (10.2.4).		
Total Cost	Payload mass and choice of propulsion scheme set the total satellite mass (11).		
	Cost constraints and launch costs set a maximum mass for each satellite as a function of number of satellites (13.3).	-	-

6.4 Interplanetary Transfer Trades[10]

One of the major system-level trades for the MINERVA constellation was the selection of a low-thrust electric versus chemical propulsion system. In order to explore this trade fully, the orbit group examined the interplanetary transfer profile for both methods to provide the bus group with an accurate assessment of the cumulative required ΔV. During early design iterations, electric propulsion appeared the most promising, so we selected that approach for our initial analysis.

Several aspects of the low-thrust transfer method make a thorough trajectory analysis considerably involved. To begin with, the near-continuous use of the electric thruster adds an external force term to the governing equation of motion. Third- and fourth-body effects from the planets' moons and the Sun are significant in several operating regimes during the transfer and cannot be neglected, as in traditional Keplerian orbit equations. Point-mass approximations are not valid for the planets, particularly since the spiraling trajectory common to low-thrust systems is sensitive to variations in the gravity field. The net result is a set of coupled, non-linear differential equations with boundary value conditions for each regime of the transfer orbit. In [Stuhlinger, 1964], Ernst Stuhlinger describes the various operating regimes:

> "A trajectory to Mars…will consist of the following phases: (1) spiral around the earth with tangential thrust until escape is achieved; (2) segment of an opening spiral around the sun with tangential thrust until the predetermined turnaround point is reached; (3) segment of a closing, but still outbound, spiral around the sun with reversed thrust until the orbit of Mars is reached; (4) motion on the Martian solar orbit, with the thrust vector turned either from forward to radially inward, or from reverse to radially outward, to obtain superorbital or suborbital velocity, in order to approach Mars in its solar orbit; (5) appropriate direction of thrust to effect the capture of the vehicle into an orbit around Mars; and (6) spiral around Mars with reverse tangential thrust until the desire orbit around Mars is reached."

The orbit group performed a preliminary analysis using several simplifying assumptions to obtain analytical approximations for the electric propulsion case. The group later expanded the analysis by performing stepwise integration on slightly improved modeling equations to obtain a numerical solution to the same problem. Due to the level of uncertainty in the preliminary analyses, however, the capture trajectory around Mars became a significant risk issue for the program.

Fortunately, the orbit group obtained a copy of two software packages used by NASA mission planners to simulate the trajectory of interplanetary missions using low-thrust electric propulsion. The first software package, ChebyTOP, was developed by Boeing in the early 1970s under a contract from NASA Ames, and maintained by the NASA Jet Propulsion Lab since its release. ChebyTOP performs moderately detailed trajectory analysis for interplanetary missions. The second software package, SEPSPOT, was developed by MIT Lincoln Labs in the mid-1970s under a contract from NASA Glenn

[10] DLF

Research Center, and also maintained by the NASA Jet Propulsion Lab. SEPSPOT calculates minimum trip time for a trajectory from one closed conic to another.

Table 6.3 summarizes the results of the low-thrust trajectory analysis. The total ΔV required for the electric propulsion method is 15.67 km/s, and the total transit time from Earth departure to Mars capture is 894 days. These values are computed using an Earth parking orbit of 185 km. Most low-thrust missions typically rely on the launch vehicle to boost into a much higher parking orbit, thereby minimizing the amount of time the spacecraft has to spend working its way from Earth. The departure trajectory is depicted in Figure 6.4, while Figure 6.5 shows the heliocentric interplanetary trajectory. Figure 6.6 completes the electric propulsion profile with the final capture trajectory around Mars.

Table 6.3: Summary of Transfer Design Trade

	Earth		**Interplanetary**		**Mars**	
	ΔV (km/s)	Time (d h)	ΔV (km/s)	Time (d h)	ΔV (km/s)	Time (d h)
Chemical	3.80	2d 17h	0.17	282d 23h	1.60	3d 17h
Electric	7.38	421d 14h	5.66	323d 3h	2.63	150d 1h

(Using parking orbit of 185 km)

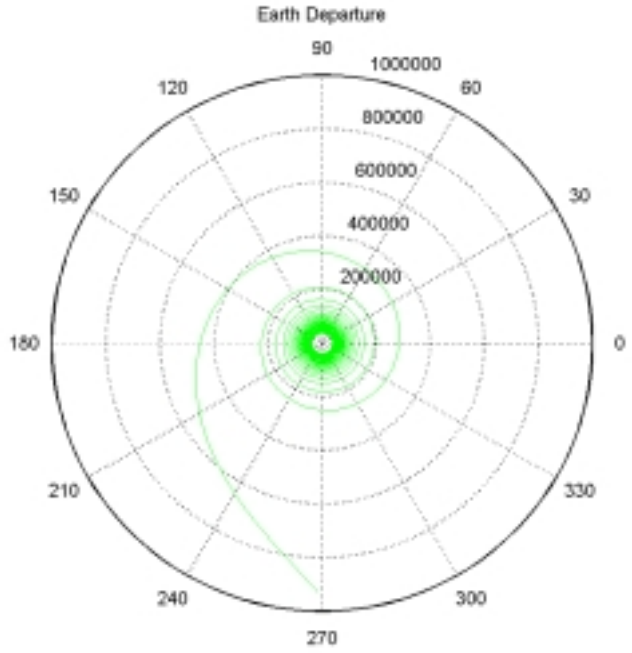

Figure 6.4: Electric Propulsion Departure Trajectory

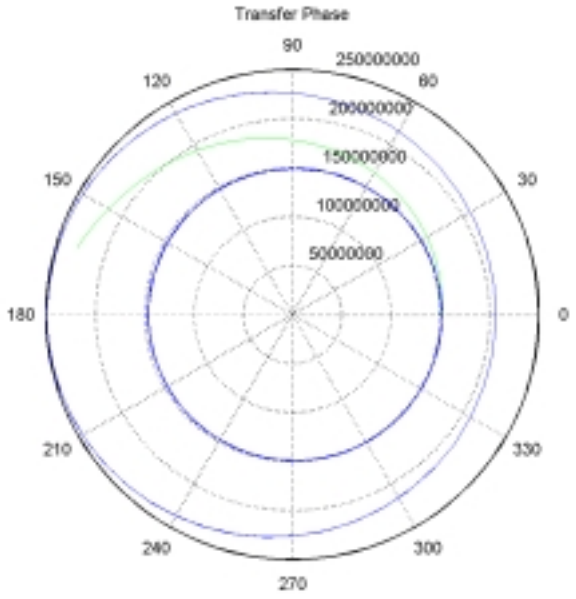

Figure 6.5: Electric Propulsion Transfer Trajectory

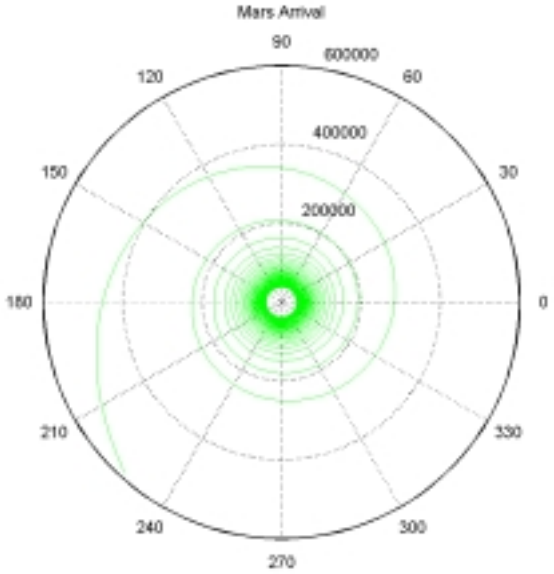

Figure 6.6: Electric Propulsion Arrival Trajectory

In addition to electric propulsion, the orbit group examined chemical propulsion methods. Once again, the group used several simplifying assumptions to perform a preliminary

analysis. In this case, the interplanetary transfer was modeled as a patched-conic problem with a simple Hohmann transfer orbit between Earth and Mars. Although this approach resulted in a fairly accurate assessment of the total ΔV required for the transfer, it did not take into consideration the plane change performed by the launch vehicle prior to achieving parking orbit, the use of the launch vehicle second stage for the initial departure burn, or the correction burns performed on the transit phase between Earth and Mars.

The second iteration of the chemical propulsion analysis took these considerations into account. In addition, the code calculated the ΔV required to boost each satellite into the Martian atmosphere and, as an alternative, to raise each satellite into a higher disposal orbit. Table 6.3 summarizes the results from the second analysis for the final system design. The total ΔV required for the chemical propulsion method is 5.57 km/s, and the total transit time from Earth departure to Mars capture is 286 days. The earth departure trajectory is depicted in Figure 6.7, the heliocentric interplanetary trajectory in Figure 6.8, and the final capture trajectory around Mars in Figure 6.9.

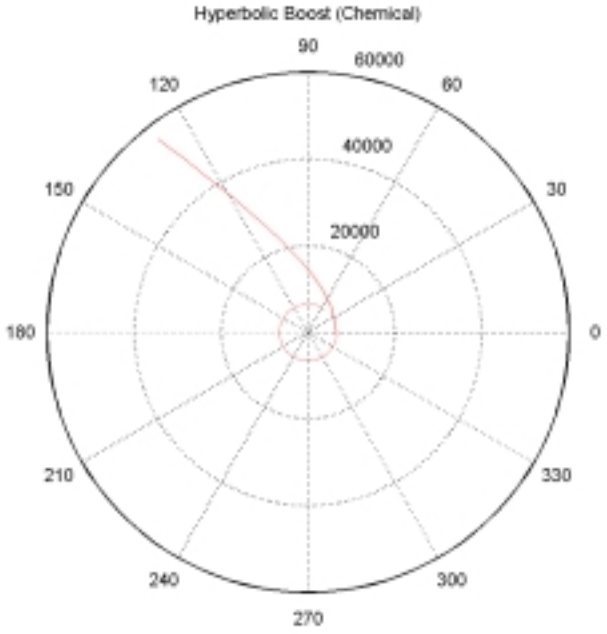

Figure 6.7: Chemical Propulsion Departure Trajectory

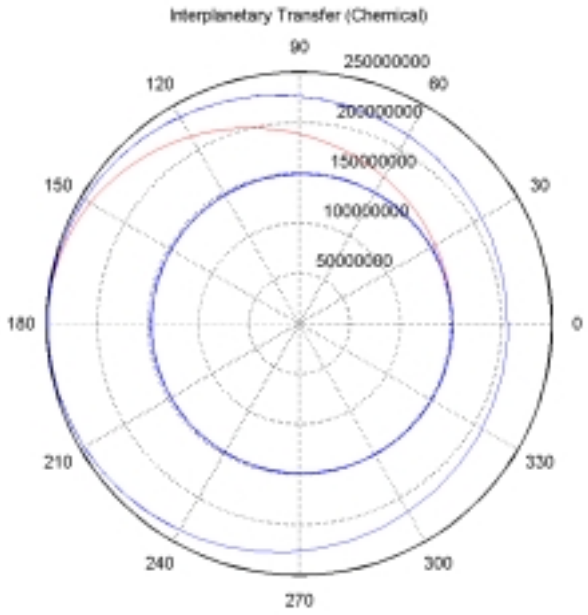

Figure 6.8: Chemical Propulsion Transfer Trajectory

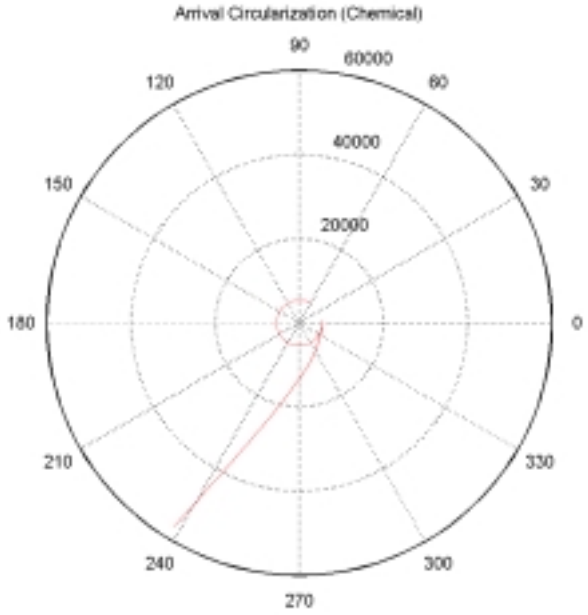

Figure 6.9: Chemical Propulsion Arrival Trajectory

Having completed the individual case analysis for both electric and chemical propulsion methods, the orbit group provided the results to the bus group and launch group for consideration in their associated trades. Strictly from an orbit standpoint, chemical propulsion not only requires less overall ΔV, but also takes less transit time to complete and is therefore the best candidate of the two methods. Given the mission operations concept – in particular, the use of the launch vehicle for a significant portion of the transfer ΔV – the integration group selected chemical propulsion for the MINERVA system design.

6.5 Constellation Design[11]

The purpose of the MINERVA system is to provide communication and positioning information to the Martian surface. More specifically, the system will be focusing on surface elements that lie between 15°N and 15°S. The satellite constellation was designed so that it maximized the performance within this latitude band.

The first step in designing the satellite constellation was creating a set of trade spaces. These trade spaces were governed by the requirements set forth in the requirements document and from the constraints placed on the system by the actual architectural design of the MINERVA system. Then the trade spaces were combined and a set of feasible designs was developed. From these designs, a single constellation was chosen so that it maximized the performance of the system within the latitude band of coverage, while at the same time minimizing the overall cost of the system.

[11] SAS

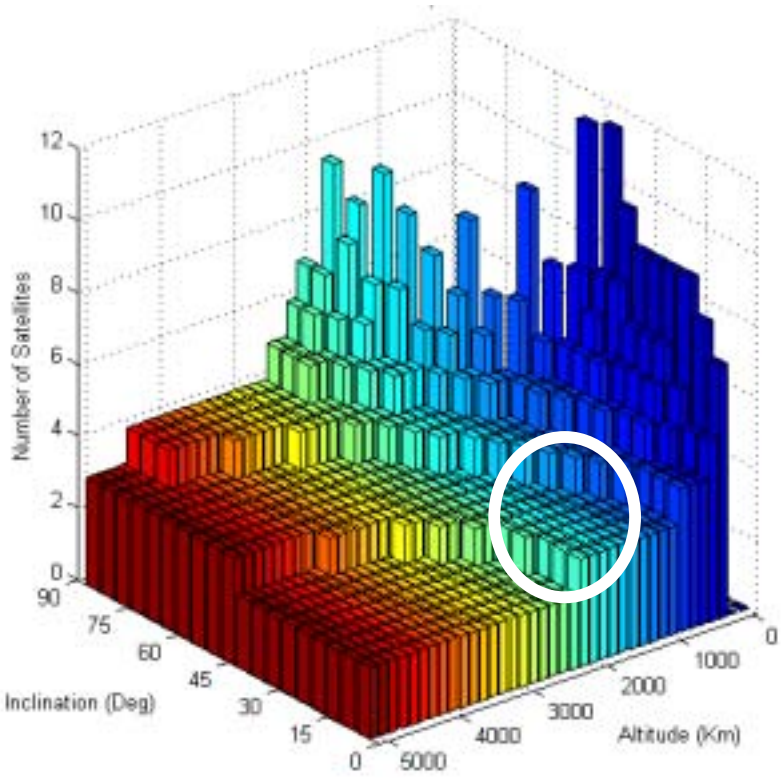

Figure 6.10: Coverage Trade Space

6.5.1 Constellation Design Trade Space

6.5.1.1 Availability and Revisit Time

Two separate requirements placed on the MINERVA system affect the coverage of the satellite constellation. Firstly, a satellite shall be available to an MSE at least 50% of the time, and secondly, the time between satellite passes shall not exceed three hours.

Using these two constraints, a separate trade space was created for each type of constellation.

For example, constellations with a different number of orbital planes, or phasing angles have their own trade space.

In each trade space the minimum number of satellites needed to satisfy the requirements was calculated for different inclinations and altitudes.

The coverage trade spaces were then combined and the resulting composite trade space is shown in Figure 6.10. From the plot we can see that as altitude increases, the number of satellites decreases. This follows from the fact that as the satellites increase in altitude, the size of their footprint also increases. The number of satellites also increases as the

inclination increases. This is because as the inclination increases, the satellites are directly above the ±15° latitude band for a smaller percentage of the orbital period.

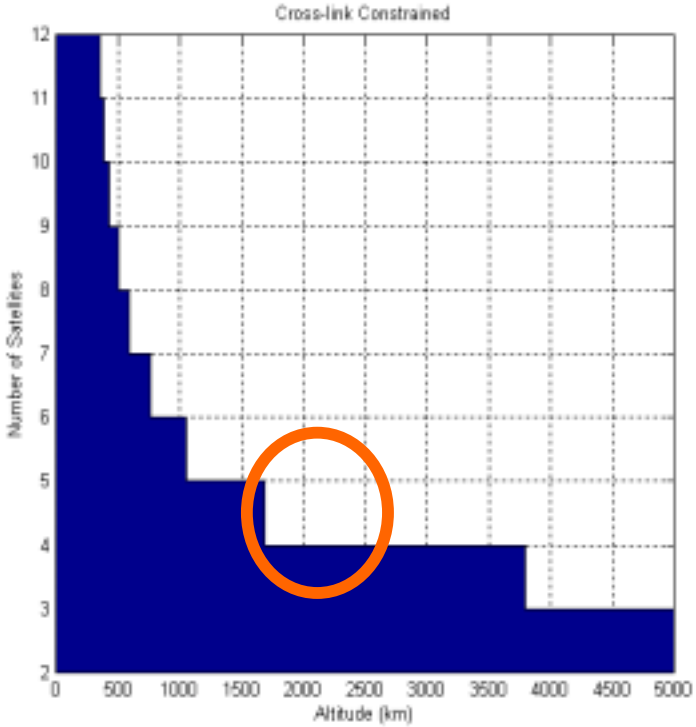

Figure 6.11: Minimum Altitude for Inter-Satellite Links

6.5.1.2 Inter-Satellite Links

Each satellite has the ability to communicate with the other satellites in orbit via inter-satellite links. In order for these links to work, the satellites require line of sight visibility. This constraint imposes a minimum altitude on the satellite constellation. Figure 6.11 shows the approximate minimum altitude necessary for line of sight communication. The figure assumes that the satellites are evenly spaced around the planet in circular orbits. Also included in the figure is the requirement that the communication links must pass 200 km above the surface. This additional requirement provides a margin of safety that takes into account the atmospheric effects and orbit insertion errors.

6.5.1.3 Position Determination Constraint

As described in section 10.2 the satellites need to be in an inclined orbital plane relative to the equator. This inclination allows the MINERVA system to calculate the position of an MSE with greater accuracy and in less time. The required inclination is 25°-30° with higher inclinations preferred.

6.5.2 Final Constellation Design

The above trade spaces placed restrictions on the constellation design. After they had been combined, they produced a set of constellations that were feasible. From this set, the final design was chosen.

The parameters that were varied include, number of satellites, inclination, and altitude. The first parameter that was chosen was the number of satellites. From the ICE sessions it was confirmed that four satellites is the maximum number of satellites that could be afforded. The decision to use four satellites was based mainly on the altitude restriction placed on the constellation by the inter-satellite links. Having four satellites allow as the constellation to orbit at a much lower altitude than three satellites. (1700 km compared to 3700 km). At 3700 km, the antenna needed to communicate to the surface would be much larger than necessary.

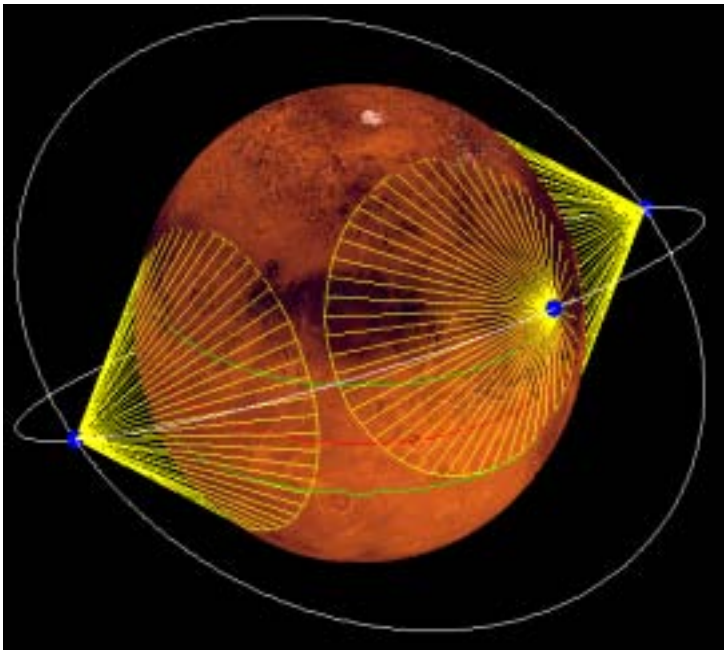

Figure 6.12: Final Constellation

Once four satellites had been chosen, the altitude and the inclination were determined. An increase in altitude increases the coverage area, but at the same time increases the antenna size. A decrease in inclination also increases the coverage within the latitude band, but at the same time decreases the performance of the position determination system. From these two trades, the final altitude was chosen to be 2000 km. This altitude corresponds to the altitude where the beamwidth of the antenna allows users to communicate with the satellite as long as the satellite is 10° above the horizon (see Figure 6.12).

Once the altitude had been set at 2000 km, the inclination was set so that the satellite can communicate with any MSE in the ±15° latitude band during every orbital period. The required inclination is 27°. This can be seen graphically in Figure 6.12. Generated in MATLAB, the figure shows the satellites in their final constellation around Mars. The yellow cones represent the areas covered by each individual satellite. The green lines represent the ±15° latitude band. In the figure, one of the satellites is at the highest point (with respect to the equator) in its orbit.

The final design is a Walker-Delta pattern, which consists of four satellites in two orbital planes. The satellites are in circular orbits with an altitude of 2000 km and an inclination of 27°.

6.5.3 Constellation Statistics

Once the constellation had been determined, the statistics of the constellation were determined. These statistics were used to evaluate different point designs. The payload group used this information to determine the communication abilities of the system.

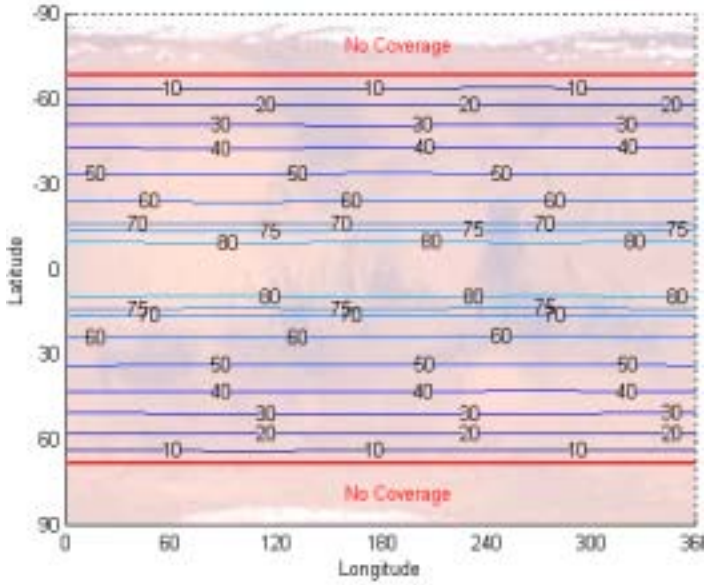

Figure 6.13: Availability Contours

Shown on Figure 6.13, Figure 6.14 and Figure 6.15 are the results of the statistical analysis of the final constellation. Figure 6.13 is a contour plot showing the percentage of time that a satellite is in view. Around the equator, a satellite is in view for at least 80% of the time, and at 15° N and 15° S, the satellite is in view 70% of the time. Above 65° the satellites are never in view.

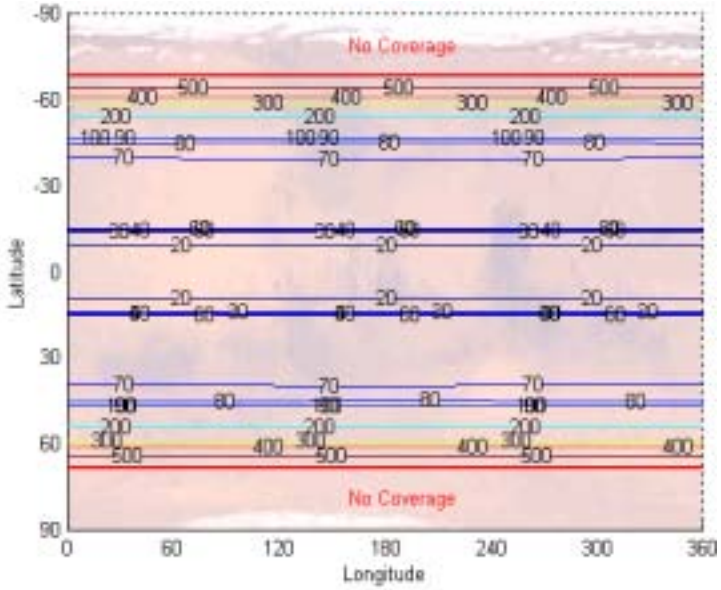

Figure 6.14: Contours of Maximum Revisit Time

Figure 6.14 shows the maximum time in minutes that a satellite will not be in view. Near the equator, this is less than 20 minutes, and less than 30 minutes at the ±15° latitudes. Just outside of this band, the maximum revisit time increases to 60 minutes. This large jump is due to the fact that during an orbit period, an MSE outside of the latitude band may not see all four satellites.

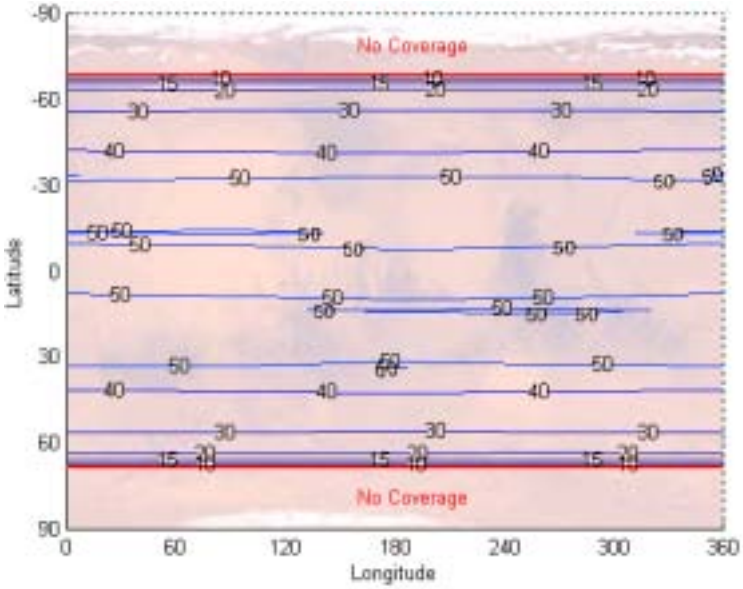

Figure 6.15: Contours of Average Time in View

Figure 6.15shows the average amount of time in minutes that a satellite will stay in view. From -30° N to 30° S, a satellite will stay in view for about 50 minutes. Notice that this corresponds to the inclination of the orbital planes, as is to be expected.

6.6 Launch Analysis[12]

Although the space launch vehicle (LV) that will transport our spacecraft into orbit is not technically part of the MINERVA system, planning for launch was critical to our design. As some launch options would cost over 30% of our total budget (to IOC), we had to carefully assess and trade those options, lest launch consume too much of the budget and unnecessarily limit other aspects of our design.

6.6.1 Launch Vehicles

The first set of launch decisions we faced concerned the boundaries of our trade space. There are a number of LVs available for commercial use worldwide, some of which are notably reliable and low-cost, but planning to use a foreign LV would involve political risk.[13] Likewise, new and improved LVs are constantly being developed, and several new systems are slated to enter service by our launch date, but as their cost, performance, and availability have not yet been demonstrated, they involve technical risks. We attempted to minimize both political and technical risks by considering only demonstrated US LVs.[14]

We took into account cost, availability, and several performance metrics, and selected the Athena II, Delta II, Delta III, and Zenit 3SL as good candidate LVs to model for our design trades. Figure 6.16, below, presents the cost per kg of payload transported to Low Earth Orbit (LEO), for a variety of US launch vehicles. (While this measure does not reflect efficiency gains that some LVs may provide at higher orbits, it is a fair overall estimate, to first order.[15]) It is clear from this chart that the four LVs identified above are among the most cost-effective options, although they differ significantly in terms of absolute cost and performance.

---

[12] JMF

[13] In the current state of the world, the feasibility of commercial launch contracts is largely determined by international relations. US ventures, in particular, must consider the possibility that national security-related investigations may delay or even prohibit launch on foreign LVs.

[14] The Zenit 3SL is the only LV we considered that might be controversial. However, we maintain that it can be included as a "US" LV, even though it is manufactured in Ukraine and Russia, because it is the LV created for Sea Launch, a multinational venture actually led by a US company (Boeing). Moreover, the Zenit 3SL has already been classified as a US system for certification and liability purposes.

[15] This data is for the 185 km, 28.5°, circular orbit. Since transporting a payload from the ground to LEO requires much more energy than transporting it from LEO to higher orbits or escape, comparing LVs on the basis of their cost-effectiveness to LEO is reasonable. It is also a convenient means of comparing the very disparate costs and performance levels of small and large LVs.

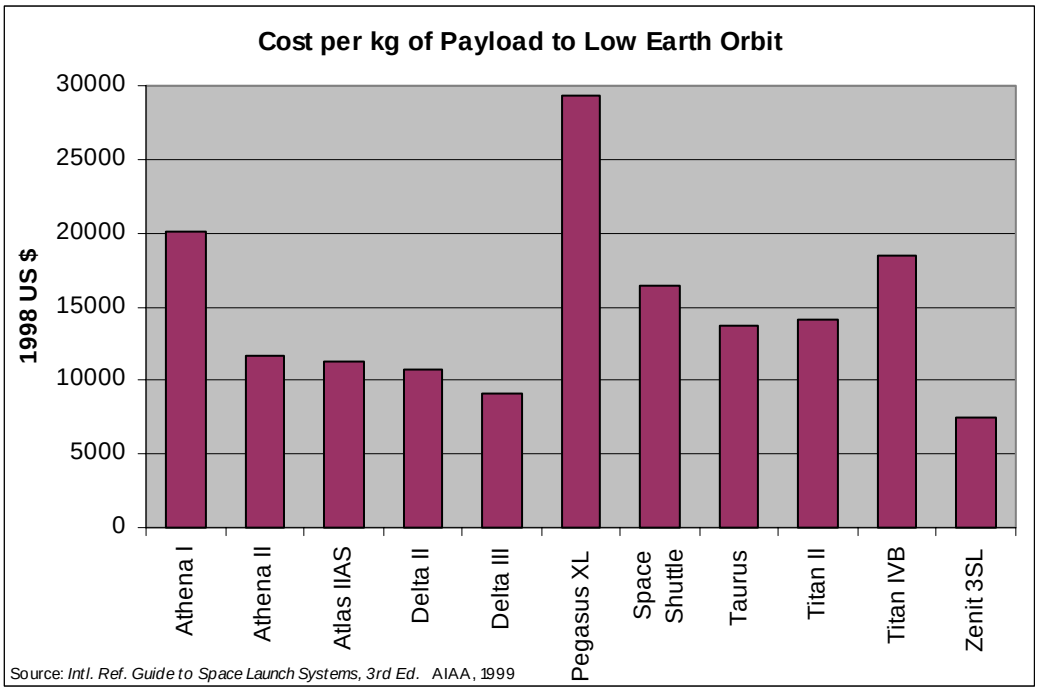

Figure 6.16: Cost per kg of Payload to LEO for Selected US Launch Vehicles

Figure 6.17 depicts the selected candidate LVs (approximately to scale), and each is briefly described below.

Figure 6.17: Launch Vehicles Included in Final Launch Trades

- **Athena II** – a small LV produced by Lockheed Martin – the least expensive launch option (even if two are required!), but with limited capability: only practical to LEO.

- **Delta II** – a medium-light LV produced by Boeing – a very reliable and fairly low cost launch option, with sufficient capability for most launch scenarios.

- **Delta III** – a new medium LV produced by Boeing – a risky option, having failed in its only two launches to date, but Boeing claims to have resolved those problems (and will have seven more years before we launch), and the Delta III offers great capability at a moderate price.

- **Zenit 3SL** – a medium multinational LV, led by Boeing – also new and fairly risky, Sea Launch is somewhat larger and slightly more expensive than the Delta III, but is designed for a different set of missions (equatorial launch to geosynchronous orbit).

Finally, Figure 6.18 presents the relative cost and performance capabilities of the Athena II, Delta II, Delta III, and Zenit 3SL. This chart shows how much payload mass each of the vehicles could boost in the two extreme launch scenarios: 400km LEO (blue columns on the left) and direct escape (green columns on the right). It also includes cost[16].

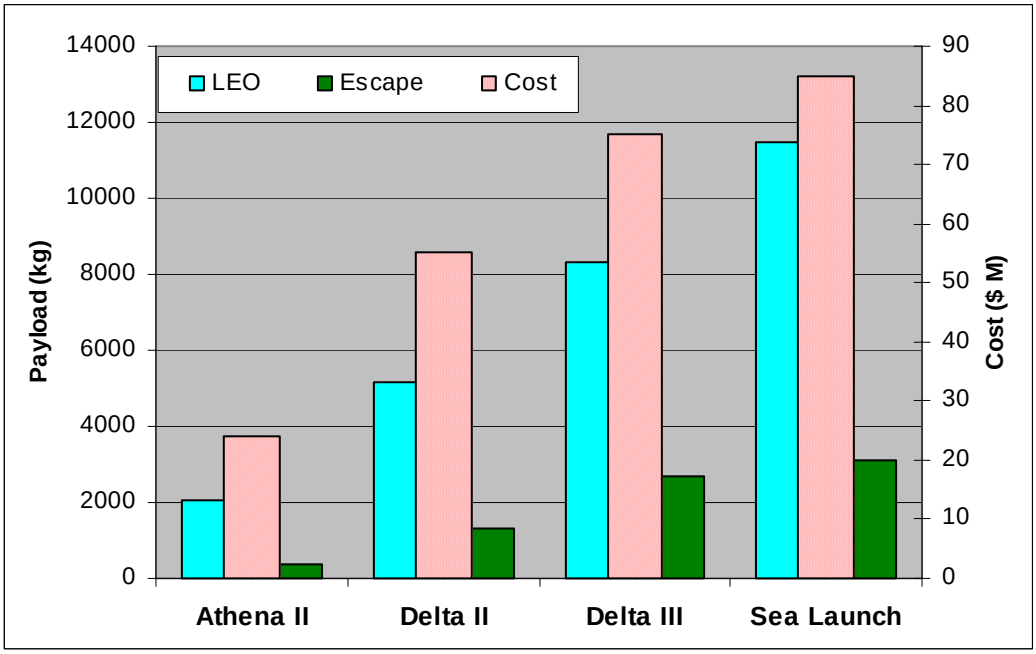

Figure 6.18: Launch Vehicle Performance and Cost Data

[16] Excel insisted on putting the cost column between the two payload columns, even though the cost ordinate is on the right.

6.6.2 Launch Trades

In order to choose between the candidate LVs we needed to compare their capabilities, which was challenging because many things were being traded simultaneously in our design sessions. For any given payload mass and launch orbit altitude, we would run a MATLAB module to determine which of the four LVs would be the most efficient. This in itself often gave us many choices, as the specified orbit and payload mass were very unlikely to precisely match an LVs capabilities. Instead, we would find that the most cost-effective LV could either transport the payload to a higher orbit, or transport more mass, without affecting the launch price. This impacted all of the other design groups, as we had to collectively determine whether it would be most beneficial to

- launch to a higher altitude and save on-board propellant, or to
- launch to the original altitude and use the extra mass somewhere else in the design (while remaining under our cost budget).

This was really a trade between propulsion from the launch vehicle and propulsion on-board the MINERVA spacecraft. For example, it would appear that we could save a lot by simply using an Athena II to just get us to LEO. In that case, however, we would need larger spacecraft equipped with a sufficient propulsion system and enough power and fuel to boost themselves to Mars. If we used an electric propulsion system, they would need radiation shielding, for they would have to spiral out through the Van Allen belts. But all the extra mass for the structures, power, propellant, and shielding might mean we would need three Athena IIs, at which point it would be more efficient to use one of the larger LVs. Or, for a less extreme example, we could use a Delta II to transport to LEO even for our largest design scenarios, but if our spacecraft could be made small enough, a Delta II could launch them directly to Mars.

At the same time, however, we had to consider that each of the LVs was designed for certain missions. While one LV would be more efficient for one launch scenario, it might not be for a slightly higher orbit – and LV performance did not usually scale linearly.[17] For example, some of the performance curves for the Delta III are given in Appendix E.

In our concurrent design sessions, we investigated four launch scenarios: LEO, middle Earth orbit between the Van Allen radiation belts, geosynchronous orbit, and direct Earth escape. It soon became clear that the best options were the two extremes: circular LEO and direct Earth escape. LEO is efficient because we can use a smaller booster for a fairly low price, and then use high-I_{sp} electric propulsion to spiral out and transit to Mars.[18]

---

[17] We actually had to contact engineers at Boeing and Lockheed Martin to ask how to extrapolate the published LV performance curves for a few of our launch scenarios, and they were very helpful.

[18] I_{sp} stands for specific impulse, which is the ratio of thrust to propellant mass flow rate. Therefore the higher the I_{sp} of the rocket propellant, the more thrust it provides to the spacecraft per pound.

This would take longer, and it would also require radiation shielding, but we could afford the extra mass if we were only launching to LEO. Direct Earth escape is efficient because it makes the most out of paying for a given LV (although it has to be a larger one), and allows us to have smaller spacecraft carrying much less propellant. Intermediate options, however, tend to combine the disadvantages of both. Launching to a high circular orbit, for example, would require as much energy from the LV as direct escape (if not more), but would also require propellant to spiral out, plus radiation shielding to protect the spacecraft from the upper Van Allen belt, both increasing our mass – for no gain (in fact, it would take longer to get to Mars then the direct escape).

After further analysis, we discovered that in the direct escape option, we could replace the electric thrusters with small, inexpensive, chemical thrusters. This, taken into consideration along with a tight budget, made direct escape via Delta III a better option than LEO. The Delta III could provide enough hyperbolic excess velocity for MINERVA to transit directly to Mars, and all we needed on the spacecraft were small chemical propulsion systems to facilitate capture at the Mars end.

6.7 References

Bottkkol, Matthew S. and Didomenico, Paul B, A Phase-Based Approach to the Satellite Revisit Problem. Advances in the Astronautical Sciences, 91-165.

Brown, Charles D. Spacecraft Mission Design. Washington, DC:AIAA Ed. Series, 1992.

Delta Launch Services. Delta II Payload Planners Guide. The Boeing Co.,(1996, 1999).

Hopkins, Joshua B. Lockheed Martin Space Systems. E-mail correspondence about the capabilities of the Athena II launch vehicle. April, 2000.

Hobbs, Richard. Marine Navigation: Piloting and Celestial and Electronic Navigation, 3rd ed. Naval Institute Press, Annapolis, MD. 1990.

Isakowitz, S. J., Hopkins, J. P., and Hopkins, J. B. International Reference Guide to Space Launch Systems (3rd Ed.). AIAA, 1999.

Jet Propulsion Laboratory. Mars Global Surveyor Project Mission Plan (Final Version, Rev. B). JPL D-12088. NASA, 1996.

Prussing, John E. and Conway, Bruce A. Orbital Mechanics. New York:Oxford Press, 1993.

Solomon, Charles. Boeing Space Systems. Telephone interview about the capabilities of Delta II and III launch vehicles. April, 2000.

Stuhlinger, Ernst. Ion Propulsion for Space Flight. New York: McGraw-Hill, 1964. Pp 120-121.

7 Constellation Set-up

To set up the MINERVA constellation requires four phases of operations: launch, interplanetary transfer, Mars capture, and deployment. This section provides an overview of each phase.

7.1 Launch[19]

MINERVA will be launched from Cape Canaveral Air Station on a Delta III launch vehicle. The daily launch window constraint is ±1 s, with opportunities occurring once every twenty-four sidereal hours between August 3 and August 18, 2007. The window is extremely tight due to the geometry of the parking orbit with respect to the ecliptic plane. As the launch site rotates around the Earth's axis, the orbit plane into which the Delta III can directly launch becomes nearly coplanar with the ecliptic plane once every sidereal day. By launching early, the satellite may remain in Earth parking orbit until the time and position for the departure burn is achieved. Considering there is little leeway for slips due to inclement weather or vehicle problems, the probability of a successful launch is improved by attempting to launch early in the launch window rather than later. The last launch opportunity occurs at 9:56 AM (GMT), August 18, 2007.

For launch, the four MINERVA spacecraft will be connected and stowed vertically within the Delta III payload fairing (refer to Table 7.1 for a detailed description of the launch sequence). About four minutes after lift-off the LV will reach an altitude of 120 km, and the fairing will jettison. Shortly thereafter, the first stage of the LV will separate, and the second stage will ignite to boost the system into a 185 km circular parking orbit with an inclination of 28.5°. Twenty-eight minutes later, the system will reach the descending node of the parking orbit and will perform a short 35 s duration burn to move into a staging orbit with an inclination of 23.45°. There the system will cruise for a minimum of three hours, and potentially several days depending on the launch date. At the precise departure point, the second stage will re-ignite and the system will be boosted into a hyperbolic, trans-Mars orbit. Once the second stage burn is complete, the second stage will drop off, and the MINERVA spacecraft will separate in preparation for the transfer phase.

[19] DLF

Table 7.1: Launch Sequence

T+ 0:00	Launch
T+ 1:19	Solid drop (6)
T+ 2:37	Solid drop (3)
T+ 3:44	Jettison fairing
T+ 4:29	Stage 1 separation
T+ 4:41	Stage 2 burn, i=28° ΔV = 4.628 km/s Duration = 8.27 min
T+ 16:00	Collision avoidance run
T+ 28:17	Stage 2 burn, i=23.45° ΔV = 0.700 km/s Duration = 35 s

7.2 Interplanetary Transfer[20]

The transit phase begins when the second stage of the Delta III is restarted to boost the system from the staging orbit around Earth into a trans-Mars trajectory (refer to Table 7.2 for a detailed description of the transfer sequence). This phase will last for approximately 283 days, until the spacecraft reach the Mars sphere of influence. The entire second stage/payload assembly will be spinning about the velocity-aligned axis to provide a small measure of stability throughout the burn and to minimize the effects of off-axis thruster pointing error. The burn will last for 5 min 35 s and will provide 3,799 m/s of additional velocity to place the stacked constellation on a hyperbolic departure trajectory, timed to coincide with the window of opportunity for the interplanetary transfer orbit. Tracking data will be collected after the burn is complete to establish the actual flight path of the second stage/payload assembly.

[20] DLF

Table 7.2: Transfer Sequence

T+ 3:23:20	Departure burn (second stage) ΔV = 3.799 km/s Duration = 5.59 min
T+ 3:29:30	Start release sequence Interval = 50.15 min
T+ 6:01:00	De-spin maneuver
T+ 6:01:50	Deploy solar arrays
T+ 6:05:00	Initial checkout
T+ 2d 16:39	Depart Earth SOI
T+ 2d 16:39	Alignment burn (four ACS thrusters) ΔV = ~0.020 km/s Duration = 48.2 s
T+ 2d 16:45	Functional testing
T+ 122d 16:00	Correction burn (four ACS thrusters) ΔV = ~0.005 km/s Duration = 12.0 s
T+ 285d 00:00	Upload precise position
T+ 285d 01:00	Spin-up maneuver
T+ 285d 14:29	Arrive Mars SOI (29 May 2008)

Shortly after achieving a stable departure trajectory, the spacecraft will be ejected from the assembly using a spring-loaded release mechanism. The mechanism will provide approximately 0.3 m/s of velocity, causing the first satellite to move slowly away from the rest of the assembly. As the first satellite is ejected, the upper stage begins a programmed timing sequence that will release the three remaining satellites at equal intervals of 50 min 9 s. The timing of the release sequence is important for proper phasing upon arrival at Mars, and will be discussed in greater detail in the following section.

Once released from the upper stage, each satellite will remain inactive for sixty minutes to ensure safe clearance distance from the rest of the assembly. At that point, the satellite will use its on-board sensors to acquire attitude data and perform a de-spin maneuver. Having achieved three-axis stabilized attitude control, the satellite will slew into an Earth-Sun facing orientation. The constellation will be ready for initial on-orbit functionality tests once all four satellites are in this transfer configuration.

As the spacecraft reach the edge of the theoretical Earth sphere of influence (SOI), each one will perform an alignment burn using four of the ACS thrusters working in tandem. The purpose of the burn will be twofold: to align the velocity vector with the interplanetary transfer trajectory within the ecliptic plane, and to correct for trajectory errors accumulated through the launch and departure phase of the mission. The four thrusters will fire for 48 sec to achieve a ΔV of 20 m/s.

Correction burns may be performed at one or two additional points along the interplanetary transfer orbit. The need for these burns will be determined real-time by the operations staff based on the projected position error upon reaching Mars. Each satellite will perform its own correction burn, but must also maintain proper inter-satellite spacing. Therefore, any and all correction burns will be coordinated for all four satellites from the Earth control center.

As each satellite approaches the Mars sphere of influence, it will perform a spin-up maneuver to obtain an angular velocity of six revolutions per minute. The satellite will spin about the velocity-aligned axis to provide stability throughout the upcoming capture burns and to minimize the effects of off-axis thruster pointing error. At this point in the mission timeline, the solar arrays will be fully extended, meaning the spacecraft will be spinning about its major axis as well as the velocity vector.

The last correction burn will be the Mars injection burn. This burn has two components: an in-plane component which aligns the velocity vector along a precise hyperbolic arrival trajectory, and an out-of-plane component which raises or lowers each spacecraft into a slightly inclined orbit with respect to the ecliptic plane. The first satellite in the formation will raise its inclination by +27°, with the following satellites alternating between lowered and raised inclination (i.e. the second satellite will change its inclination by –27°, the third by +27°, etc.). Although the actual plane change will be very small, it is a critical maneuver that ensures each satellite will arrive at Mars with the correct distance from the ecliptic plane to achieve a mission orbit of the desired inclination. Because the

burn will be performed at the sphere of influence rather than a lower orbit, the desired plane change occurs with minimal ΔV of 167 m/s.

7.3 Mars Capture[21]

The Mars capture phase begins as each satellite reaches the theoretical sphere of influence of Mars, at an altitude of roughly 577,000 km. This point will occur on or about May 29, 2008, depending on the precision of the correction burns made en-route. The subsequent sequence of events for the capture regime is outlined in table 3. If the satellite is properly positioned at arrival, it will naturally enter a hyperbolic trajectory around Mars in the same plane as one of the two mission orbits, designated for reference here as the 'A' plane. When the hyperbolic capture trajectory approaches the desired mission orbit altitude of 2,000 km, the on-board systems will automatically initiate a 19-second circularization burn. This burn will slow the satellite by a ΔV of 1,602 km/sec, placing it in the desired mission orbit.

Table 7.3: Capture Burns

T+ 285d 14:29	Injection burn (main kick motor) ΔV = 0.167 km/s Duration = 2.1 s
T+ 290d 08:22	Circularization burn (main kick motor) ΔV = 1.602 km/s Duration = 19.1 s
T+ 290d 08:23	De-spin maneuver

Precisely 50 minutes after the first satellite reaches the Mars sphere of influence, the second satellite begins heading toward the planet for capture. The satellite will follow the same sequence outlined above, except that it will enter a hyperbolic capture trajectory in the same plane as the second mission orbit, designated the 'B' plane. Since the second satellite arrived at the sphere of influence 50 minutes – which is ¼ the period of the 2,000 km mission orbit – after the first satellite, it will complete its circularization burn 90° out of phase with the first satellite as desired for the constellation configuration. The third and fourth satellites will arrive in a similar fashion, the third being placed in the A plane

[21] JMF, DLF, RLM

180° out of phase of the first satellite, and the fourth being placed in the B plane 180° out of phase with the second satellite.

7.4 Deployment[22]

The deployment phase begins after each satellite completes its respective circularization burn. Each satellite will perform a de-spin maneuver to return to three-axis stabilized attitude control. In the meantime, ground controllers will obtain position fixes for all four satellites and determine what type of station-keeping burn each one will perform to configure the constellation as closely as possible to the specified design parameters. Once the station-keeping burns are complete, the satellites will slew into operational nadir-pointing attitudes and deploy the large high-gain antennas. Following an additional checkout period, the constellation will achieve Initial Operational Capability (IOC) on July 9, 2008.

Table 7.4: Deployment Sequence

T+ 290d 08:24	Deploy large antenna
T+ 290d 10:54	All satellites in place
T+ 291d 12:00	Correction maneuvers (as necessary)
T+ 296d 12:00	Test and calibration
T+ 326d 01:40	IOC: 9 July 2008

[22] DLF

8 On-Orbit Operations[23]

This chapter begins with an overview of normal MINERVA operations. It then goes into a more detailed functional analysis of four main categories of operations: Earth Uplink, Mars Uplink, Positioning Loop, and Anomaly Resolution. This functional analysis includes a combination of functions and data flow due to the highly coupled nature of the MINERVA communication tasks and information.

8.1 Overview

Once the MINERVA constellation set-up is complete, normal on-orbit operations can commence, so IOC should be reached around July 9, 2008. This phase is to last for at least five years.

Figure 8.1 diagrams the system's top-level functional flow, in which Normal Operations appears as block 5 (a more detailed functional flow diagram is found in Appendix D).

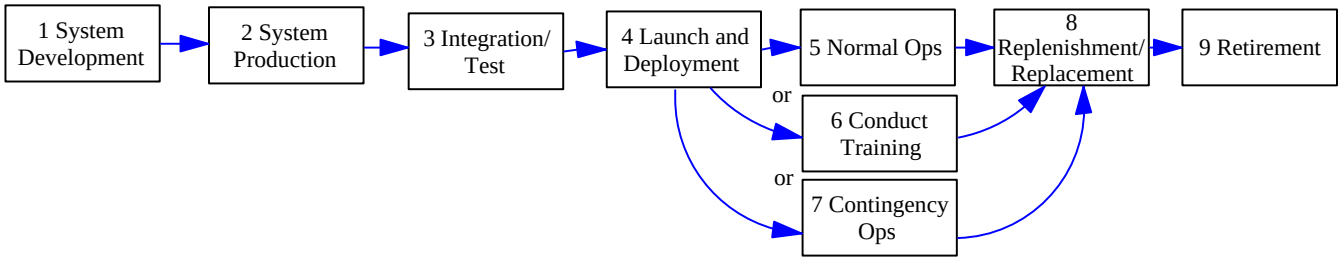

Figure 8.1: MINERVA Funcitonal Flow Diagram

The MINERVA satellites will be responsible for:

- Maintaining their orbits (station-keeping)
- Relaying communication between MINERVA satellites (cross-linking)
- Relaying communication between MINERVA satellites and Earth
- Relaying communication between Mars surface explorers (MSEs) and Earth
- Providing position information to MSEs

The MINERVA constellation described above will provide coverage for all MSEs within 60° latitude of the Martian equator, and exceed coverage requirements for MSEs within 15° latitude. In this band, assuming an elevation angle of 10° is required for a clear line-

[23] RLM, JMF

of-sight, a satellite should come into view at least every twenty minutes and it should remain in view for an average of fifty minutes per pass.

As long as at least one satellite is in view, an MSE will be able to send or receive communication data, except for the nineteen-day exclusion period when the Sun is on the Earth-Mars axis. Since the four MINERVA satellites will be equally distributed around Mars, at least two will be in view of Earth at all times. Accordingly, those two satellites will conduct communication with DSN. Meanwhile, all four satellites will be able to transmit to and receive from MSEs and the other MINERVA satellites. Any satellites not in view of Earth can still relay communication to Earth by cross-linking. That was the rationale for making all four MINERVA satellites identical.Any MINERVA satellite can provide position information to MSEs, through the use of two-way Doppler radar and two-way ranging techniques (which require only one satellite in view to function). The satellite will initiate the procedure by sending a signal to the MSE as it comes into view. When the MSE receives this query, it will send an acknowledgment reply. Doppler and range data are taken as the satellite overflies the MSE, and on-board satellite computers determine the MSE's position. (The altitude of the MSE is known from MOLA mission data.) While not quite a real-time solution, this process can provide a quick approximate answer (on the order of tens of kilometers), which can be improved through integration over time (see section 10.2.4.3.2 for further details).

To perform these functions for MSEs, MINERVA will operate according to a user table. Each satellite will have a copy of this table, which will list all the MSEs along with their last known (or expected) locations, their individual communication codes, and their action schedules. Thus the table tells each satellite which MSEs should be in view at any given time, how to contact them, and whether or not they need communication or positioning services. The unique communication codes enable MINERVA to distinguish between different MSEs, and to serve multiple MSEs simultaneously. (If multiple MSEs are in view at the same time, the data rate for each may have to be limited; this could be determined on Earth and added to the user table.)

All satellites constantly poll all MSEs they expect to be in view. Every satellite will know where all satellites and MSEs are at all times, because the user table and satellite ephemeris data will be shared. This will enable MINERVA to direct information for a given MSE to the closest satellite, either currently in view of the MSE or next to come into view.

Any MSE that receives a query with its communication code is required to send a response. Upon receipt of the response, MINERVA will downlink any information it has from Earth for that MSE. In addition, the satellite can uplink information to be transmitted back to Earth, and/or provide position information to the MSE, as the user table dictates. Principal Investigators can modify the user table entries pertaining to their MSEs at any time. (Changes should be sent at least thirty minutes to one hour before they are to take effect, in order to travel to Mars and get processed in time.)

The MINERVA satellites also have a search mode, in which all satellites poll a specific target MSE, whether they expect to be in view or not, in an effort to find it. This mode

might be used if an MSE fails to respond after MINERVA satellites have tried to poll it several times, for example.

Finally, to minimize loss of data, MINERVA will store every transmission until it receives confirmation of receipt, a new command to abort that transmission, or until the backup storage buffer is full (at least three days).

8.2 Earth Uplink

The Earth uplink function initiates with the collection of data and commands from Principal Investigators for uplink to MINERVA. This information is interleaved with all of the data, commands, updates, and ephemeris information generated at the Earth Ground Station for the MINERVA satellites. Processing at the Ground Station will include time and destination tagging of the information. This is an important step in the function of the system, because a majority of the information required by the MINERVA system is generated and processed on the ground rather than by an autonomous system aboard the MINERVA spacecraft. This information includes which users the MINERVA system is to accommodate, at specific times, for specific durations. Tables of information tell the satellites where the users should be, and how to process uplink and downlink information for the users.

This single data stream generated at the Earth Ground Station passes by way of the Deep Space Network to the MINERVA spacecraft. The appropriate destination spacecraft and time required for transmission are determined through analysis at the Ground Station. Upon arrival, the receiving spacecraft checks the transmission for completeness and integrity, and de-interleaves the signal. Each specific segment of the signal will have both the destination and time tags mentioned earlier.

1) If the message is to be relayed to other system elements or users, the segment is sent to a buffer until the appropriate time. The MINERVA satellite initiates a communication request to the destination element (other MINERVA satellites or Mars Surface Elements) at the appropriate time, and sends the transmission upon acknowledgement of the initialization. The sending MINERVA satellite will then erase the data segment from the buffer once a confirmation is received from the destination element.

2) If the transmission segment is for use of the receiving MINERVA satellite, the data segment is sent to the main computer for processing. This segment includes any updates to the list of communication and positioning users that MINERVA will be accommodating, as well as ephemeris data with which the satellite updates its position. The satellite then maneuvers if necessary. Figure 8.2 presents a diagram of the Earth uplink functions.

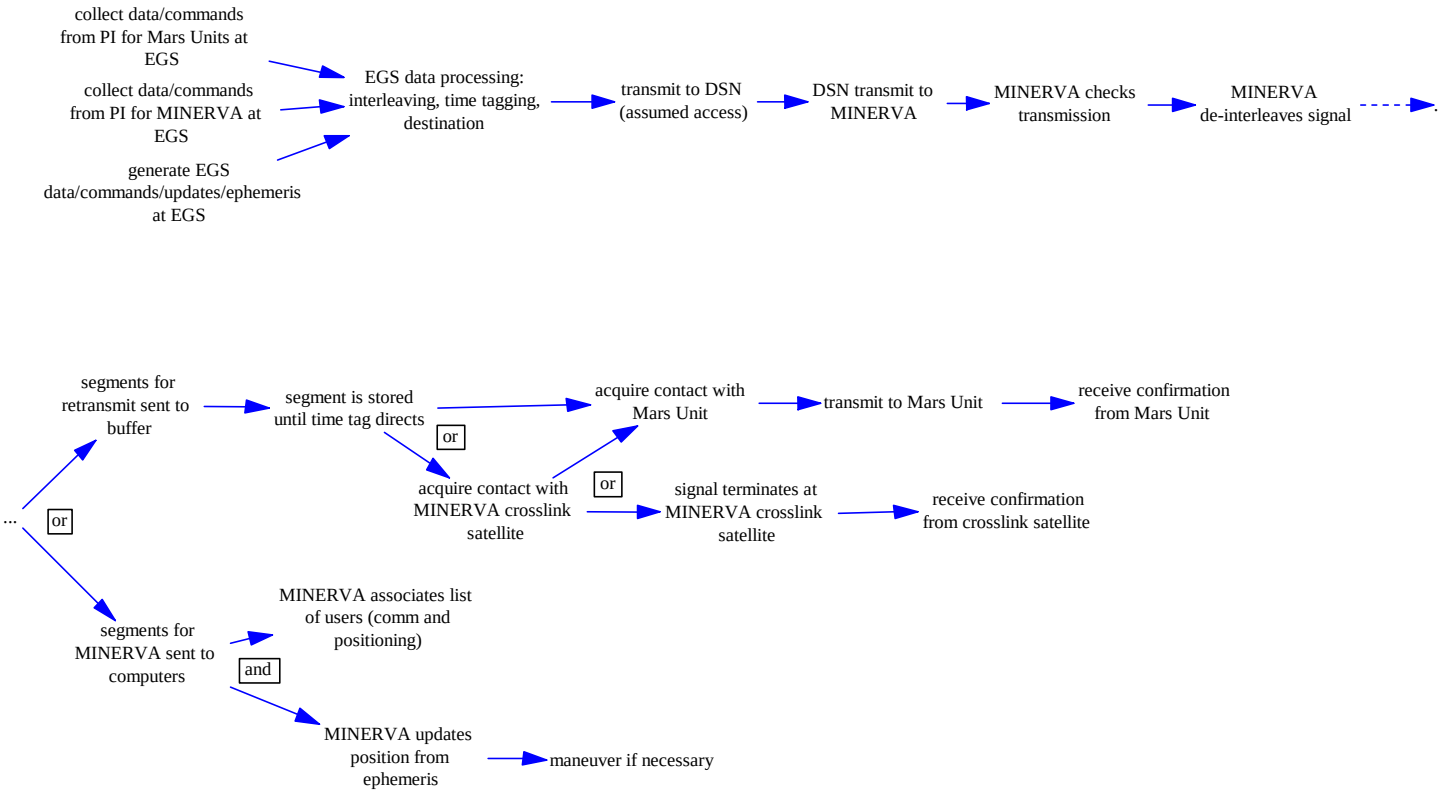

Figure 8.2: MINERVA Earth Uplink Stream

8.3 Mars Uplink

Once MINERVA has received instructions to provide communication service for an MSE, the appropriate MINERVA satellite sends a communication initialization signal to the user. The user then uplinks the data to the MINERVA satellite, where it is stored in a data buffer. For the sake of risk reduction, this buffer will allow three days worth of data storage to account for anomalies within the communication stream. MINERVA then sends a confirmation to the user and interleaves the data with the next transmission to the Earth Ground Station. The data buffer is cleared when MINERVA receives transmission confirmation from the Earth Ground Station. Not including processing time, this cycle will occur in a minimum of two time lengths of data transmission between Earth and Mars (about 45 minutes). Figure 8.3 is a diagram of the Mars uplink functions.

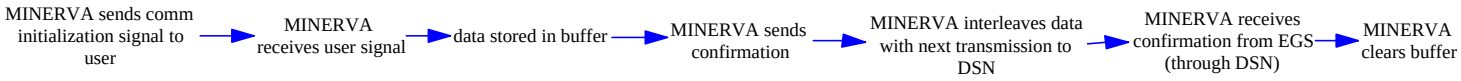

Figure 8.3: MINERVA Mars Uplink Stream

8.4 Positioning Loop

The method by which MINERVA provides positioning to its users includes the majority of the set-up analysis provided by the Earth Ground Station, and the actual calculation of the positioning solution performed aboard the spacecraft. The positioning solution loop begins with service instructions provided by the Earth Ground Station, and an update of the MINERVA satellite's position from on-orbit and Earth-generated orbit propagation analysis. These service instructions will include which MSE to provide service for, approximate location of the MSE, and the length of time for which to provide service. Similarly to the Mars Uplink stream, the appropriate MINERVA satellite sends a positioning initialization signal to the user. Once the MINERVA satellite receives a reply, it calculates the positioning solution and sends the solution to the user, and the cycle repeats itself for an allotted amount of time. Should this positioning cycle require a handoff of users between satellites, this information will be included in the instructions uplink from the Earth Ground Station. The MINERVA satellite then ends the positioning cycle per the positioning instructions. Figure 8.4 presents a diagram of the positioning loop functions.

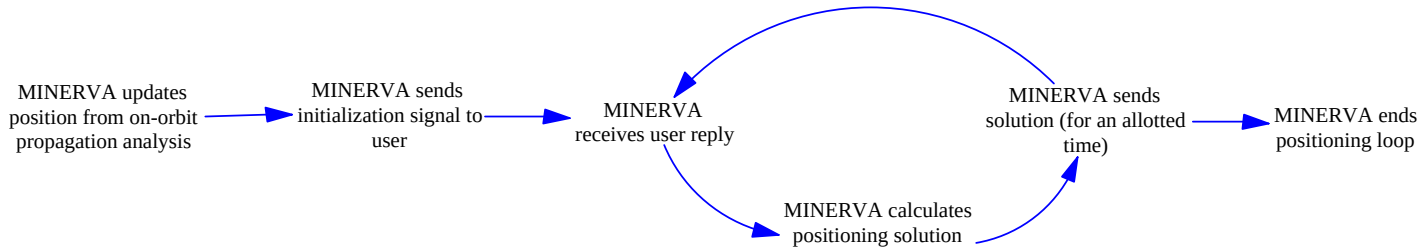

Figure 8.4: MINERVA Positioning Loop

8.5 Anomaly Resolution

The anomaly/fault resolution stream will run continuously within each MINERVA satellite. Should a satellite's regular subsystem checkout identify a problem, or a subsystem send an anomaly flag, the spacecraft will enter Safe Mode 1 (see section 14.2 for further description of safe modes). This mode includes an autonomous analysis of the anomaly, and any autonomous attempt at correcting or rerouting around the anomaly. If the autonomous analysis cannot resolve the anomaly, the satellite enters Safe Mode 2 or 3. These modes then require a notification to the Earth Ground Station for help in resolving the problem. MINERVA then receives the instructions back from the Ground Station and implements the instructions in the effort to return to normal operations status. Figure 8.5 is a diagram of the anomaly resolution functions.

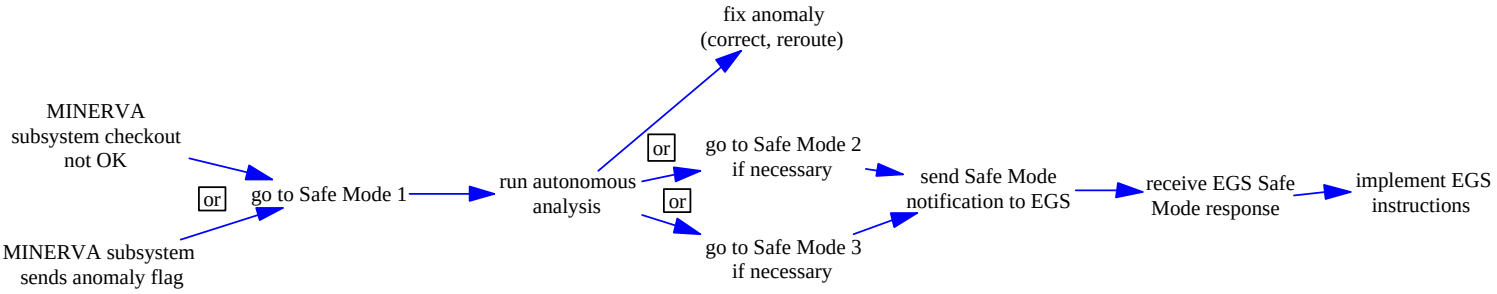

Figure 8.5: MINERVA Anomaly Resolution Stream

9 Disposal

As each MINERVA satellite's on-orbit operations phase is concluded (as it exceeds its design lifetime or is otherwise no longer useful), that satellite enters its final mission phase, and has the capability to be boosted into a disposal orbit with an altitude of 2150 km.

10 Payload

10.1 Communication System Design[24]

10.1.1 Overview

The communication system consists of the hardware and software that allows the exchange of data between different MSEs, or between MSEs and the Earth. Enabling a user on Mars to communicate through MINERVA reduces the amount of hardware that it has to carry on board. Data exchange consists of commands sent to MINERVA or to MSEs, scientific data sent back to Earth, or navigation signals sent to MSEs.

To provide communication on the other side of Mars, when the MSE and the satellite covering it are hidden from the Earth, it has been decided to implement cross-links between the satellites. Satellite cross-links also increase the fault tolerance of the system. For example, if a satellite loses its Earth communication link, it can still communicate with Earth through another satellite's communication system using the cross-link capability (see Figure 10.1).

The presence of cross-links allows communication to Earth to be split between two satellites, which reduces the effective data rate per satellite.

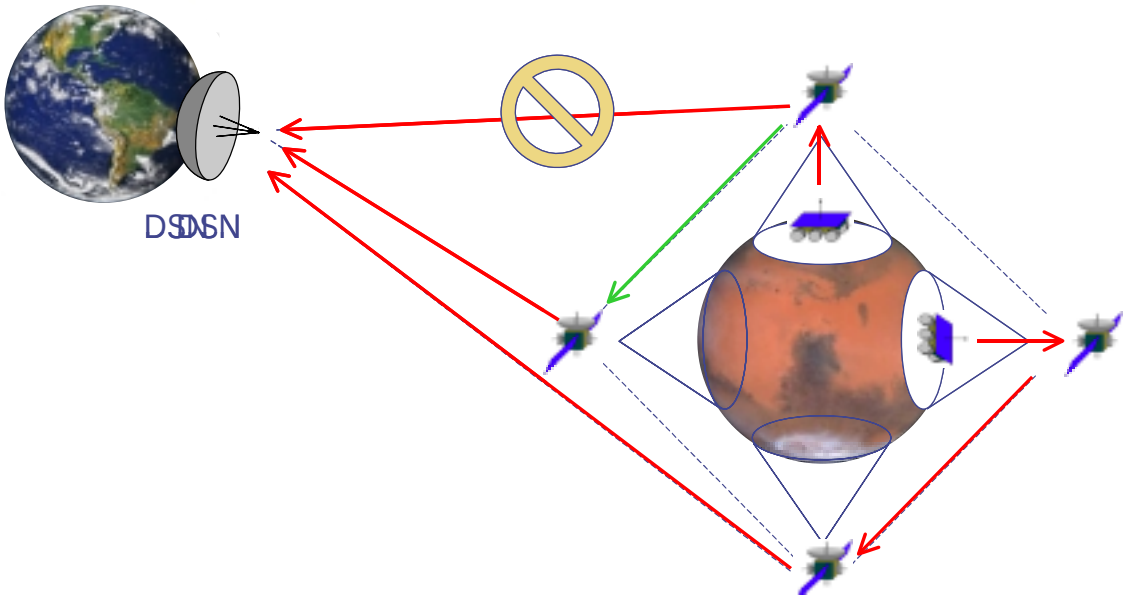

Figure 10.1: Use of a Cross-link Antenna in Case of Loss of the High Gain Antenna

[24] SN, AO

On Earth, the Deep Space Network, which is used for most deep space missions and Mars missions, will be used to provide communication with MINERVA.

The communication system has been divided into different subsystems for each of the types of links described in Figure 10.2.

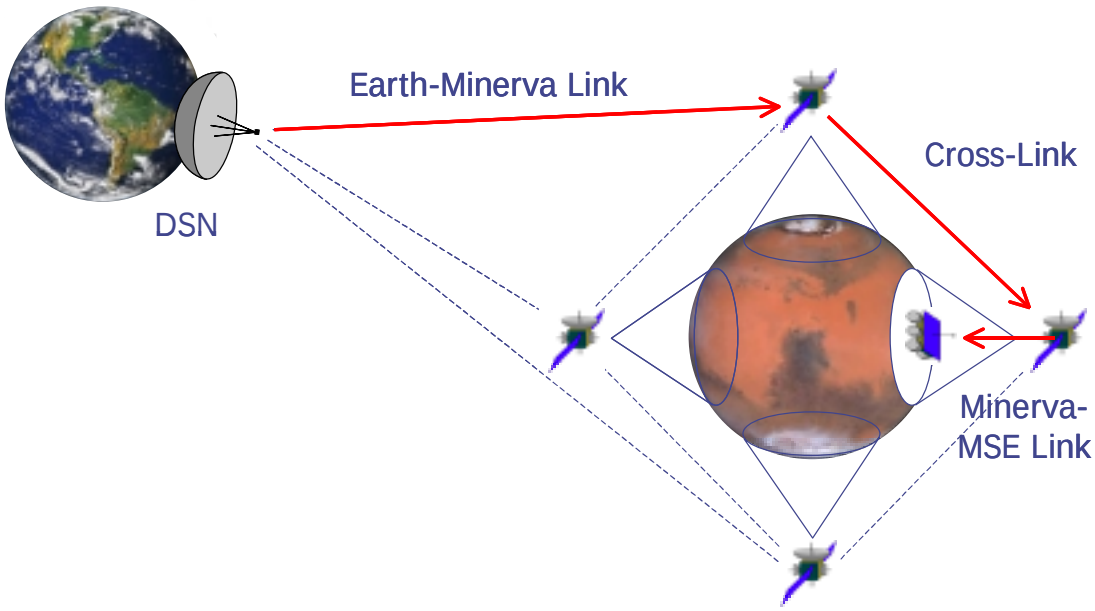

Figure 10.2: The Three Different Types of Links

All the communication links have been designed using a margin of at least 3 dB, to compensate for the fact that a user might be located at the edge of half-power beamwidth of the satellite's antenna beam[25]. The communication links have been designed using the longest path length possible for each link.

To reduce the hardware required onboard the satellites, it has been decided to use the same hardware for communication and for position determination. In fact, as explained in section 10.2, the principle of the position determination system is to send a signal to an MSE and analyze the response.

[25] Beamwidth refers to the half-power beamwidth of the antenna, which is the angle across which the gain is within 3 dB (50%) of the peak gain.

10.1.2 Top-Level Trade Analysis

This section presents the top-level trades that led to the choice of communication system hardware. The goal was to choose a type of antenna for the three communication links (MINERVA-Earth, MINERVA-Mars and cross-links).

The first section summarizes the different possible types of antennas, which were used as the basis for the trade studies. The next sections examine the possibility of integrating as many links as possible.

10.1.2.1 Antenna Types

Horn type antennas were abandoned after preliminary calculations because of their relatively high mass and volume for the same performance as a helix type antenna (see Table 10.1).

Table 10.1: Performance Comparison Between a Horn and a Helix Type Antenna

Type of Antenna	Helix	Horn
Gain	6.89 dB	6.5 dB
Beamwidth	77°	76.7°
Characteristics used [SMAD 1, 1999]	D = 25 cm C = 79 cm L = 31 cm λ = 75 cm η = 0.70 $\varnothing$base = 60 cm	D = 70 cm C = 2.2 m h = 22 cm λ = 75 cm η = 0.52

Lens antennas with switched-feed array were also abandoned because of their high mass and their limitation in terms of diameter [SMAD 2, 1999].

Images removed due to copyright restrictions.

Figure 10.3: Different Types of Antennas Used in the Trade Analysis: a) Horn, b) Helix, c) Lens, d) Parabola, e) Omni-Directional, f) Phased Array

10.1.2.2 Integrating the Three Link Types

Integrating the three communication links has the advantage of minimizing the number of receiving and transmitting systems. This option was quickly rejected because of some obvious technical difficulty, as explained below:

The simplest solution for communicating in different directions is an omni-directional antenna. However, long distance communication would require excessively high transmission power (Figure 10.4).

The next option is to use a directional antenna with a single main lobe. Such an antenna must be mechanically or electronically steered to allow communication in different directions, as shown in Figure 10.5. It follows that simultaneous communication in different directions is not possible.

The last option is to use another category of directional antennas, such as phased array antennas, which can produce multiple electronically steered beams. In this case, the antenna would have to electronically steer the beams over an angle of at least 180°. Using current technology, this is not feasible. Producing several beams with a parabolic antenna is possible if using off-axis feeds, but is not a viable option either since these beams would still have to be mechanically steered.

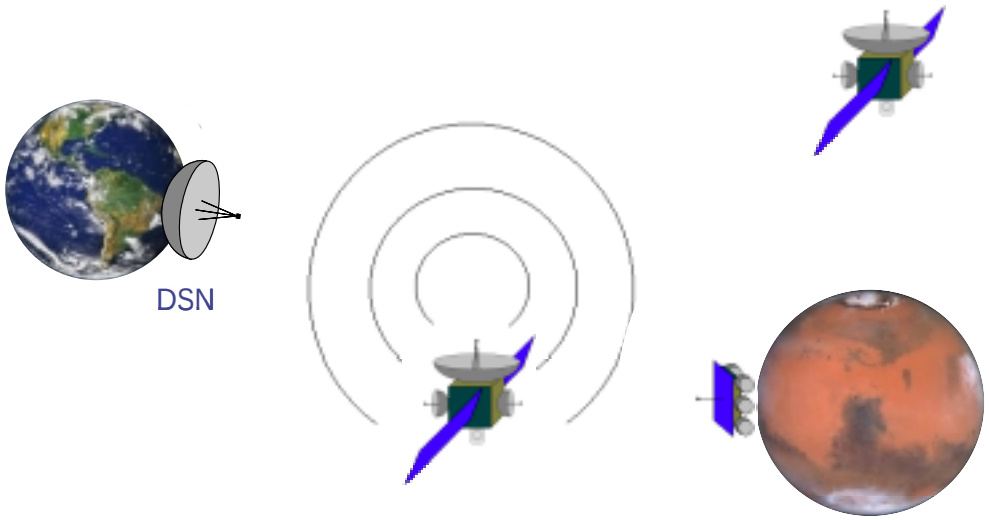

Figure 10.4: Use of an Omni-directional Antenna to Integrate all Three Different Links

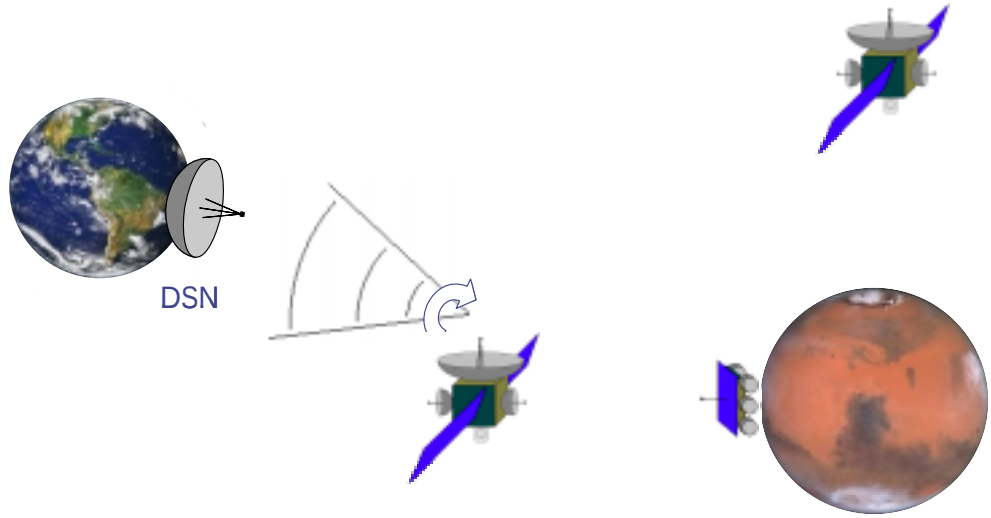

Figure 10.5: Use of a Directional Antenna to Integrate the Three Different Links

In any case, integrating all the links reduces the system reliability, as all the links are dependent on a single antenna. Adding a redundant antenna defeats the purpose of integrating the links in the first place.

10.1.2.3 Integrating Cross-links and MINERVA-MSE Communication

Another option we looked at was to integrate the short-range communication links (MINERVA-MSE link and Cross-Link) and to use a separate system for long-range communication (see Figure 10.6). The frequency for such an integrated link would have to be UHF, for compatibility with MSEs [Edwards, 2000].

The first option is to use a single-beam antenna. In this case, the minimum required beamwidth to enable simultaneous communication between satellites and with MSEs was determined by the orbit group as 101.9°, independently of altitude.

The corresponding gains for parabolic and helix antennas are 4.1 dB and 4.5 dB respectively (see SMAD, Table 13-14). This is too low for cross-links.

The cross-link link budget shows that an Effective Isotropic Radiated Power (EIRP) of 29.2 dBW is required for MINERVA cross-links. The transmitted power for the parabolic and helix antennas is therefore approximately 600W.

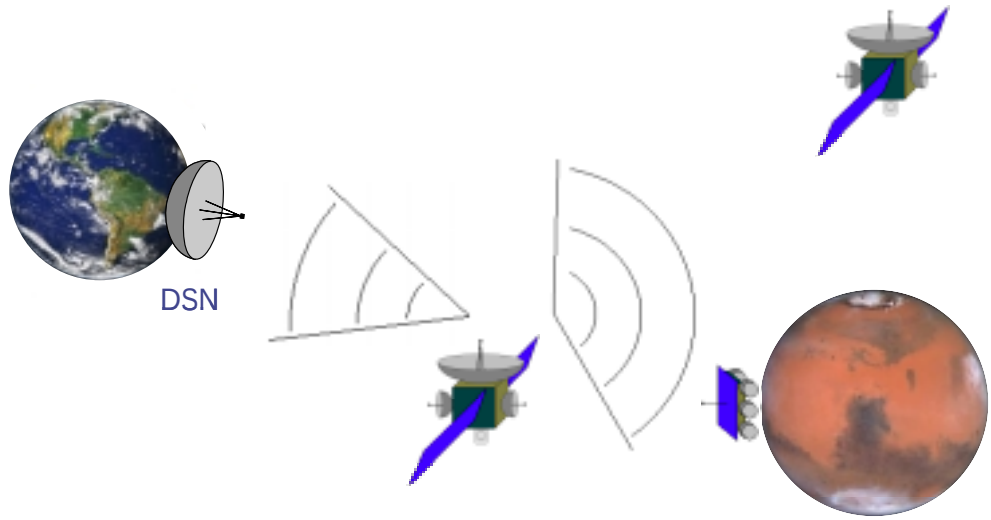

Figure 10.6: Integrating MINERVA-MSE Link and Cross-Link

This power level is unrealistically high for our system, and this option is therefore not feasible.

The second option is to use a phased array antenna. This option is particularly interesting since phased array antennas can form multiple medium-to-high gain beams inside a total beamwidth angle of more than 120° [26]. This technology is more reliable than mechanically steered antennas. Though it has not been used in deep space yet, it has been proven in many Earth missions similar to MINERVA.

However, most of the phased array antennas used in existing systems are X-band, Ka-band or Ku-band. Only a few of them are UHF, and are used as radars by the US Air Force and the Royal Air Force, not as communication systems [Daher, 1998].

For this reason, we put aside the idea of integrating the MINERVA-MSE link with cross-links.

10.1.2.4 Considering Each Type of Link Separately

The option finally chosen was to implement each type of link separately (see Figure 10.7).

---

[26] A Ka-Band phased array antenna is under development at NASA that will be able to scan anywhere within a 60° half angle cone as measured from the antenna boresight, while maintaining all other performance specifications [http://www530.gsfc.nasa.gov/tdrss/kaband.html].

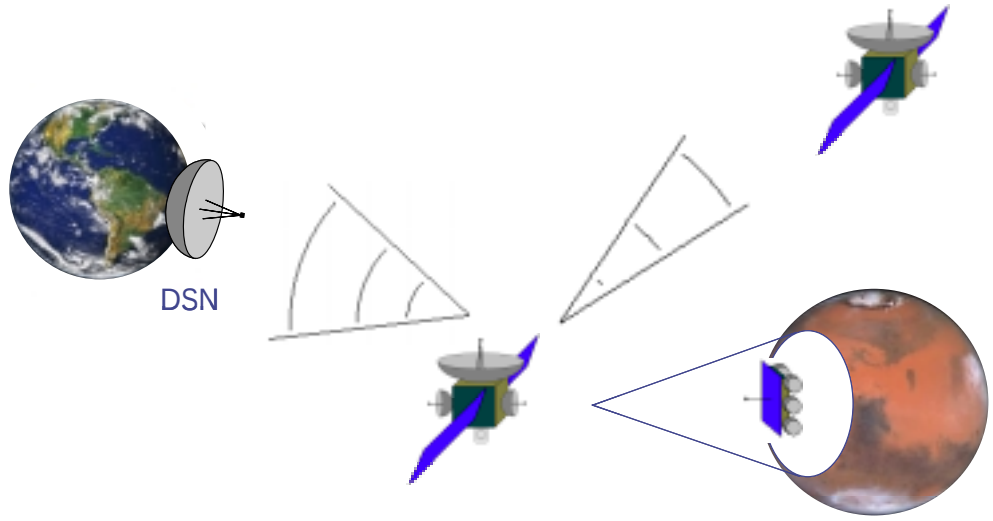

Figure 10.7: Considering each Type of Link Separately

This solution means that one communication subsystem will be used for the Earth-MINERVA link, one for the MINERVA-MSE link and one for the Cross-Links.

10.1.2.5 Modulation and Coding Techniques

This section refers to SMAD Section 13.3.3. Modulation in SMAD is defined as "the process by which an input signal varies the characteristics of a radio frequency carrier (usually a sine wave)". These characteristics are amplitude, phase, frequency and polarization. On the receiver side, demodulation of the signal measures the variations in the characteristics of the received carrier and deduces what the original signal was. For space applications, phase or frequency modulation techniques are preferred because the transmitter can operate at saturation for maximum power efficiency.

The most common modulation techniques used in satellite systems are (see SMAD Figure 13-8):

- Binary Phase Shift Keying (BPSK)

  Set the carrier phase at 0° to transmit a binary 0, and at 180° to transmit a binary 1.

- Quadrature Phase Shift Keying (QPSK)

  Take two bits at a time to define one of the four following binary symbols: 00, 01, 10, 11. Each of those symbols corresponds to one of the four carrier phases: 0°, 90°, 180°, 270°. This results in a better use of the spectrum than BPSK, but is more susceptible to phase disturbances.

- Frequency Shift Keying (FSK)

  Set the carrier frequency at a frequency F1 to transmit a binary 0 and at a frequency F2 to transmit a binary 2. It is not susceptible to phase disturbances. However, it requires a higher E_b/N_o and results in a poor use of the spectrum.

BPSK is the standard deep space telemetry modulation format.

To demodulate a digital bit reliably, the amount of energy received for that bit, E_b, must exceed the noise spectral density, N_o, by a minimum factor.

By reducing the E_b/N_o required to achieve a given BER, the required transmitter power and the antenna size are reduced, or the link margin is increased. A technique to reduce the required E_b/N_o is to insert extra bits, called parity bits, into the data stream at the transmitter. These bits enable the receiver to detect and correct a limited number of bit errors, which might occur in the transmission because of noise or interference. This technique is called forward error correction coding. It is common in deep space missions. For example, the Pioneer deep-space communication link uses this technique to obtain the performance required to overcome the large space loss.

A common type of error correction technique is convolutional coding with Viterbi decoding, which greatly reduces the minimum E_b/N_o to obtain a specific BER. A rate-1/2 convolutional code is implemented by generating and transmitting two bits for each data bit. The data rate is therefore one-half the transmitted bit rate (hence “rate-1/2”). However, recent techniques can achieve significant coding gains without increasing the bandwidth. [Sklar, 1988]

The MINERVA communication system design is based on BPSK R-1/2, K=7 Viterbi Soft DEC modulation that requires an E_b/N_o of 5.1 dB for a BER of 10^{-6} (see Figure 10.8).

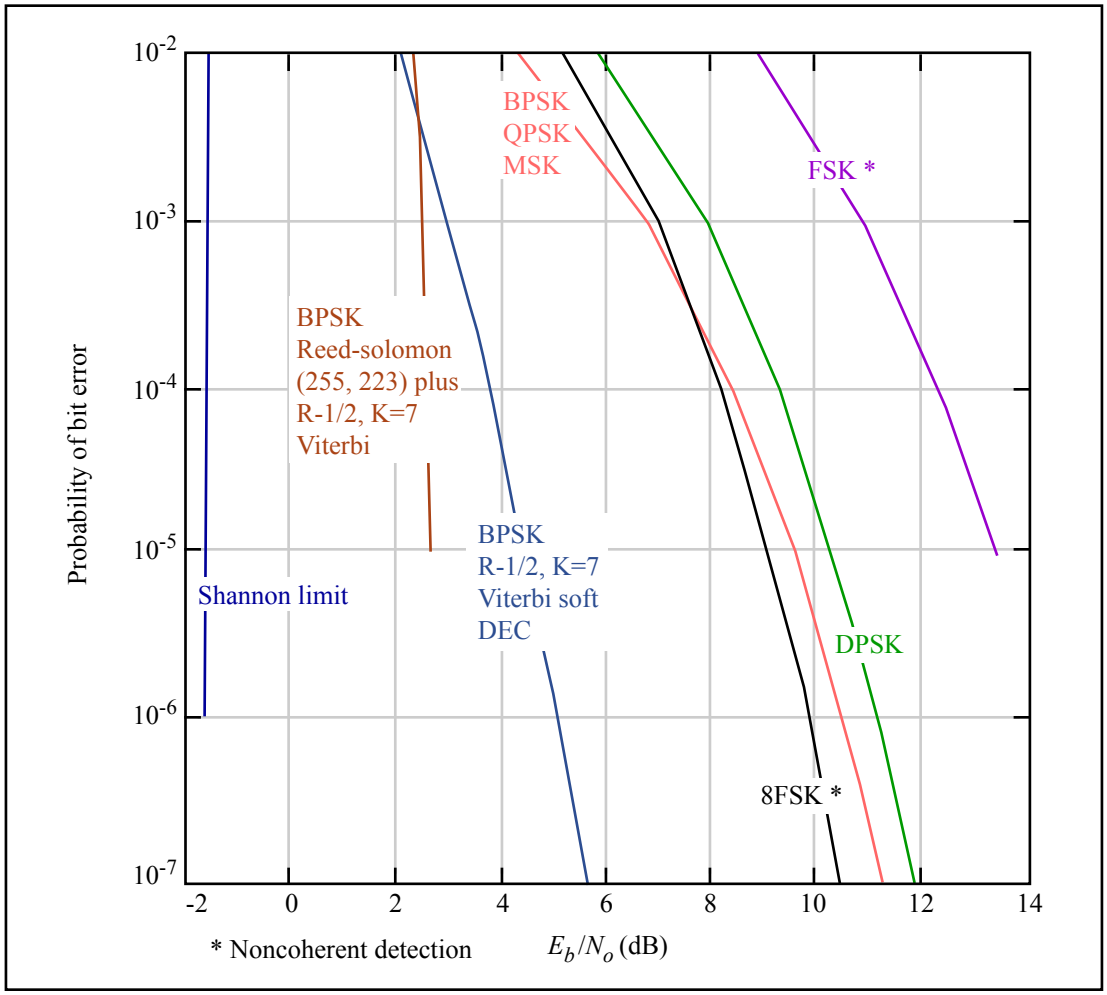

Figure by MIT OpenCourseWare.

Figure 10.8: Bit Error Probability as a Function of Eb/No [Wertz, 1999]

The value of E_b/N_o below which error-free communication cannot take place regardless of the data rate, is known as the Shannon limit and is equal to –1.6 dB. The MINERVA communication system was designed by taking this constraint into account. All the values given in Figure 10.8, including the Shannon limit, are theoretical and based on infinite bandwidth transmission channels and ideal receivers. These values were used as good approximations for communication systems around Mars since there is no bandwidth limitation there. Losses to account for hardware imperfections were included in the link budgets.

10.1.3 Link Design

10.1.3.1 Parameters and Equations

This section contains equations and definitions of parameters that are used for link budget designs in subsequent sections.

10.1.3.1.1 Link Design Equations

The link equation is :

Equation 1: Link Equation

$$\frac{E_b}{N_o} = \frac{PL_l L_s L_a L_{pt} L_{pr} G_t G_r}{kT_s R}$$

where E_b / N_o is the ratio of received energy-per-bit to noise-density, P is the transmitter power, L_l is the transmitter-to-antenna line loss, G_t is the transmit antenna gain, L_s is the space loss, L_a is the transmission path loss, L_{pt} is transmit antenna pointing loss, L_{pr} is receive antenna pointing, G_r is the receive antenna gain, k is Boltzmann's constant, T_s is the system noise temperature, and R is the data rate.

The following is Equation 1 rewritten in decibel form:

Equation 2: Link Equation (dB)

$$\frac{E_b}{N_o} = P + L_l + G_t + L_{pt} + L_{pr} + L_s + L_a + G_r + 228.6 - 10\log T_s - 10\log R$$

The pointing loss equation is given by:

Equation 3: Pointing Loss

$$L_{pt} = -12\left(\frac{e}{\theta}\right)^2$$

where e is the pointing error and θ is the antenna half-power beamwidth.

The space loss is (in decibel form):

Equation 4: Space Loss (dB)

$$\begin{aligned} L_s &= 20\log(3\times10^8) - 20\log(4\pi) - 20\log S - 20\log f \\ &= 147.55 - 20\log S - 20\log f \end{aligned}$$

where S is the path length and f is the carrier frequency.

The carrier-to-noise-density-ratio equation in decibel form is:

Equation 5: Carrier-to-Noise Density Ratio (dB)

$$\frac{C}{N_o} = \frac{E_b}{N_o} + 10\log R = (EIRP) + L_s + L_a + \frac{G_r}{T_s} + 228.6$$

where $(EIRP)$ is the effective isotropic radiated power defined in decibels as follows:

Equation 6: Effective Isotropic Radiated Power (dB)

$$(EIRP) = P + L_l + G_t$$

10.1.3.1.2 Parabolic Antenna Design Equations

The gain for a parabolic antenna is given by (in decibel form):

Equation 7: Parabolic Antenna Gain

$$G = 20\log\pi + 20\log D + 20\log f + 10\log\eta - 20\log c = -159.59 + 20\log D + 20\log f + 10\log\eta$$

where G is the antenna gain, D is the antenna diameter, η is the antenna efficiency and c is the speed of light in vacuum.

The relation between half-power beamwidth, frequency and antenna diameter is:

Equation 8: Parabolic Antenna Half-Power Beamwidth

$$\theta = \frac{21}{f_{GHz} D}$$

10.1.3.1.3 Helix antenna design equations:

The possible range of diameters for a helix antenna is determined by:

Equation 9: Limits on Helix Antenna Diameter

$$0.8 \le \frac{c}{\lambda} \le 1.2$$

where D is the antenna diameter, λ is the wavelength and $c = \pi D$.

The antenna length L is related to the antenna diameter and half-power beamwidth by:

Equation 10: Helix Antenna Length

$$L = \frac{52^2 \lambda^3}{c^2 \theta^2}$$

The gain is then (in decibel form):

Equation 11: Helix Antenna Gain

$$G = 10.3 + 10\log\left(\frac{c^2 L}{\lambda^3}\right)$$

10.1.3.2 Earth-MINERVA Link Design

The main functions of the MINERVA-Earth link include telemetry and data return from Martian missions as well as command and control of Martian missions from Earth, including possible software uploads to Martian craft.

The Deep Space Network (DSN) will be used for communication between MINERVA and the Earth.

10.1.3.2.1 Design Trades

Two of the four satellites will have simultaneous Direct-To-Earth (DTE) links. The total communication bandwidth will be divided between these two links.

The requirement for data return is 10 Gb/sol. This translates into an average data rate of 112 kbps (kilobits per second) over a day. The data rate actually used must take DSN's availability into account:

- MINERVA will be allocated one DSN pass per day. This corresponds to ten continuous hours of communication per day.
- Five minutes are allocated at the beginning of each DSN pass for DSN pointing set-up. An additional minute is allocated for satellite acquisition each time a satellite comes out of eclipse from behind Mars. With three satellites periods during each DSN pass and four satellites, this translates into a total minimum of 17 min per DSN pass without actual data exchange.
- For Mars Global Surveyor (MGS), DSN guarantees that less than 5% of the transmitted data will be lost or corrupted everyday.

Taking all these factors into account, the effective DSN availability is 37%. To transfer 10 Gb/sol, each of the two satellites sustaining a DTE link must therefore transmit at a data rate of 150 kbps.

The Earth-MINERVA link budget was calculated for a maximum distance between Mars and Earth equal to 401,300,000 km. For lower distances, data rates can be increased.

For the design of the MINERVA-Earth link antenna a trade analysis was performed between the following types of antennas. The primary driver for the choice of antenna type is the distance between Mars and the Earth, which ranges from a minimum of approximately 50 million km to a maximum of 400 million km. This link requires a high gain antenna.

Phased array antennas, such as the ones used on LEO satellites to communicate with TDRSS, have an EIRP of approximately 33 dBW as opposed to the 71 dBW MINERVA requires. This type of antenna is more suited to medium to high gain applications with high data rates (over 1 Mbps) than to relatively low data rate deep space missions with power constraints.

Parabolic antennas are therefore the best choice for this link. As the frequency is increased, the antenna diameter for a given gain decreases. Therefore, to minimize the antenna diameter, Ka-band was chosen as the frequency for this link.

Table 10.2 contains numerical values for the link budget design for the MINERVA-Earth link.

10.1.3.2.2 Link Budget

Table 10.2: MINERVA-Earth Link Budget

Item	Symbol	Units	Source	Uplink	Downlink
Frequency	f	GHz	Input	32	32
Transmit					
Power	P	W	Input	3500	130
Power	P	dBW	10 log P	35.44	21.14
Line Loss	L_l	dB	Input	-3.0	-2.5
Beamwidth	θ_t	deg	Input	0.074	0.32
Antenna Efficiency	η_t	-	Input	0.70	0.55
Diameter	D_t	m	Equation 8	34.00	2.05
Peak Gain	G_{pt}	dB	Equation 7	79.6	54.2
Pointing Offset	e_t	deg	Input	0.0100	0.1
Pointing Loss	L_{pt}	dB	Equation 3	-0.22	-1.17
Effective Gain	G_t	dB	$G_{pt} + L_{pt}$	79.4	53.0
EIRP	EIRP	dBW	$P + L_l + G_t$	111.82	71.62
Path Length	S	km	Input	401,300,000	401,300,000
Space Loss	L_s	dB	Equation 4	-294.6	-294.6
Propagation Loss	L_a	dB	SMAD Fig. 13-10	-0.1	-0.1
Rain Loss	L_r	dB	SMAD Fig. 13-10	-8.0	-8.0
Receive					
Diameter	D_r	m	Input	2.05	34.00
Antenna Efficiency	η_r	-	Input	0.55	0.70
Peak Gain	G_{pr}	dB	Equation 7	54.2	79.6
Beamwidth	θ_r	deg	Input	0.32	0.017
Pointing Offset	e_r	deg	Input	0.1	0.0050
Pointing Loss	L_{pr}	dB	Equation 3	-1.17	-1.04
Effective Gain	G_r	dB	$G_{pr} + L_{pr}$	53.0	78.6
System Noise	T_s	K	Input	600	28
Data Rate	R	bps	Input	500	138,000
E_b/N_0	E_b/N_0	dB	Equation 2	35.90	10.19
Carrier-Noise Ratio	C/N_0	dB-Hz	Equation 5	62.89	61.58
Bit Error Rate	BER	-	Input	1.E-09	1.E-06
Modulation Method	-	-	Input	BPSK + R1/2	BPSK + R1/2
Required E_b/N_0	Req E_b/N_0	dB-Hz	SMAD Fig. 13-9	5.1	5.1
Implementation Loss	L_i	dB	Estimate	-2.0	-2.0
Margin	-	dB	E_b/N_0 - Req $E_b/N_0 + L_i$	28.80	3.09

10.1.3.3 MINERVA-Mars Link Design

10.1.3.3.1 Design Trades

The main purpose of the MINERVA-Mars link is to provide communication between MINERVA satellites and MSEs.

The distinctive features of the MINERVA-Mars link are:

- 0.4 GHz uplink
- 0.437 GHz downlink
- High beamwidth to maximize surface coverage area (77° for 2000 km altitude)
- Low gain

The necessity of supporting existing assets on the Martian surface determined the choice of UHF band for the MINERVA-Mars link. In designing this link, it was assumed that MSEs transmit at least 10 W of RF power using an omni-directional antenna (gain 0 dB).

The coverage analysis following from the constellation design determined that each MSE is in view of a satellite 65% of the time. MINERVA must be able to receive a total of at least 10 Gb/sol from the MSEs. Assuming that at least two users equally share the link this corresponds to a minimum data rate of 86 kbps per user.

For the design of the MINERVA-Mars link parabolic, helix, and phased array antennas were considered.

A parabolic antenna with the required gain and beamwidth would have a diameter of approximately 70 cm, which is smaller than the UHF wavelength (75 cm). Since parabolic dishes do not work unless their diameter is several wavelengths, a parabolic antenna is not appropriate for this link.

Helix antennas are well suited for applications with frequencies below 2 GHz and high beamwidth. A phased array antenna with the same beamwidth and gain characteristics would be more costly and complex.

Therefore we selected a non-steerable helix antenna for the MINERVA-Mars link.

Since the antenna beam is conical, two different cases can be distinguished: a user located at the edge of the cone, and a user located right under the satellite in the center of the cone. The MINERVA-Mars link budget was calculated for the worst case (maximum range), which is at the edge of the cone.

10.1.3.3.2 Link Budget

Table 10.3 contains numerical values for the link budget of the MINERVA-Mars link[27].

Table 10.3: MINERVA-Mars Link Budget

Item	Symbol	Units	Source	Uplink	Downlink
Frequency	f	GHz	Input	0.400	0.437
Wavelength	λ	m	c / f	0.750	0.686
Transmit					
Power	P	W	Input	10.000	21.000
Power	P	dBW	10 log P	10.000	13.222
Line Loss	L_l	dB	Input	-2.000	-2.000
Beamwidth	θ_t	deg	Input	180.000	77.000
Antenna Efficiency	η_t	-	Input	0.550	0.700
Antenna Length	L	m	Equation 10	N/A	0.239
Antenna Diameter	D_t	m	Equation 9	N/A	0.250
Antenna Reflector	B	m	0.8λ	N/A	0.549
Peak Gain	G_{pt}	dB	Equation 11	0.000	6.890
Pointing Offset	e_t	deg	Input	0.000	0.000
Pointing Loss	L_{pt}	dB	Equation 3	0.000	0.000
Effective Gain	G_t	dB	$G_{pt} + L_{pt}$	0.000	6.890
EIRP	EIRP	dBW	$P + L_l + G_t$	8.000	18.112
Path Length	S	km	Input	2980.000	2980.000
Space Loss	L_s	dB	Equation 4	-153.976	-154.744
Propagation Loss	L_a	dB	SMAD Fig. 13-10	0.000	0.000
Rain Loss	L_r	dB	SMAD Fig. 13-10	0.000	0.000

[27] The influence of Mars' atmosphere was neglected for the link design.

Item	Symbol	Units	Source	Uplink	Downlink
Receive					
Antenna Length	L	m	Equation 10	0.312	N/A
Antenna Diameter	D_r	m	Equation 9	0.250	N/A
Antenna Reflector	B	m	0.8λ	0.600	N/A
Antenna Efficiency	η_r	-	Input	0.700	0.550
Peak Gain	G_{pr}	dB	Equation 11	6.890	0.000
Beamwidth	θ_r	deg	Input	77.000	180.000
Pointing Offset	e_r	deg	Input	0.000	0.000
Pointing Loss	L_{pr}	dB	Equation 3	0.000	0.000
Effective Gain	G_r	dB	$G_{pr} + L_{pr}$	6.890	0.000
System Noise	T_s	K	Input	600.000	600.000
Data Rate	R	bps	Input	86000.000	172000.000
E_b/N_0	E_b/N_0	dB	Equation 2	12.388	11.832
Carrier-Noise Ratio	C/N_0	dB-Hz	Equation 5	61.733	64.187
Bit Error Rate	BER	-	Input	1.E-06	1.E-06
Modulation Method	-	-	Input	BPSK + R1/2	BPSK + R1/2
Required E_b/N_0	Req E_b/N_0	dB-Hz	SMAD Fig. 13-9	5.100	5.100
Implementation Loss	L_i	dB	Estimate	-2.000	-2.000
Margin	-	dB	E_b/N_0 - Req E_b/N_0 + L_i	5.288	4.732

(Table 10.3: MINERVA-Mars Link Budget, continued)

10.1.3.4 Cross-Link Design

10.1.3.4.1 Design Trades

The advantages of implementing cross-links are:

- Data being transmitted to Earth can be split between two satellites, which reduces the data rate requirements for each DTE link.
- MSEs located on the other side of Mars can still communicate with Earth through MINERVA.
- Different MSEs located beyond line-of-sight of each other can communicate with each other through MINERVA.

X-band was chosen for the cross-links because it provides a larger beamwidth than Ka-band or Ku-band for a given antenna diameter. This reduces the constraints on antenna steering. Furthermore, X-band allows for a smaller antenna size than lower frequency bands such as S-band or C-band.

Communication availability between the MINERVA satellites is required to be at least 90%. The link is designed for the worst-case data rate, when 10 Gb/sol must be transferred between two satellites. This translates into a maximum data rate of 125 kbps for cross-links.

Trade study options for the antenna type included parabolic, helix, and phased array antennas. Helix and phased array antennas can provide a larger beamwidth, which is desirable for cross-links because it minimizes the need for mechanical steering.

However, the choice of antenna type was finally determined by the decision to use the cross-link antenna for communication with the Earth during the transfer phase. The main Earth-link antenna cannot be used during the transfer phase because the insertion burns produce acceleration on the order of ten g's which the antenna boom structure cannot handle.

A parabolic antenna that is designed to give a wide beamwidth at X-band, will have a narrow beamwidth with high gain at Ka-band. This gives good cross-link and transfer link capability in a single antenna, provided the transfer link frequency is chosen to be Ka-band. Both bands will not be used simultaneously. Two feeds are included in the antenna, one for each band[28].

To increase the reliability of the system, two omni-directional antennas are included in each satellite to be used for cross-links in case the attitude control is lost.

10.1.3.4.2 Link Budget

The link budget was calculated for the maximum distance between the satellites orbiting Mars, which is equal to 7633 km at an altitude of 2000 km.

Table 10.4 contains numerical values for the link budget for the MINERVA cross-links at X-band.

Table 10.5 contains numerical values for the link budget for the MINERVA cross-link antennas to be used with Ka-band for the DTE link during Mars approach.

Table 10.6 contains numerical values for the link budget for the MINERVA cross-links using X-band and an omni-directional antenna.

[28] Note that the use of cross-link antenna during Mars approach will be possible only at a distance less than 289,000,000 km.

Table 10.4: MINERVA Cross-Link Budget

Item	Symbol	Units	Source	Uplink	Downlink
Frequency	f	GHz	Input	7.2	7.2
Transmit					
Power	P	W	Input	5	5
Power	P	dBW	10 log P	6.99	6.99
Line Loss	L_l	dB	Input	-3.0	-3.0
Beamwidth	θ_t	deg	Input	5.8	5.8
Antenna Efficiency	η_t	-	Input	0.55	0.55
Diameter	D_t	m	Equation 8	0.5	0.5
Peak Gain	G_{pt}	dB	Equation 7	29.0	29.0
Pointing Offset	e_t	deg	Input	0.1	0.1
Pointing Loss	L_{pt}	dB	Equation 3	0.00	0.00
Effective Gain	G_t	dB	$G_{pt} + L_{pt}$	29.0	29.0
EIRP	EIRP	dBW	$P + L_l + G_t$	32.98	32.98
Path Length	S	km	Input	7,633	7,633
Space Loss	L_s	dB	Equation 4	-187.3	-187.3
Propagation Loss	L_a	dB	SMAD Fig. 13-10	0.0	0.0
Rain Loss	L_r	dB	SMAD Fig. 13-10	0.0	0.0
Receive					
Diameter	D_r	m	Input	0.5	0.5
Antenna Efficiency	η_r	-	Input	0.55	0.55
Peak Gain	G_{pr}	dB	Equation 7	29.0	29.0
Beamwidth	θ_r	deg	Input	5.8	5.8
Pointing Offset	e_r	deg	Input	0.1	0.1
Pointing Loss	L_{pr}	dB	Equation 3	0.00	0.00
Effective Gain	G_r	dB	$G_{pr} + L_{pr}$	29.0	29.0
System Noise	T_s	K	Input	600	600
Data Rate	R	bps	Input	125,379	125,379
E_b/N_0	E_b/N_0	dB	Equation 2	24.55	24.55
Carrier-Noise Ratio	C/N_0	dB-Hz	Equation 3	75.53	75.53
Bit Error Rate	BER	-	Input	1.E-06	1.E-06
Modulation Method	-	-	Input	BPSK + R1/2	BPSK + R1/2
Required E_b/N_0	Req E_b/N_0	dB-Hz	SMAD Fig. 13-9	5.1	5.1
Implementation Loss	L_i	dB	Estimate	-2.0	-2.0
Margin	-	dB	E_b/N_0 - Req E_b/N_0 + L_i	17.45	17.45

Table 10.5: DTE Link Budget Using a Cross-Link Antenna at Ka-Band

Item	Symbol	Units	Source	Uplink	Downlink
Frequency	f	GHz	Input	32	32
Transmit					
Power	P	W	Input	3500	120
Power	P	dBW	10 log P	35.44	20.79
Line Loss	L_l	dB	Input	-3.0	-3.0
Beamwidth	θ_t	deg	Input	0.017	1.30
Antenna Efficiency	η_t	-	Input	0.70	0.55
Diameter	D_t	m	Equation 8	34.00	0.5
Peak Gain	G_{pt}	dB	Equation 7	79.6	42.0
Pointing Offset	e_t	deg	Input	0.01	0.1
Pointing Loss	L_{pt}	dB	Equation 3	-4.15	-0.07
Effective Gain	G_t	dB	$G_{pt} + L_{pt}$	75.4	41.9
EIRP	EIRP	dBW	$P + L_l + G_t$	107.88	59.7
Path Length	S	km	Input	289,000,000	289,000,000
Space Loss	L_s	dB	Equation 4	-291.8	-291.8
Propagation Loss	L_a	dB	SMAD Fig. 13-10	-0.1	-0.1
Rain Loss	L_r	dB	SMAD Fig. 13-10	-8.0	-8.0
Receive					
Diameter	D_r	m	Input	0.5	34.00
Antenna Efficiency	η_t	-	Input	0.55	0.70
Peak Gain	G_{pr}	dB	Equation 7	42.0	79.6
Beamwidth	θ_t	deg	Input	1.3	0.017
Pointing Offset	e_r	deg	Input	0.1	0.01
Pointing Loss	L_{pr}	dB	Equation 3	-0.07	-4.15
Effective Gain	G_r	dB	$G_{pr} + L_{pr}$	41.9	75.4
System Noise	T_s	K	Input	600	600
Data Rate	R	bps	Input	500	500
E_b/N_0	E_b/N_0	dB	Equation 2	23.75	10.07
Carrier-Noise Ratio	C/N_0	dB-Hz	Equation 5	50.74	36.09
Bit Error Rate	BER	-	Input	1.E-06	1.E-06
Modulation Method	-	-	Input	BPSK + R1/2	BPSK + R1/2
Required E_b/N_0	Req E_b/N_0	dB-Hz	SMAD Fig. 13-9	5.1	5.1
Implementation Loss	L_i	dB	Estimate	-2.0	-2.0
Margin	-	dB	E_b/N_0 - Req E_b/N_0 + L_i	16.65	2.97

Table 10.6: MINERVA Cross-Link Budget with an Omni-Directional Antenna

Item	Symbol	Units	Source	Uplink	Downlink
Frequency	f	GHz	Input	7.2	7.2
Transmit					
Power	P	W	Input	5	5
Power	P	dBW	10 log P	6.99	6.99
Line Loss	L_l	dB	Input	-3.0	-3.0
Beamwidth	θ_t	deg	Input	180.000	5.8
Antenna Efficiency	η_t	-	Input	0.55	0.55
Diameter	D_t	m	Equation 9	0.00	0.5
Peak Gain	G_{pt}	dB	Equation 7	0.0	29.0
Pointing Offset	e_t	deg	Input	0.00	0.1
Pointing Loss	L_{pt}	dB	Equation 3	0.00	0.00
Effective Gain	G_t	dB	$G_{pt} + L_{pt}$	0.0	29.0
EIRP	EIRP	dBW	$P + L_l + G_t$	3.99	32.98
Path Length	S	km	Input	7,633	7,633
Space Loss	L_s	dB	Equation 4	-187.3	-187.3
Propagation Loss	L_a	dB	SMAD Fig. 13-10	0.0	0.0
Rain Loss	L_r	dB	SMAD Fig. 13-10	0.0	0.0
Receive					
Diameter	D_r	m	Input	0.5	0.00
Antenna Efficiency	η_t	-	Input	0.55	0.55
Peak Gain	G_{pr}	dB	Equation 7	29.0	0.0
Beamwidth	θ_t	deg	Input	5.8	180.0
Pointing Offset	e_r	deg	Input	0.1	0.0
Pointing Loss	L_{pr}	dB	Equation 3	0.00	0.00
Effective Gain	G_r	dB	$G_{pr} + L_{pr}$	29.0	0.0
System Noise	T_s	K	Input	600	600
Data Rate	R	bps	Input	500	500
E_b/N_0	E_b/N_0	dB	Equation 2	19.55	19.55
Carrier-Noise Ratio	C/N_0	dB-Hz	Equation 5	46.54	46.54
Bit Error Rate	BER	-	Input	1.E-06	1.E-06
Modulation Method	-	-	Input	BPSK + R1/2	BPSK + R1/2
Required E_b/N_0	Req E_b/N_0	dB-Hz	SMAD Fig. 13-9	5.1	5.1
Implementation Loss	L_i	dB	Estimate	-2.0	-2.0
Margin	-	dB	E_b/N_0 - Req E_b/N_0 + L_i	12.45	12.45

Figure 10.9: Communication Scheme shows the overall communication scheme with data rates and availability for each of the links.

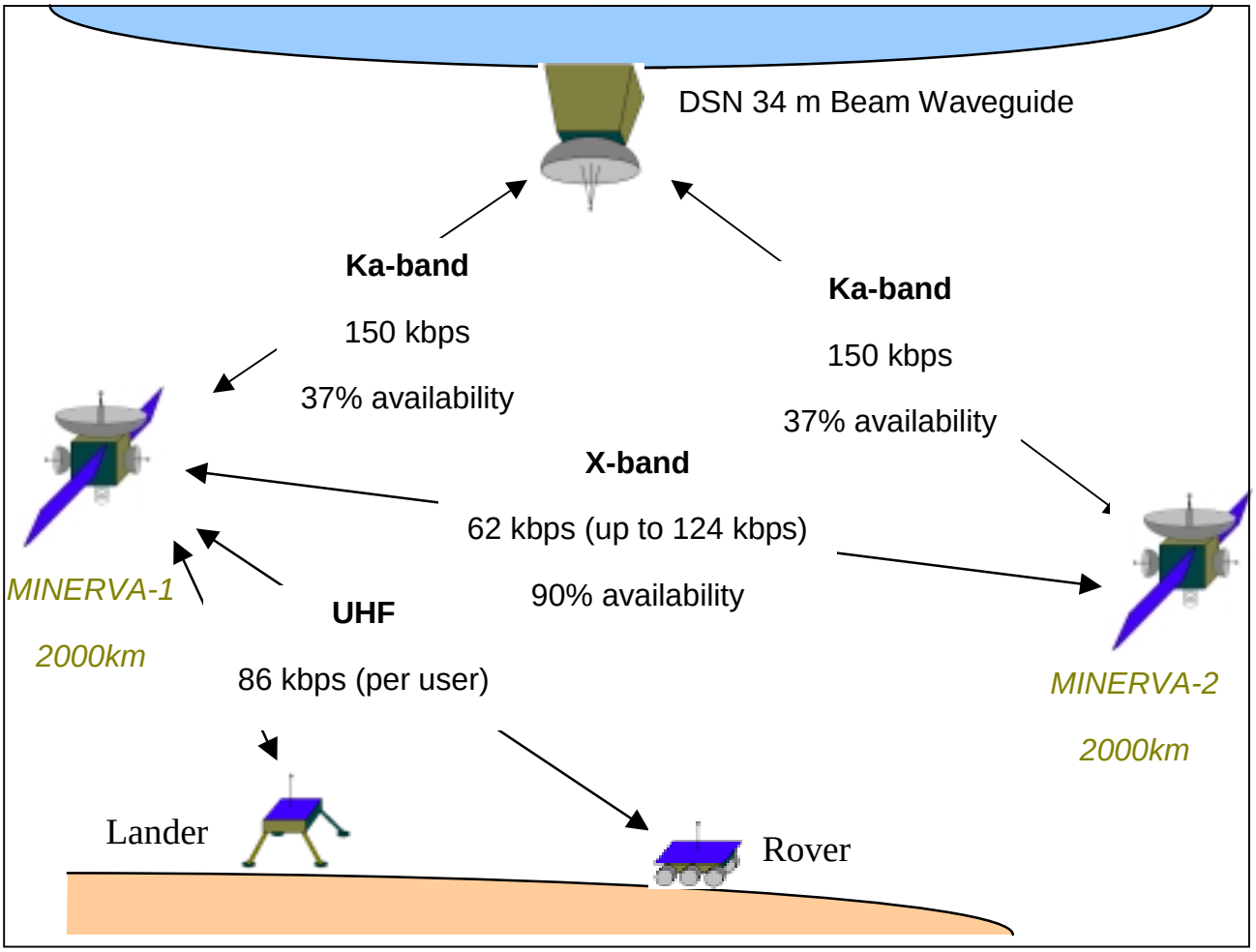

Figure 10.9: Communication Scheme

10.1.4 Communication Procedures

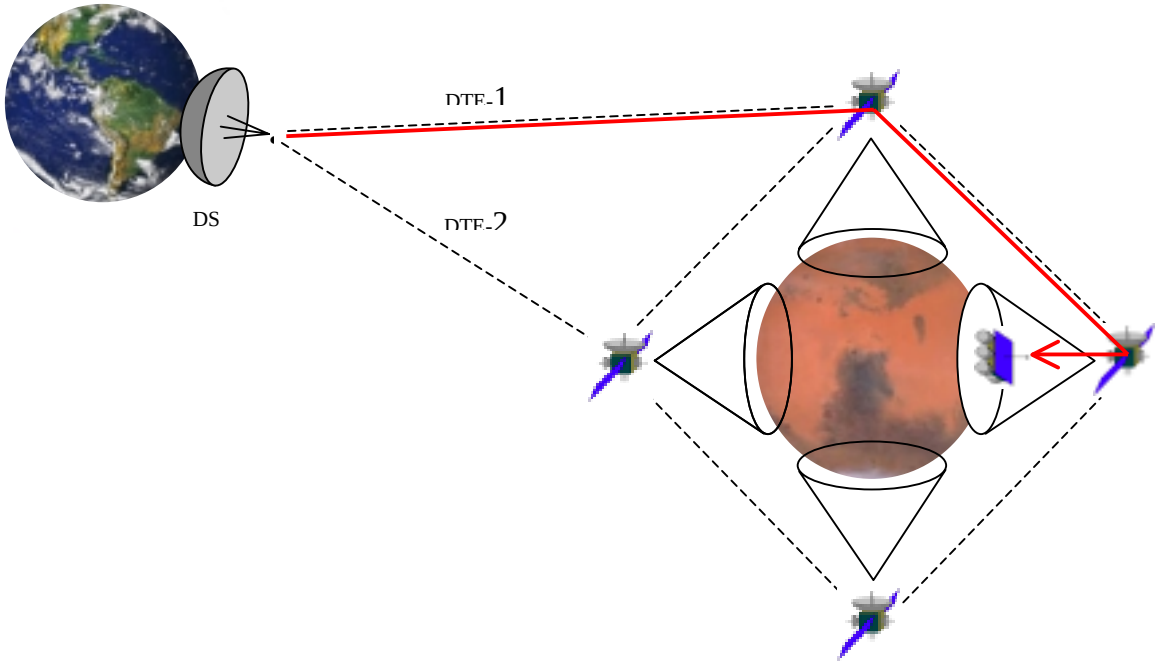

Figure 10.10: Virtual Connection

By default, data routing in the MINERVA constellation will be pre-planned on Earth assuming that the location of each MSE involved in the communication procedures is known. For a detailed description of the Earth-based routing algorithm, see section 8.

Automatic routing was also included in the MINERVA system as an alternative routing solution. This section describes the automatic routing procedure to be performed onboard MINERVA satellites when MSE locations are unknown or when direct data transfer between MSEs is required.

To ensure that data from Earth reaches its destination on the Mars surface and that data from MSEs reaches the Earth, MINERVA will use the principle of virtual connections.

As shown in Figure 10.10, data can follow several possible paths. One of these paths will be established as a virtual connection in accordance with the following procedure:

> When data has to be uploaded to some specific craft on the Martian surface, a packet is first broadcast to all satellites containing information identifying the craft. Then each of the satellites tries to establish a connection with this craft. One of the satellites will be successful. A virtual connection will be established through this satellite and whichever of its closest neighbors that has a link with the Earth, unless the satellite itself has a link with the Earth (see Figure 10.10). The newly established virtual connection becomes the path followed by all signals.

To implement this feature each satellite will have a routing table including entries of the following form:

Next host address	Next router address
…	…

'Next host address' contains all data destinations including MINERVA satellites, MSEs, and Earth ground stations. 'Next router address' corresponds to MINERVA satellites. The meaning of each entry is as follows: data for a 'next host' will be sent to a 'next router', unless the 'next host' is in the subnet of the router that received a packet. A subnet can be as small as a single Martian craft.

As satellites move around Mars, the routing tables are dynamically updated. This means that when the MSE moves out of the coverage area of a particular satellite and the link between them is lost, every satellite tries to establish connection with the MSE again. This time a different satellite will be successful, and the same procedure as before will be used to establish a virtual connection.

The same procedure will apply to data return from an MSE to Earth. In each packet of data sent by an MSE, Earth will be indicated as the destination address. A satellite receiving the packets will forward them in accordance with its routing table to whichever of its closest neighbors has a link with Earth, unless the satellite itself has a link with Earth.

10.1.5 Payload Risk Tolerance

10.1.5.1 Failure Modes Analysis

The MINERVA communication network has been designed to allow for a graceful degradation of performance in case of a failure.

This section summarizes the possible impacts of a failure in the communication system.

10.1.5.1.1 Ka-band Communication Subsystem Failure

The Ka band communication subsystem can fail if the antenna, the steering motor or the two Ka-band transponders fail.

Whatever the number of Ka-band failures in the constellation, the availability and data rate of the MINERVA-Mars link do not change (65%).

However, the Earth-link will be affected as follows:

- If the Ka-band subsystem fails on one out of the four satellites, the availability of the link to Earth does not change (37%). The data return rate (10 Gb/sol at the farthest distance from the Earth) does not change, because three satellites are always in view of the Earth. Therefore, MINERVA can still have two active DTE links by choosing two operational satellites from the three in view.
- If the Ka-band subsystem fails on two out of the four satellites, the availability of the link to Earth does not change (37%) because at least one operational satellite will always be in view of the Earth. The instantaneous data rate with the Earth decreases by a factor of two when both of the failed satellites are in view of the Earth because only the third satellite in view of the Earth can be used. When one or none of the failed satellites are in view of the Earth, the instantaneous data rate does not change. There will therefore be a slight degradation in the total data return only if the two antennas fail on two adjacent satellites.
- If the Ka-band subsystem fails on three out of the four satellites, the availability of the link to Earth is degraded because no link is possible when the only operational satellite is in eclipse behind Mars. The instantaneous data rate to Earth is zero when the operational satellites is in eclipse and is divided by two when it is in view of the Earth. The total data return thus decreases by slightly less than a factor of four.
- If the Ka-band subsystem fails on all four satellites the cross-link antennas can be used to communicate with Earth, at a very low data rate.

10.1.5.1.2 Cross-Link Subsystem Failure

Whatever the number of cross-link failures, the link availability to MSEs remains the same (65%). Only a fraction of the opportunities for near-real time communication with Earth is lost.

If one cross-link fails, the same amount of data can be transferred through the system. The only difference is that there is only one path the data can follow. The performance of the system does not degrade.

If two cross-links fail, the constellation is divided into two parts that cannot communicate with each other directly. The total data return to the Earth decreases if the data collected from the MSEs over one day happens to be unevenly distributed among these two parts of the constellation.

10.1.5.1.3 UHF Subsystem Failure

If a UHF subsystem fails on one satellite, the MINERVA availability to MSEs degrades to 50%, which still meets the minimum requirements. The total data return to the Earth will depend on the data that MINERVA can get from the MSEs with this slightly degraded availability. If enough power is available on the MSEs or if a slight degradation in BER is acceptable, the link data rate will be increased and the total data return will still exceed 10Gb/sol. In the worst case, the data return will be 8 Gb/sol.

As several UHF subsystems fail, the availability and total data return continue degrading similarly, as shown in Table 10.7: Graceful Degradation of Availability

Table 10.7: Graceful Degradation of Availability[29]

Number of satellites with link to Mars	MINERVA-MSE link Availability
4	65%
3	50%
2	35%
1	18%
0	0%

10.1.5.1.4 Amplifier Failure

If a single satellite loses one of its three amplifiers, the total available payload RF output power drops to 110W. This power is sufficient to fully maintain the link with the MSEs and the cross-links, and to communicate with the Earth at a reduced data rate. Because

[29] Acknowledgment SAS

two other satellites will always be in view of the Earth, the total data rate to Earth still exceeds the requirements.

If several satellites lose one of their three amplifiers, the only performance degradation is a reduction in the total data return to the Earth at the farthest Earth-Mars distance.

10.1.5.2 Alternative Earth Ground Station

In case DSN goes down or is available less than ten hours per day, other radio telescopes could be used to communicate with MINERVA.

An example is the Sardinia Radio Telescope (SRT), which is being built in Italy. Tracking NASA/ESA deep space probes is one of its goals. It will be able to receive both at Ka-band and at X-band, but transmit only at X-band.

The main antenna on MINERVA satellites will have an additional X-band feed to use in case such a telescope has to be used. This adds flexibility to the system without adding significant mass or cost, because the transponders used already support both Ka-band and X-band.

Assuming we can use an alternative telescope like SRT, the main effect of losing the DSN link is a reduction in the availability of the Earth-Mars link, and a degradation of the total data return per sol.

Refernced from: http://www.ira.bo.cnr.it/srt

10.2 Position Determination System Design[30]

The top-level position determination requirement is to provide positioning to all MSEs in the ±15° latitude band with an accuracy of 100 m. We break this requirement into two main steps:

1. Determine the MINERVA satellites positions with respect to a Mars-fixed reference frame with an accuracy of at least 100 m. This will hereafter be called *orbit determination*.

2. Determine MSEs positions with respect to MINERVA satellites with an accuracy of at least 100 m. This is the step usually described under the name *position determination*.

The positioning information has no time constraint other than that naturally imposed the MSE velocity. This velocity limits the time to gather measurements for one positioning estimate. It does not limit the time to process this information, which is left to the choice of the MINERVA team.

---

[30] EL, KM

10.2.1 Position Determination Design Trades

This section explains the designs trades that led to the choice of a position determination method.

10.2.1.1 Active versus Passive Position Determination

Position determination may be performed with or without input from the user. The first case is referred to as ‘active position determination’ and the second ‘passive position determination’.

Passive position determination may be performed using the same systems used in target tracking, for example, IR (infrared) and radar systems. The advantage of passive position determination is that it does not require communication with the user. The primary disadvantage of passive systems is the increase in the computational burden.IR detection uses the heat emitted by objects to detect them. Successful detection therefore requires a temperature difference between the object being detected and the ambient. Since dust storms can raise the ambient temperature by 10°C, detection in storms may be difficult. Accurate position determination requires precise attitude control of the satellite, and the strictness of this requirement increases with altitude. Once an IR image has been collected, it has to be processed in order to identify the target. This implies that there will be a high computational requirement per position determination solution.Radar position determination involves bouncing an RF signal off the target and using the time delay from transmission to reception to determine the target range. Unfortunately, the surrounding ground also reflects the radar signal. Unwanted ground return is called ground clutter. If the target is moving, its Doppler frequency may be used to distinguish it from the ground clutter. Stationary targets may be detected using high resolution SAR or similar systems to map the ground and target. Since the entire search area has to be mapped in order to identify the target, this results in a very high computational load per position determination solution.

Since the communication requirement means that there will be a communication link between the satellites and the rovers, and given the above disadvantages of passive systems, we decided to use active position determination.

10.2.1.2 One-way versus Two-way Position Determination

In the presence of a communication link between the satellites and the MSEs, range or Doppler shift measurements provide useful positioning information and are not computationally demanding.

Active positioning methods can use either a one-way or a two-way communication link. Systems that require only a one-way link, like the Global Positioning System (GPS), present the advantage of being available to any number of simultaneous users. On the other hand, measuring a one-way time delay adds the satellite/user clock offset as a new unknown, unless their clocks are perfectly synchronized. Similarly, measuring one-way Doppler shift adds the satellite/user frequency offset as a new unknown, unless they both have precise frequency references. Such an unknown offset is time varying. Solving for it

therefore requires simultaneous redundant measurements, which means increasing the number of satellites.

Since the number of Mars surface elements (MSEs) is limited and since they will all establish a two-way communication link with the MINERVA system, we decided to use a two-way positioning method.

Table 10.8: Characteristics of Different Positioning Methods

Positioning methods	**One-Way Ranging (GPS type)**	**Two-Way Ranging**			**Infra Red**
		Range	**Range & Doppler**	**Doppler**	
Advantages	Clock problems 'GPS receivers'	Limited number of users Users require transponders			Never used Limited by attitude control
Disadvantages	Proven method	Proven method (Transit) No clock problem			No ambiguity 2D at once
2D Solution	Triple coverage	3	1 *(2)*	1 *(2)*	1
3D Solution	Quadruple coverage	2	2 *(3)*	2 *(3)*	2
Altitude	High	High	Medium	Low	Low

The advantages and disadvantages of the different possible positioning methods are summarized in Table 10.8. Numbers in italics indicate the number of satellites necessary to resolve the ambiguity in real time. With inclined orbits, ambiguities can also be resolved by waiting long enough for the planet's rotation to break the symmetry around the satellite ground track.

10.2.1.3 2D versus 3D Position Determination

Determining an MSE position involves solving for three unknown coordinates, which a-priori requires at least three independent measurements. Prior to any measurement, we know that MSEs are located near the Mars surface. Operators of Mars surface missions require their spacecraft's position with respect to a Martian surface grid of reference. This means that only two-dimensional positioning is required, provided the Martian topology can be estimated to the required accuracy.

We decided to capitalize on the data currently being collected by the Mars Orbiter Laser Altimeter (MOLA) on board the Mars Global Surveyor (MGS) spacecraft. This experiment has already determined the Martian topology with an accuracy of 13 m on a 0.25° x 0.25° surface grid [Smith, 1999]. This means that the altitude of the Martian surface is known at points placed every 15 km over the whole planet. The accuracy of an interpolation between these reference points is limited by the surface topology variability. Slopes of up to 4 km elevations over 300 to 1300 km are observed in the transition phase between the smooth Northern hemisphere and the rough Southern hemisphere of Mars [Aharonson, 1998]. This corresponds to 200 m elevation over 15 km.

We decided to perform two-dimensional position determination assuming knowledge of the Martian altitude at any point with an accuracy of 200 m. Knowledge of the Martian topology is still being improved by the MOLA experiment and can be expected to give better estimates by the time the MINERVA mission is operational.

10.2.1.4 Instantaneous versus Long-term Position Determination

Instantaneous two-dimensional positioning requires taking two independent simultaneous measurements. This can be done by measuring both two-way range and two-way Doppler shift between one satellite and the MSE. This is easily done with typical communication hardware [Levanon, 1998], which already exists on the MINERVA satellites to meet the communication requirements. Simply adding a stable frequency reference improves the measurement accuracy.

However, this method leads to ambiguous solutions and singularities that can be resolved only by the use of a second satellite. Continuous double coverage would therefore be required to provide instantaneous position determination with 100 m accuracy.

Since most Mars surface elements are very slow moving, instantaneous positioning is not required. Determining an MSE's position with 100 m accuracy makes sense if the MSE has traveled less than 50 m during the measurement period. The requirement is therefore to gather sufficient positioning information in less than three hours (three hours positioning update rate).

This time period enables the MINERVA system to gather enough positioning information without the need for either double or continuous coverage.

We therefore decided to provide positioning by measuring two-way range and two-way Doppler shift between an MSE and one satellite at a time.

10.2.1.5 Communication Signal versus Positioning Signal

Communication between a MINERVA satellite and an MSE during the time in view is continuous and performed at a relatively high data rate. Positioning measurements on the other hand can be performed at discrete instants during a satellite pass and can use a very low data rate.

In order to simplify the concurrent handling of these two functions, MINERVA allocates a dedicated frequency channel to the positioning message.

Code division multiplexing is used on this channel. A separate spread spectrum code will be allocated to each MSE. This code will enable MINERVA to isolate signals from different MSEs within the same satellite footprint. CDMA provides a convenient method for measuring range, as used by GPS.

Range measurement accuracy is inversely proportional to the frequency used for coding. This frequency must however be at least an order of magnitude smaller than the carrier frequency, namely 400 MHz. MINERVA will use pseudo-random codes at about 4 MHz.

Overlap of satellite footprints can occur in the existing MINERVA constellation and is expected to increase as the mission expands. Therefore, satellites must isolate their positioning signals from those originating from different satellites. This is achieved by assigning each satellite a low frequency code, which is superimposed on the MSE code.

10.2.2 Orbit Determination

This section explains the trades that led to the choice of an orbit determination method and summarizes the orbit determination scheme.

10.2.2.1 Orbit Determination Design Trades

The requirement to provide positioning with 100 m accuracy places an upper bound on the accuracy in the satellite's orbit (namely 100 m).

Two main kinds of orbit determination methods exist:

Earth tracking and processing

The first method is to have Earth ground stations determining the orbits completely, from satellite tracking to orbit reconstruction. This has been the method used by most space missions to date. DSN is designed to perform one-way, two-way and even three-way[31] range and Doppler tracking of deep space satellites. The only requirement on the spacecraft is to have a communication link with the ground station, which will necessarily be the case for MINERVA. This method is relatively easy and has been extensively proven on Mars missions.

However, there is a mathematical upper bound on the accuracy achievable by such a method [Wood, 1986]. Furthermore, in order to reach good accuracy, the satellites must be tracked over a long period of time (typically a whole DSN pass). Additional delay is added by light travel time between the Earth and Mars, and orbit processing

[31] Three-way Doppler corresponds to performing Very Long Baseline Interferometry with two DSN stations at a time.

time. This method is therefore useful for daily orbit reconstruction, but cannot be used to update the satellites' ephemeredes in real time.

On-board Orbital Propagator

If 100-m-accuracy positioning is required in real time, the satellites' positions must be determined in real time with better than 100 m accuracy. For a Mars orbiting spacecraft, this instantaneous accuracy cannot be reached by measurements from the Earth. A solution is to carry a high precision orbital propagator on-board the satellites and take local measurements to continuously update the satellite ephemeredes. Earth could still determine the initial ephemeredes on a daily basis. The local measurements can be of several types:

- Ground Beacon Positioning

Beacons on Mars could play the role of a ground network. Earth could initially determine their location with an accuracy of a few meters by simultaneously tracking the beacons and the satellites over several days [Vijayaraghavan, 1992]. The same method used for positioning of Mars surface elements could then be used to determine the satellites' positions with respect to these Mars references. A fairly intense and homogeneous network of ground stations would be needed to continuously maintain the required accuracy.

- Altimetry

An instrument such as a laser altimeter can be used to accurately measure the distance from a satellite to the Martian surface. The Mars Orbiter Laser Altimeter (MOLA) used on the Mars Global Surveyor (MGS) spacecraft measures altitude with an accuracy of tens of centimeters. Altimeter crossovers also enable the MGS team to determine the satellite's orbit with an accuracy of a few meters. Such a method avoids the complexity associated with landing a network of beacons on Mars. However, the mass of such an instrument (44 kg) exceeds the maximum payload mass on a MINERVA satellite.

- Satellite Relative Positioning

Satellite cross links can be used to measure range and Doppler shift between two satellites. However, the satellite's positions with respect to a Mars-fixed frame cannot be known without reference to a Mars fixed point. This method can therefore be used only to improve the accuracy of orbit determination using ground beacons.

In addition to the disadvantages mentioned above, this second type of orbit determination places a very high computational load on the constellation. Such a level of computational autonomy has never yet been used in space.

We therefore decided to determine the satellites' orbit by DSN tracking and Earth post-processing. 100-m-accuracy position determination will not be available in real time.

10.2.2.2 Orbit Determination Method

10.2.2.3 Satellite Ephemeris

DSN will help determine MINERVA orbits with a similar process to that used for MGS.

Precise orbit determination requires:

- The tracking data recorded over a whole DSN pass (ten hours)

  MGS is tracked by DSN with 0.54 mm/s (3σ) accuracy in the Doppler shift measurement and 13.4 m (3σ) accuracy in the range measurement [MGS_Reqs, 1995]. This performance corresponds to an X-band communication link. MINERVA will use Ka-band to communicate with DSN. Since the wavelength at Ka-band is shorter than at X-band, DSN may be able to reach even better accuracy for MINERVA.

- A high degree and order standard gravity field model

  The gravity field model is itself continuously improved by the MGS orbit determination process. It currently consists of 70×70 gravity coefficients and can be expected to be even better by 2008 [Lemoine, 1999].

- A high precision model for non-conservative forces

  Since the MINERVA orbital altitude is above the Mars atmosphere, the main non-conservative force acting on the satellites will simply be solar radiation pressure. Modeling the radiation pressure effects requires a precise model of the geometry and material properties of the spacecraft, together with a precise satellite attitude determination.

The orbit determination software developed for MGS reconstructs the spacecraft position with a radial accuracy of less than 50 m, and hundreds of meters along-track and cross-track. This accuracy keeps improving as the gravity field model improves [Lemoine, 1999] and much better results can be expected by 2008. Furthermore, the orbit determination accuracy can be improved by capitalizing on concurrent tracking of MINERVA satellites.

We assumed that an orbital accuracy of less than 20 m in radial, along-track, and across-track directions will be achievable by post-processing of the DSN tracking data measured over one DSN pass (ten hours) [Ely, 2000].

10.2.2.4 Satellite Clock Offset

During each DSN pass, clock signals from each MINERVA satellite will be tracked to determine the absolute clock offset in the satellite clock and its first two time derivatives (satellite clock drift and clock drift rate). This information is necessary to place the correct time tag on each positioning measurement taken by MINERVA. The correction can be performed either on Earth or on each satellite. In the latter case, MINERVA simply needs to regularly upload clock offset, clock drift and clock drift rate to MINERVA satellites.

10.2.3 Position Determination Method

This section explains the principles of the MINERVA positioning method. The geometry of the problem is summarized in Figure 10.11.

10.2.3.1 Positioning Method Overview

Each MINERVA satellite is equipped with a UHF communication subsystem to communicate with MSEs as described in section 10.1. For positioning purposes, this subsystem will be linked to an Ultra Stable Oscillator (USO) providing a highly reliable and predictable frequency reference.

Each MINERVA satellite at any instant *t* has a list of MSEs for which it is required to take positioning measurements. The USO provides the carrier for the positioning message at the specific downlink frequency allocated to positioning. For each MSE, the positioning message is encoded with the MSE-specific 4 MHz pseudo-random noise (PSN) code, superimposed on the satellite-specific low chip rate code.

Each MSE is required to isolate and retransmit that part of the positioning message that carries its code. The retransmission process must conserve the phase and multiply the carrier by a specified ratio so that it fits into the positioning uplink frequency channel.

Upon reception, each satellite isolates its part of the message and isolates each MSE's message. Cross-correlating each message with the relevant MSE's code provides the range to that MSE. The Doppler shift of each MSE message is also measured.

Positioning measurements can be taken as often as every five minutes (at least). They are stored in the satellite for up to three days carrying a satellite tag, an MSE tag and a time tag.

If both orbit determination information and MSE positioning measurements are available, MSE positions at the times of measurement can be reconstructed.

10.2.3.2 Two-Way Ranging

The range between two objects is directly proportional to the time it takes a signal to travel between them. This is the principle that radar works on. In two-way ranging the satellite transmits a signal to the MSE on the ground. The transmitted signal carries an

MSE-specific code so that the data from each MSE can be isolated and treated separately. The MSE retransmits this signal back to the satellite, which can use a system similar to GPS code acquisition. The received signal is cross-correlated with a replica of the initial code. If this code is pseudo-random with a period much longer than the transit time, the cross product is negligible unless both signals are exactly in phase. The phase of the replica is adjusted until the amplitude of the cross product reaches a peak value. The phase needed to reach this resonance is the time lag of the received signal.

This time lag is the sum of two terms. The first term is the light roundtrip travel time between the satellite and the MSE, which is what we want to measure; the second is the time it took the MSE to process the signal and send it back. This last term can be predicted and automatically subtracted from the measured time.

The range between the satellite and the MSE is then given by:

$$R = \frac{c \cdot \left(t_{receive} - t_{transmit} - t_{process} \right)}{2} \text{ -}$$

where c is the speed of light[32].

A single range measurement places the user on a sphere centered on the satellite. If the satellite position with respect to Mars is known, the intersection of the sphere with the Mars surface can be determined. This places the user on a small circle.

To estimate user location with ranging only, MINERVA would need at least a second measurement, either from a second satellite or from the same satellite at a later time. This would result in a second small circle and two possible target positions. Otherwise, a third measurement should be taken to resolve the ambiguity.

10.2.3.3 Doppler Ranging

MINERVA satellites measure their Doppler shift with respect to objects on the surface of Mars by determining the frequency offset of the received signal with respect to the signal they transmitted. Two methods can be used to estimate the frequency of the received signal:

1 Take the Fourier transform of the signal, which is very accurate but computationally intensive.

2 Count the number of cycles in a given time period. This was the method used by the *Transit* positioning system [Leondes, 1980].

---

[32] The time difference is actually a measure of the distance travelled by light on a straight line in inertial space, which is different from the instantaneous range because of the satellite movement with respect to the planet. This slight difference is easily accounted for in positioning calculations and was not detailed here for the sake of clarity.

The Doppler shift is related to the angle between the line-of-sight (LOS) from the satellite to the MSE and the LOS relative velocity. If the satellite velocity is known, and the MSE velocity is assumed to be negligible, the angle may be determined:

$$
\begin{aligned}
f_D &= 2\frac{v_{LOS}}{\lambda} \\
&= 2\frac{v_{sat} \cdot \cos(\alpha)}{\lambda} \\
&\therefore \\
\alpha &= \arccos\left(\frac{f_D \cdot \lambda}{2 \cdot v_{sat}}\right)
\end{aligned}
$$

The angle measurement places the user on a cone, with its apex at the satellite and its axis along the satellite velocity. If the satellite position with respect to Mars is known, the intersection of this cone with the Mars surface can be determined. This places the user on a hyperbola.

Capitalizing on the small circle given by the range measurement, there are two possible target positions. If the user position can be estimated from a previous measurement cycle, the correct intersection point may be identified. Otherwise, a third measurement must be taken to resolve the ambiguity.

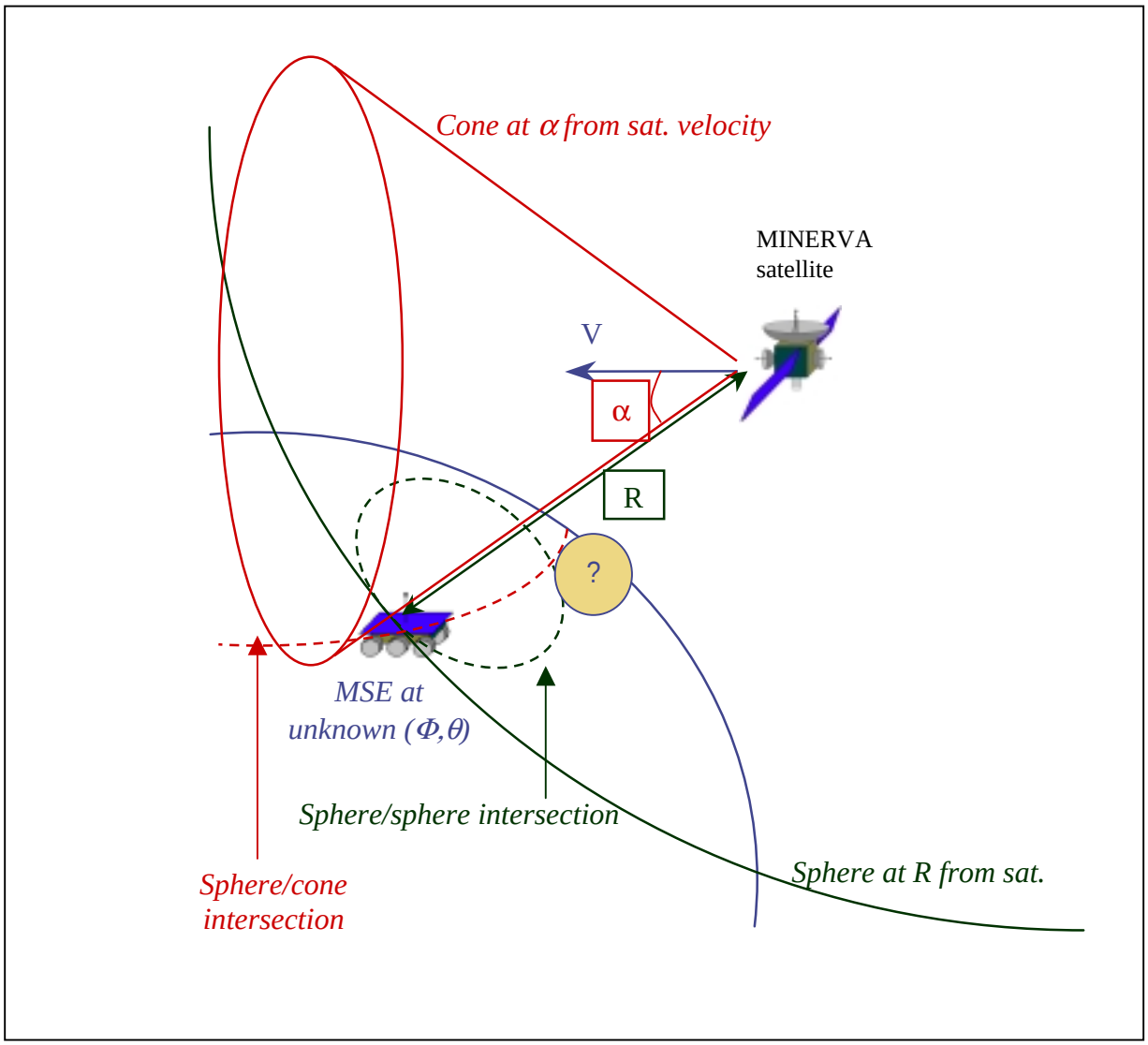

Figure 10.11: Position Determination Method

10.5.2.3 Ambiguity Resolution

Ambiguity in the position determination results from the instantaneous symmetry of the positioning problem with respect to the satellite's orbital plane. At any instant *t*, the planet, the ranging sphere and the Doppler cone are symmetric with respect to this plane and therefore have two symmetric intersection points on either side of the satellite ground track. This ambiguity can be resolved only by taking a new measurement with different symmetry characteristics. MINERVA will use three methods to solve the ambiguity problem:

1 If the MSE's position has been estimated in a previous positioning cycle, and if it is known that this MSE cannot have traveled the distance between the two solution points, we can eliminate one of the two solutions directly.

2 The use of inclined orbits enables MINERVA satellites to break the positioning symmetry as the planet rotates below the orbital plane. This situation is illustrated in Figure 10.12 in the unfavorable case where the planet's movement does not suffice to move the MSE on to the other side of the satellite ground track. Consider a planar planet and let *h* be the distance between the satellite ground track and the MSE. During a time Δt, the planet's rotation makes both the MSE and its symmetrical point travel a distance $l = R_M . \omega_M \Delta t . \cos(latitude)$, which corresponds to 72.1 km displacement on the equator and 69.6 km at 15° latitude. Making the approximation $l \approx 70 km$ at all latitudes, the distance between the new MSE's symmetrical point and the displaced old symmetrical point is:

$$\Delta x = 2(h - h') = 2 \cdot l \sin(i)$$

The ambiguity resolution is thus improved with increasing orbital inclination. For 27°, $\Delta x \approx 63\ km$. As soon as this distance is bigger than the positioning accuracy, the second measurement will suffice to solve the ambiguity.

3 When taking measurements over one entire satellite pass is not sufficient to resolve the ambiguity (MSEs close to the satellite ground track), the symmetry will be broken with the next satellite pass. Using distinct orbital planes improves ambiguity resolution.

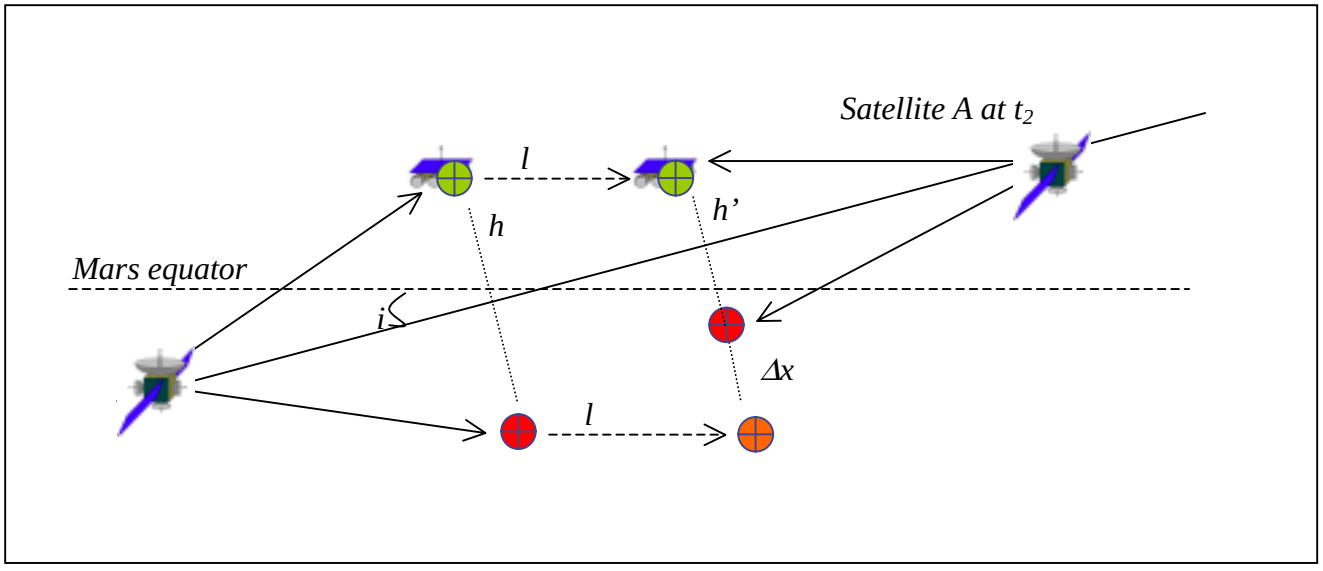

Figure 10.12: Ambiguity Resolutiion

10.2.4 Position Determination Error Estimation

10.2.4.1 Sources of Error

Two kinds of errors limit the accuracy of the positioning function:

1 Random errors, which correspond to noise in the measurements, and cancel out as several measurements are taken.

2 Bias errors, which correspond to uncertain knowledge of one of the parameters and will repeat over several consecutive measurements.

10.2.4.1.1 Random Error Sources

- Two-way range measurement noise:

  Range is measured as the time it takes for signal transmitted by a MINERVA satellite to be received again after having been retransmitted by an MSE. The accuracy in this difference in time is limited by the chip rate used to encode the signal. Since time delay is measured by cross-correlation between transmitted and received signal, the chip period limits the measurement accuracy. Communicating at UHF (400 MHz), MINERVA can use a code bandwidth of $\nu = 4$ MHz. The resulting range accuracy is:

  $$\sigma_R \approx \frac{0.1c}{\nu} \approx 7.5m$$

  Therefore $\sigma_R = 10\ m$ has been used in positioning accuracy calculations.

- Two-way Doppler shift measurement noise:

  Doppler shift is measured by determining the frequency offset of the received signal.

  Whether it is done by taking the Fourier transform of the signal or by counting the number of cycles in a given time period, an Ultra Stable Oscillator (USO) will be used on board each MINERVA satellite to generate the frequency reference for positioning signals. The accuracy will be limited by:

  - Integration time

    Frequency resolution is improved by increasing the time over which the signal is integrated[33]. As an example, Table 10.9 gives the frequency measurement stability as a function of integration time for the USO used on board the Mars Global Surveyor Spacecraft (MGS) [MGS_Reqs].

[33] As the integration time increases, what is actually measured is an average Doppler shift over the time of integration. If the MSE's velocity is neglected and the satellite orbit known, this average Doppler shift can easily be related to the MSE position. The overall positioning scheme remains the same as described.

Typical integration times for positioning application range from 100 ms to 1 minute. A conservative estimate of the measurement accuracy is over such a time: $1.0 \times 10^{-11} f = 4.10^{-3}$ Hz .[34]

Table 10.9: USO Characteristics on MGS Spacecraft

Integration time (seconds)	USO requirement
1	1.0×10^{-12}
10	4.0×10^{-13}
100	4.0×10^{-13}
1000	4.0×10^{-13}

- Satellite oscillator stability

  The Doppler shift is obtained by subtracting the initial frequency. Therefore both methods are limited by the satellite oscillator stability over the integration time. USOs at UHF were used on the *Transit* system with a frequency change over one satellite pass of less than a part in 10^{11} [Leondes, 1980]. A very conservative upper bound on the frequency offset over a light roundtrip time (tens of milliseconds) is therefore $\Delta f < 4.10^{-3}$ Hz.

- Uplink frequency

  The MSE has to retransmit the satellite signal at an accurate predefined uplink frequency. This will be done by using specific components on all MSEs, which directly multiply the incoming frequency by a specific ratio and conserve its phase information [Ely, 2000]. Therefore the error added in the return link is just a ratio of the initial frequency error:

$$\Delta f_u \approx \frac{f_u}{f_d} \Delta f_d$$

  The final Doppler measurement accuracy can be expressed in terms of range-rate accuracy:

[34] This consideration is highly conservative since the actual behaviour of the Doppler shift over the integration time is known and can be modelled into the software. Such a method could yield much better accuracy. ***

$$\sigma_{\dot{R}} = \frac{\Delta f}{\lambda} < 1cm/s$$

10.2.4.1.2 Bias Error Sources

Bias errors are errors in the parameters used to calculate the positioning fix. They repeat over several consecutive measurements. They include:

- Orbit determination errors

  Satellite position and velocity with respect to a Mars-fixed coordinate frame are critical to the estimation process. Their accuracy places an absolute upper bound on the positioning accuracy. As explained in *Orbit Determination* (10.2.2), post-processing of MINERVA orbits should provide an accuracy σ_o = 20 m in all three directions (radial, along-track, across-track). This corresponds to a velocity accuracy of 1 cm/s in all three directions:

$$V_S = \sqrt{\frac{GM_M}{(R_M + h_S)}}$$

$$\therefore \sigma_v \approx \sqrt{\frac{GM_M}{(R_M + h_S)^3}}\sigma_o$$

- Time errors

  Once accurate orbits are determined, knowledge of the satellite's positions at the time of measurement relies on precise time tagging of the measurements. Since the satellites travel at a velocity $V_S \approx 2$ km/s, the time of measurement must be known to less than ten milliseconds to keep the satellite position accuracy below twenty meters. During each daily ten-hour DSN pass, satellite clocks will by synchronized with terrestrial reference atomic clocks. In addition, DSN will measure satellite clock drifts and drift rate (first and second derivative of the satellite clock offset). This information will be stored on board MINERVA and used to keep the time within 10 ms of the absolute time during the daily 14-hour period when the Earth is not available.

- Altitude errors

  Short term positioning by MINERVA assumes the user altitude is known for a given latitude and longitude. As explained in section 10.2.1, the altitude accuracy can be expected to be σ_a = 200 m.

  By taking measurements over several satellites passes, the altitude estimate may be adjusted to the value that provides the best accuracy in latitude and longitude. Therefore altitude error does not limit the achievable positioning accuracy on the long

run. It will however represent an absolute upper bound on the short-term accuracy and be a limiting factor for quickly moving MSEs.

- User velocity errors

  The proposed positioning scheme relies on a Doppler shift measurement, assuming the relative velocity between the satellite and the MSE is known. For slowly moving objects, as most MSEs are, this velocity is simply the satellite's velocity. The positioning analysis is valid for MSEs moving at less than 1 cm/s (assumed Doppler accuracy).

  For moving objects, the accuracy of the Doppler measurement degrades proportionally to the object's velocity. Moreover, in this case MINERVA cannot rely on several measurements to improve its positioning accuracy. MSEs wanting to benefit from the MINERVA system while moving at significantly more than 1 cm/s will have to carry Inertial Measurement Units to estimate the direction and magnitude of their velocity.

- Atmospheric delays

  Two other sources of error encountered by Earth orbiting satellites are atmospheric and ionospheric delays, which cause errors in the range of meters. These errors are respectively proportional to atmospheric and ionospheric densities. Since the density of both the Martian atmosphere and ionosphere are negligible with respect to Earth's densities, we can safely ignore these delays for Mars at the level of accuracy required.

10.2.4.2 Mathematical Framework

The user's position is obtained by iterating from an initial guess using a weighted least squares estimation[35]. The goal is to estimate a vector quantity **x** (containing longitude and latitude) by measuring a second vector quantity **y** (containing range and Doppler at several times) using have a theoretical model $\mathbf{y} = \mathbf{f}(\mathbf{x}) + noise$. From a first estimation $\mathbf{x}_0$, the problem can be linearized to give:

$$\Delta\mathbf{y} = \mathrm{H} \cdot \Delta\mathbf{x}$$

where **H** is the Jacobian matrix for **f** (often called design matrix):

$$\mathrm{H} = \left[\frac{\partial \mathbf{f}}{\partial \mathbf{x}} \right]$$

[35] A Kalman filter type of estimation may be better suited. This does not change the results of the following analysis.

10.2.4.2.1 Error Due to Noise

From a stochastic model of the noise in the measurements, the standard deviation (σ_n) of each measurement is estimated. A weight matrix giving more importance to those measurements with less error is defined. This matrix **W** is diagonal with the n^{th} element being $1/\sigma_n^2$.

If $\Delta\mathbf{y}$ is the difference between $\mathbf{f}(\mathbf{x_0})$ and the measured value of **y**, then the new best estimate of **x** becomes:

$$\Delta\mathbf{y} = \mathbf{x}_0 + \Delta\hat{\mathbf{x}}$$
$$\Delta\hat{\mathbf{x}} = H^{(-)}\Delta\mathbf{y}$$
$$H^{(-)} = (H^T W H)^{-1} H^T W$$

where $\mathbf{H^{(-)}}$ is called the generalized inverse for **H**.

The process is integrated until convergence within available accuracy.

With such an estimation process, the standard deviation for the final components of **x** are given by the diagonal terms in the Dilution Of Precision matrix (DOP), called **Q**:

$$\left\langle \Delta\hat{\mathbf{x}}\,\Delta\hat{\mathbf{x}}^T \right\rangle_{noise} = Q = (H^T W H)^{-1}$$

such that for the i^{th} component of **x**: $\sigma_i^2 = q_{ii}$.

10.2.4.2.2 Error in the Model

Additional errors in the estimation of **x** result from imperfections in the model **y** = **f**(**x**) + *noise*. Let **z** be a vector parameter used in the model (for example, the satellite orbital velocity) and let the **y** = **f**(**x,z**) be the relation between the parameter value and the measurement. An error $\Delta\mathbf{z}$ in **z** will result in a measurement error:

$$\Delta y = \left[\frac{\partial f}{\partial z}\right]\Delta z = L.\Delta z$$

Define $\mathbf{V_{\Delta z}}$ the covariance matrix for the errors in **z.** The covariance matrix for the resulting error in the estimate of **x** is:

$$\left\langle \Delta\hat{\mathbf{x}}\Delta\hat{\mathbf{x}}^T \right\rangle_z = H^{(-)}(LV_{\Delta z}L^T)H^{(-)T}$$

10.2.4.3 Application to MINERVA Accuracy Estimate

The above method was used to estimate the accuracy of two-dimensional positioning with MINERVA. Satellites orbits were simulated over four orbital periods. Positioning accuracy has been estimated at each point on a Martian surface grid within the ±15° latitude band, adding measurements every five minutes over each satellite pass. Specific equations and corresponding MATLAB code are given in Appendix B.

Table 10.10 summarizes the baseline assumptions and the main conclusions of this analysis.

Table 10.10: Positioning Accuracy Analysis Summary

Source of error	Determining factors	Standard deviation	Effect on positioning
Range measurement noise	Code chip rate (4 MHz)	10 m	Pos. error of same order of magnitude, attenuated with time
Doppler shift measurement noise	Integration time (<100 s) Designed for small user velocity (< 1cm/s)	3 mm/s 1 cm/s	Much smaller than other error sources
MSE altitude knowledge	Knowledge of Mars topology	200 m	Pos. error of same order of magnitude, corrected with several satellite passes
MINERVA orbits knowledge	Orbit prediction	100 m – 10 km	Absolute upper bound on positioning accuracy
	Orbit determination	20 m	

Below are the definitions for a few terms used in the rest of this section.

- Positioning accuracy

  In this discussion, measurement accuracy refers to the standard deviation (1σ) of the measurement.

  In one dimension, an accuracy of 1σ is called linear error probable. It means that 68.3% of the data points will be within σ of the actual value.

In two dimensions, as is the case for positioning accuracy, an accuracy of 1σ is called standard ellipse. It means that 39.4% of the data points will be within σ of the actual position, 50% within 1.18σ, 86.5% within 2σ, 98.2% within 3σ.

The accuracy hereafter given assumes 20 m accuracy in MINERVA satellites orbital positions. It therefore corresponds to a potential accuracy, which will be achieved with post-processing.

- Time to accuracy

  The potential accuracy of the position estimate improves over time as more measurements are taken. The time to accuracy at a given location is defined as the time after which the potential accuracy goes below the required value (100 m). For a slowly moving MSE, this accuracy level will then be maintained or improved with each additional measurement.

  The actual time to reconstruct the MSE position differs from the time to accuracy. It includes time to wait for ground station availability and time for orbital determination post-processing.

- Maximum, minimum and average time to accuracy

  The time to reach accuracy at a given point on Mars depends on the planet's angular phase with respect to the MINERVA constellation. The exact same constellation geometry observed by an MSE at a certain time will be observed at a different longitude later on.

  Therefore maximum, minimum and average time to accuracy are defined for any given latitude as maximum, minimum and average time over all longitudes.

- Average accuracy over time

  Similarly, the average accuracy at any given time is the accuracy averaged over all longitudes for a given latitude.

10.2.4.3.1 Positioning Accuracy versus Orbital Parameters

Positioning performance improves as the variety of satellite pass geometries increases. This corresponds to taking measurements from several viewpoints. For a given constellation, the achievable positioning accuracy is a function of MSE latitude. From a positioning viewpoint, the constellation architecture is considered optimal if minimizes the maximum time to accuracy over the ±15° latitude band.

- Orbital altitude

  Accuracy of positioning by range measurement usually increases with increasing orbital altitude because the same range error has relatively less effect if the total range is increased. On the other hand, the accuracy of positioning with Doppler shift measurement improves with decreasing altitude, which corresponds to increasing

orbital velocity. The choice to use both methods concurrently makes the MINERVA system instantaneous positioning performance almost independent of orbital altitude.

The main effect of orbital altitude on positioning is linked to coverage performance: as coverage time over an MSE increases, more measurements can be taken.

- Orbital inclination

A way of achieving satellite pass variety is to increase the orbital inclination. On the other hand, coverage performance over the ±15° latitude band degrades with increasing orbital inclination, meaning that fewer measurements can be taken over a given area. This trade was the main driver for the choice of orbital inclination. 27° was identified as the optimal orbital inclination as illustrated by

Figure 10.13 and Figure 10.14.

This result is due to coverage performance. 27° corresponds to the highest possible inclination for which a satellite can reach both edges of the ±15° latitude band at all times. The maximum revisit time increases dramatically if the inclination exceeds this threshold.

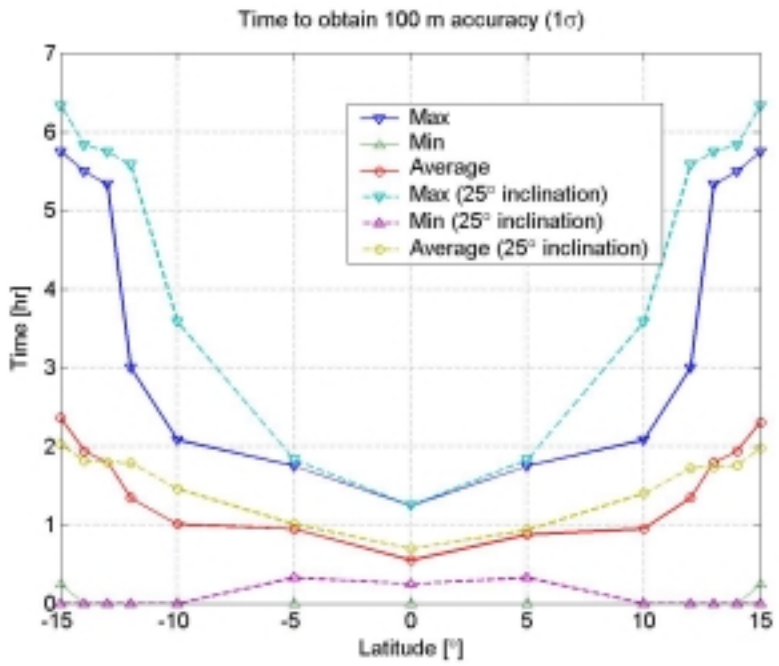

Figure 10.13: Time to Accuracy: 27° Versus 25° Orbital Inclination

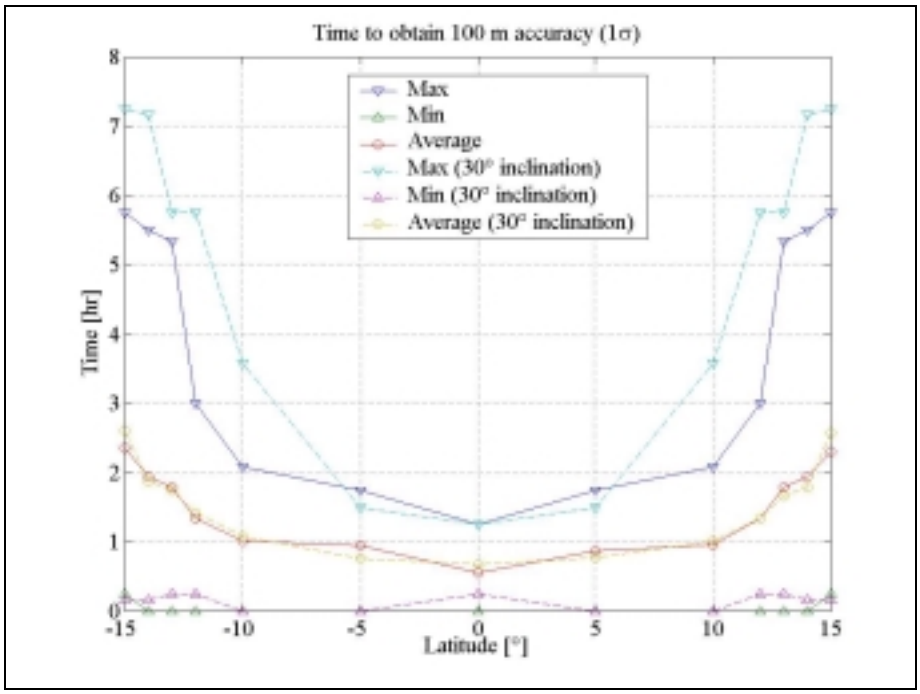

Figure 10.14: Time to Accuracy: 27° Versus 30° Orbital Inclination

- Number of orbital planes

  Using two distinct orbital planes improves the variety of satellite pass geometries and facilitates ambiguity resolution.

10.2.4.3.2 MINERVA Positioning Performance

Figure 10.15 illustrates how accuracy improves over time due to two factors.

1 The error due to measurement noise is to first order inversely proportional to the square root of the number of measurements. This factor actually plays a minor role because measurement errors are negligible compared to errors due to orbital and altitude knowledge errors.

2 The variety of viewpoints improves when more measurements are taken. This effect is very slight over one satellite pass but improves the accuracy significantly each time a new satellite comes into view. The main effect of each new satellite pass is to help correcting the error related to MSE altitude estimate.

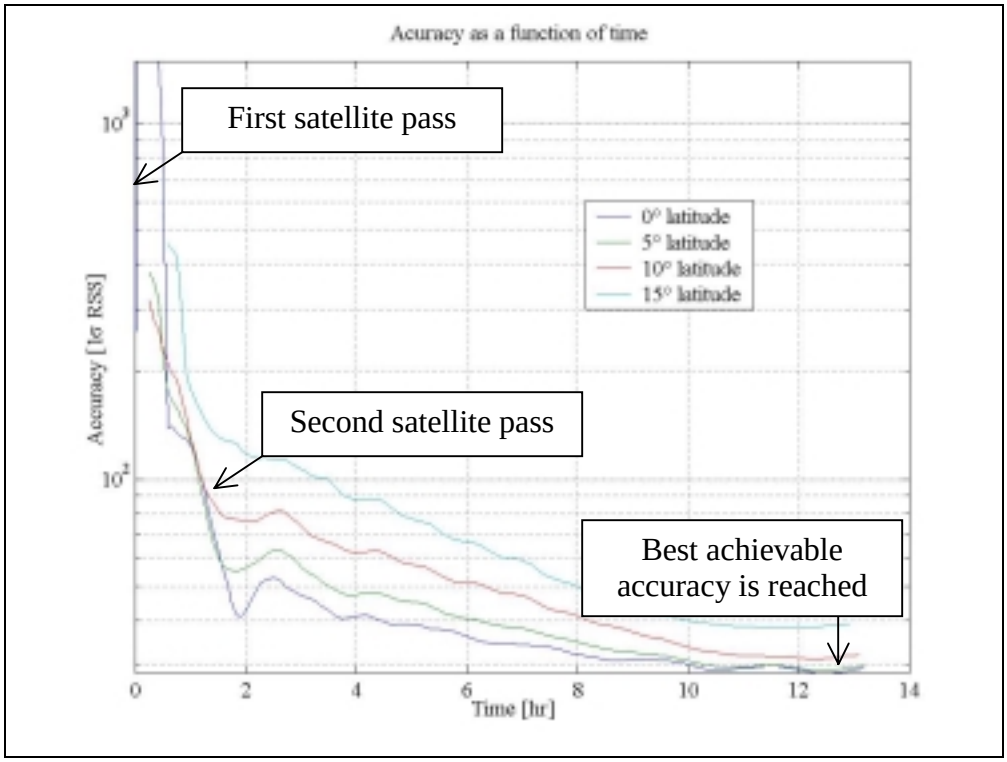

Figure 10.15: Average Accuracy as a Function of Time

The position of an MSE is determined with respect to the MINERVA constellation. This is inherent to satellite positioning. Therefore the accuracy of MINERVA satellites' positions represents the best achievable positioning accuracy. As illustrated by Figure 10.15, the accuracy will not improve beyond an asymptotic value even with an infinite number of measurements.

Positioning performance is a function MSE latitude and is symmetric with respect to the equator. The line of sight between an MSE and a satellite travels over a wider range of directions for MSEs located near the equator. The positioning accuracy thus improves with decreasing MSE latitude. Conversely, the time to reach 100 m accuracy is lowest around the equator.

Figure 10.13 shows that the maximum time to accuracy can be greater than three hours for latitudes above 12°. Figure 10.16 and Figure 10.17 give the probability to reach accuracy within a certain time for the locations of best (0° latitude) and worst (15° latitude) positioning performance. It shows that the probability for an MSE to require more than three hours of measurement data to reach accuracy will always be smaller than 30%. Since the positioning geometry rotates with the planet, this means that 'good geometries' will occur more than 70% of the time at each surface location.

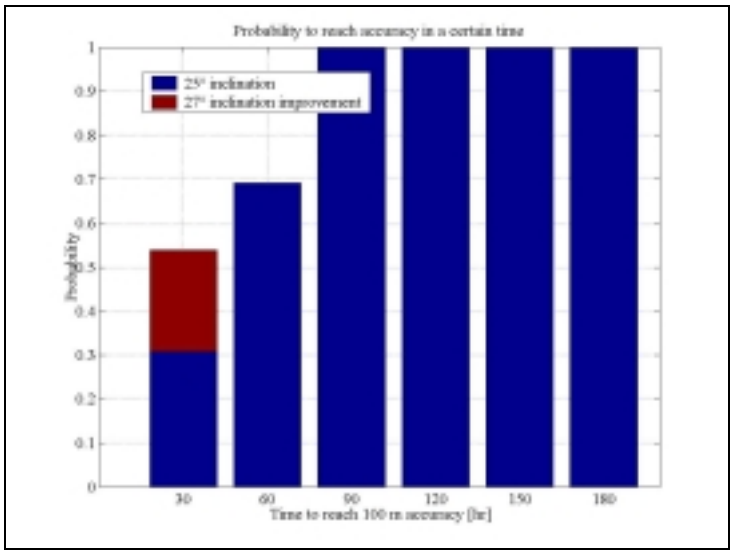

Figure 10.16: Time to Accuracy at 0° Latitude

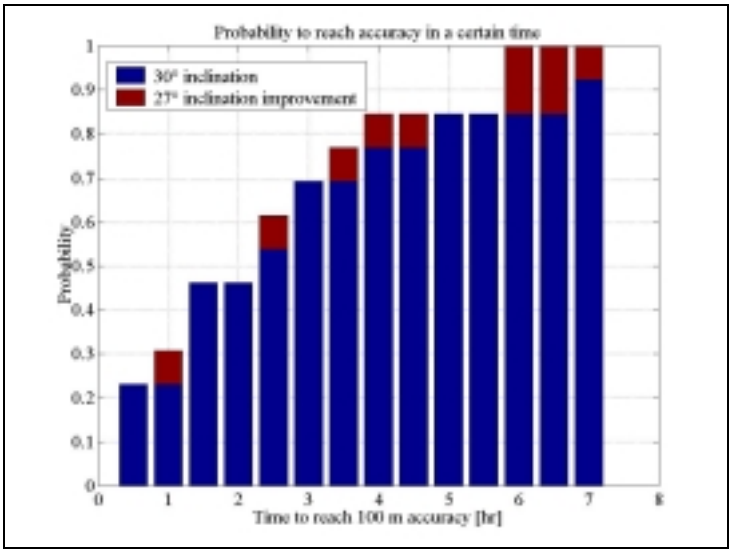

Figure 10.17: Time to Accuracy at 15° Latitude

10.3 Communication and Position Determination Hardware Summary

Table 10.11 summarizes the physical characteristics of all the payload hardware used on each MINERVA satellite. It also lists the assumptions made to estimate payload mass. Existing components were taken as baseline wherever possible. Where necessary, approximations are based on MIT faculty's expertise [Staelin, 2000] and kept conservative.

For a total RF output power of around 165 W, the payload will use three solid-state power amplifiers of 55 W each. These amplifiers will be shared among the three types of links and each will weight around 2.2 kg (see SMAD, Figure 13-15).

Table 10.11: Payload Hardware Mass Summary

Component	Characteristics	Value	Source of Information
Earth-MINERVA link			
Parabolic reflector	Diameter (m)	2.05	
	Effective Area (m2)	4.95	
	Thickness (m)	0.002	
	Mass (kg)	9.9	Density of water
Struts	Mass (kg)	4.95	50% Antenna Mass
Steering device	Mass (kg)	2	Approximation
Electronics	Transponder Mass (kg)	3.1	Motorola Small X-Band and Ka-Band Deep Space Transponders
	Amplifiers Mass (kg)	6.6	3 Motorola Ka-Band Solid State Power Amplifiers
Total Earth-MINERVA System Mass		26.55	

Component	Characteristics	Value	Source of Information
Cross-link			
Parabolic Reflector	Diameter (m)	0.50	
	Effective Area (m2)	0.3	
	Thickness (m)	0.002	
	Mass (kg)	0.59	Density of water
	Total Mass (kg)	1.18	For 2 reflectors
2 Omni-directional	Mass (kg)	0.3	Approximation[36]
Struts	Mass (kg)	0.59	50% Antenna Mass
2 Steering Devices	Mass (kg)	1	Approximation
Electronics	Transponder Mass (kg)	3.1	Motorola Small X-Band and Ka-Band Deep Space Transponders
	Amplifier Mass (kg)	0	Share 3 amplifiers used for Earth link
Total Cross-Link System Mass		5.87	
MINERVA-MSE link			
Helix Antenna	Antenna Diameter (m)	0.25	
	Wire Diameter (m)	0.005	
	Wire Length (m)	3.142	Approximation
	Wire Volume (m3)	0.00006	
	Mass (kg)	0.167	Assuming density of aluminum
Struts	Mass (kg)	0.40	Approximation
Electronics	Transceiver Mass (kg)	2.3	Motorola Multimode S-Band NASA/GN Transceiver
	Amplifier Mass (kg)	0	Share same 3 amplifiers
Total MINERVA -MSE System Mass		2.87	
Ultra-Stable Oscillator	Mass (kg)	0.2	Datum FTS 9700 series
Computer	Mass (kg)	5	Two RAD6000 (<1 kg) + housing
Additional equipment	Mass (kg)	2	Switches, diplexer, etc
TOTAL PAYLOAD MASS		**42.50**	

(Table 10.11: Payload Hardware Mass Summary , continued)

[36] Considered equivalent to 2 antennas of diameter 0.015 m, length 0.3 m, with density of aluminium

10.4 Computer Hardware

The flight computer of a modern spacecraft is a very important component. It controls the spacecraft functions and must therefore be extremely reliable. It must be radiation hardened to survive in the harsh environment of space. In case of failure, it must have a back-up system. It also connects to all the other sensors and actuators on the spacecraft, acting as the central brain.

The following definitions will come in handy in the next sections (for those readers unfamiliar with computer terminology) [AOL, 2000]:

Random Access Memory (RAM)

> In common usage, the term RAM is synonymous with main memory, the memory available to programs. One type of RAM is dynamic random access memory (DRAM). Dynamic RAM needs to be refreshed thousands of times per second. RAM is volatile memory, meaning that it loses its contents when the power is turned off.

Read-Only Memory (ROM)

> Computer memory on which data has been prerecorded. Once data has been written onto a ROM chip, it cannot be removed and can only be read. ROM is non-volatile memory, meaning that it retains its contents even when the computer is turned off.

Electrically Erasable Programmable Read-Only Memory (EEPROM)

> EEPROM is a special type of programmable ROM that can be erased by exposing it to an electrical charge. EEPROM retains its contents even when the power is turned off. EEPROM is similar to flash memory (sometimes called flash EEPROM). The principal difference is that EEPROM requires data to be written or erased one byte at a time whereas flash memory allows data to be written or erased in blocks. This makes flash memory faster.

10.4.1 Main Processor

The RAD 6000 computer was chosen as the flight computer for the MINERVA satellites. It is a radiation hardened IBM Risc 6000 Single Chip CPU. Lockeed-Martin Federal Systems developed this radiation-hardened version of the IBM R6000 [Mars_FAQ, 2000]. It was chosen for its proven reliability on missions such as Mars Pathfinder, Globalstar, and SBIRS Low SMAD. Two identical RAD6000 computers will be flown (two-for-one redundancy), with one acting as a back-up that can handle all of the functions of the primary computer. Table 10.12 shows the characteristics of the RAD 6000.

Table 10.12: RAD 6000 Characteristics

Word Length	32 bits	
Memory	128 MB of DRAM 16 GB of EEPROM	[Wertz, 1999]
Throughput Performance	Up to 20 MIPS	
Radiation Hardness	100 KRad	
Mass	~5 kg for both processors	[Warfield, 2000]
Chip Dimensions	8" x 9" x 2"	
Processing Speeds	20 MHz (22 MIPS) using 9 W 10 MHz (11 MIPS) using 5.5 W	[Mars_FAQ, 2000]

In section 10.5.2, the required memory and throughput for the flight software was estimated to be a maximum of 8 MB and 5 MIPS, respectively. From the table above, it can be seen that the RAD 6000 exceeds the requirements of our software.

The MINERVA system is designed to hold up to three days of data from the MSE in the case of DSN downtime when data cannot be transmitted. The requirement of our system is to transmit 10 Gb/sol. Therefore, we must be able to hold up to 30 Gb of data in memory. Note that this 30 Gb capacity has been divided among the satellites. Since each satellite can hold roughly 15 Gb of data, at least two satellites are required to meet the data holding requirement of 30 Gb. During nominal operations, this memory acts as a holding buffer in which to hold data until a receipt confirmation from Earth is received.

10.4.2 Computer Hardware Fault Tolerance and Reliability

As mentioned in section 10.4.1, two-for-one redundancy will be used for the flight computer. Two identical processors will be available. One will act as the main processor, with the backup processor taking over when necessary.

Error detection and correction (EDAC) circuitry will be included to reduce the chance of failure due to single event upsets (SEU). Watch dog timers will be used to restart the computer when problems occur. Watchdog timers are special circuits that count down from a predetermined time. Anomalous computer operation would prevent the timer from being reset. If the timer is not reset by the computer before the time is up, the computer is reset [Wertz, 1999]. This helps alleviate problems with computer hang-ups. Also, scrubbing programs will be used to correct single bit errors [Wertz, 1999]. The critical flight software will be duplicated in physically isolated sections of the non-volatile

memory. This reduces the chances of the loss of a spacecraft due to software failure [Wertz, 1999].

10.5 Software[37]

Software is an important part of modern space missions. In recent times, the concept of highly autonomous spacecraft has become very popular as a way to decrease mission operations costs. However, autonomy software is complex, expensive to develop, and difficult to test.

This section describes the method used to estimate the size of the flight software. It also describes the trade made between spacecraft autonomy, high software development costs, and mission operations costs.

Three distinct categories of software were identified:

1) **Flight Software**

   This is the software that actually resides on the spacecraft.

2) **Test, Integration, and Simulation Software**

   This includes software that is used to verify the flight software, and any updates to the flight software. It is also used by systems engineers to aid in anomaly resolution during operations. This software resides on the ground.

3) **Operations Software**

   This is the software used by the mission operators to control and monitor the spacecraft. Operations software includes many different software packages, which may be commercial-off-the-shelf (COTS) or developed in-house. Some may be used on-line for real-time operations, and some may be used off-line for analysis or planning. These software packages are used for several different types of jobs, including [Wertz, 1999]:

   Mission & Activity Planning - Aids in management of MINERVA resources, including user resource allocation, scheduling of MINERVA maintenance, and other mission consumables. This software is mostly used off-line.

   Mission Control - Aids mission controllers in real-time monitoring and commanding of spacecraft.

   Navigation and Orbit Control - Determines the position and velocity of the MINERVA satellites; aids in design of trajectories and maneuvers. Due to the

[37] JRR

large distances between Earth and the MINERVA system, this software is used off-line.

Spacecraft Operations - Helps monitor the health and performance of the spacecraft. It also helps to analyze anomalies. This is used off-line.

Data Delivery, Processing, and Archiving - Manages the data flow from MINERVA, including system engineering data from the satellites and MSE user data. This includes delivery of the data to the proper users on Earth, pre-processing of engineering data before it is sent to the system engineers, and archiving of all data.

In the following sections, the size and cost of the MINERVA software will be estimated. The computer requirements of the flight software will also be estimated. The computer requirements will be in the form of memory and throughput requirements. These are defined below [Wertz, 1999]:

Memory - Size of the software in Kilowords or megabytes (MB). The flight computer must have enough memory to hold the flight software.

Throughput – A measure of the processing time required by the flight software. This is measured in units of "thousands of instructions per second (KIPS)" or "millions of instructions per second (MIPS)." One measure of computer performance is the number of MIPS processed.

10.5.1 Flight Software Size Estimation

The MINERVA flight software was planned used the technique of "estimation by similarity" described in SMAD Chapter 16. The idea of this technique is to look at the frequency of execution, memory requirements, and throughput of certain typical spacecraft functions and to estimate the size of similar functions from this data. The number of source lines of code (SLOC) for the flight software are then estimated. From the number of SLOC, a cost is estimated as shown in section 10.5.4.

In order to estimate the flight software, the main functions of the flight computer are first defined. Table 10.13 shows the general functions of a MINERVA satellite.

Table 10.13: Flight Computer Functions

Flight Computer Functions	
1) MSE Position Fixing	5) Routine Housekeeping
2) Communications	6) System Monitoring and Safe Moding
3) Attitude Determination and Control	7) Operating System (O/S)
4) Guidance, Navigation, and Control	

Two trades were studies for the flight software.

The first trade was the programming language. Only C and Ada were considered for our software, as these are the most widely used languages used on deep space and science missions [Fesq, 2000].

The second trade was between different levels of autonomy. The next section describes the three different levels of flight software autonomy that were considered.

10.5.1.1 Flight Software Autonomy

Three levels of autonomy were explored for the flight software:

Table 10.14: Possible Flight Software Autonomy Levels

Autonomy Level	Description
1	Highly Autonomous
2	Partially Autonomous
3	Minimally Autonomous

Note that some autonomy will be necessary due to the large communications latency between Earth and Mars. The capabilities of each computer function are described below for each level of autonomy.

1) MSE Position Fixing

Autonomy Level 1 -- Highly Autonomous Spacecraft

When an MSE has landed, the EGS can send a simple command to MINERVA to “find the new MSE”. MINERVA will then initiate a search. If the MSE is able to respond,

MINERVA will collect the necessary radiometric data and compute the position of the MSE. The MSE will be provided with its location, and the radiometric data and position of the MSE will be sent to the EGS. If the MINERVA system has proven to be reliable, the radiometric data could be sent back to Earth only if MINERVA detects a possible error, or on request.

Once MINERVA has tracked the new MSE, it stores the last calculated position in memory. It then determines when the next possible contact will occur. During each possible contact, MINERVA will search for the MSE, and ask if it needs a position update. It will also be possible for Earth operators to direct MINERVA to search in certain locations on Mars if an error is detected.

Autonomy Level 2 -- Partially Autonomous Spacecraft

MINERVA will not store the positions of the MSEs in memory and will not determine the next possible contact for the MSEs. Instead, each MINERVA satellite will continuously send out a ping message to alert MSEs when a satellite is overhead. This will allow autonomous MSEs to initiate a position fix when the system is available.

When an MSE has landed, the EGS can send a simple command to MINERVA to “find the new MSE”. MINERVA will then initiate a search. If the MSE is able to respond, MINERVA will collect the necessary radiometric data and send it to Earth for processing.

Position fixes will be initiated from the EGS. The EGS will command MINERVA to find a position fix for a given set of MSEs (each MSE will have a predefined, unique identifier). Along with this command, the EGS will send updated MINERVA satellite position information. The EGS may also send estimated positions for the MSEs. On receiving this command, each satellite will search for the given MSEs. When an MSE is found, the position determination process will begin. As soon as enough radiometric data has been recorded, the positions of the MSEs will be calculated on-board the satellites. This position information will be sent to the EGS and the MSE if this is commanded. The radiometric data may also be sent to the EGS if commanded. It will still be possible for Earth operators to direct MINERVA to search in certain locations on Mars if an error is detected. Note that the position fix commands could be uploaded in the form of timetables for each satellite. These tables would tell each satellite when to look for a given MSE and when to provide a position fix.

Autonomy Level 3 -- Minimally Autonomous Spacecraft

When an MSE has landed, the EGS can send a simple command to MINERVA to “find the new MSE”. MINERVA will then initiate a search. If the MSE is able to respond, MINERVA will collect the necessary radiometric data and send it to the EGS for processing.

The EGS will initiate a position fix for an MSE. MINERVA will send the recorded radiometric data back to the EGS. The actual position fixing calculations will be done on Earth. The EGS may send a timetable of when and where each satellite should look for a given MSE.

2) Communications

Autonomy Level 1 -- Highly Autonomous Spacecraft

When the EGS wishes to communicate with an MSE, it will send the message to MINERVA and tell it which MSE it should go to. Since MINERVA will always have a good indication of where the MSE is located, it will then be able to determine which satellite will be the best to send the message. Note that this may require that the message be passed via cross-link to the satellite in view of the MSE.

When an MSE wants to communicate with another MSE or the EGS, it will send a request message to MINERVA. This request message will include the amount of data to be sent and its final destination. Once MINERVA receives the request message, it will collect the message from the MSE and send it to its final destination. If the MSE wants to communicate with another MSE, MINERVA will send a copy of the message to Earth. This may also require the MSE message to be transmitted via cross-link to a satellite in view of the Earth.

For both of these processes, MINERVA will determine the best data rate to use. It will also allocate a given amount of memory for each MSE, depending on the expected data volume.

MINERVA will actively listen for signals from both the EGS and the MSEs. If the EGS wishes to update the MINERVA software or send a command to MINERVA, the message is labeled as a MINERVA message. Each satellite will have a unique identifier, so commands can be sent to a particular satellite if desired. If the desired satellite is not in view of Earth, the receiving satellite will pass the message via cross-link to the correct satellite.

If one of the satellites goes into a safe mode, it will be able to tell Earth about it directly or via cross-link.

Autonomy Level 2 -- Partially Autonomous Spacecraft

When the EGS wishes to communicate with an MSE, it will send the message to MINERVA. It will also tell MINERVA which satellite should send the message, at what time, and to which MSE. For example, if the EGS wishes to communicate with an MSE that is out-of-view of Earth, it must first contact a satellite that is in view. Then, it must tell the satellite in view which satellite to cross-link the message to, and which satellite should send the message to the MSE.

MINERVA will send the message until a receipt confirmation is received, which it will relay to the EGS. If no receipt confirmation is received in a preset amount of time, MINERVA will inform the EGS and await further instructions.

If the EGS does not know where an MSE is located, it will send the message to MINERVA and tell it which MSE it should go to. MINERVA will then initiate a search where each satellite pings for the specified MSE. When one of the satellites finds the

MSE, it alerts the other satellites and sends the message to the MSE. A confirmation message is then sent to Earth. Note that this may require that the message be passed via cross-link to the satellite in view of the MSE.

When an MSE wants to talk to the EGS or another MSE, MINERVA will use the same process of pinging for the final destination. If one of the satellites is already in contact with the EGS, MINERVA will be able to detect this.

For all communications processes, MINERVA must be told what data rate to use, else it will use a default setting.

Autonomy Level 3 -- Minimally Autonomous Spacecraft

Same as Autonomy Level 2.

3) Guidance, Navigation, and Control

Autonomy Level 1 -- Highly Autonomous Spacecraft

Each satellite will be able to find its own position around Mars with an accuracy of at least 100 m. The satellites will work together using radiometric data from DSN and their own cross-links to determine their positions. VLBI on Earth will be used to augment the on-board position fixing. Once an accurate fix is found, an on-board, high precision orbit propagator will allow the satellite to accurately estimate its position until the next precision fix is available.

Autonomy Level 2 -- Partially Autonomous Spacecraft

The position fixing of the satellites will be done on Earth using the DSN. An on-board, low precision orbit propagator will allow the satellites to know their position within 1 km, given an initial starting point as a reference. Earth will provide accurate satellite positioning as uplinked ephemeris data.

Autonomy Level 3 -- Minimally Autonomous Spacecraft

Same as Autonomy Level 2.

4) Attitude Determination and Control

All Autonomy Levels

The attitude of each spacecraft will be controlled autonomously on-board. Each satellite will have a nominal attitude where the UHF antenna points towards Mars, the cross-link antennas point toward the satellites ahead and behind, the Earth-Mars antenna points towards Earth, and the solar arrays are kept in the best attitude for power generation, given the antennae directions.

When a satellite is in safe mode, the attitude will be controlled such that solar arrays are in the best position for power generation. Depending on the nature of the safe mode, either the Earth-Mars antenna will be pointed to Earth, or the cross-link antennas will be pointed to another satellite (for failure of the main Earth-Mars antenna).

5) Routine Housekeeping

All Autonomy Levels

Routine housekeeping will be done autonomously. Spacecraft momentum will be monitored and dumped via momentum wheel de-spins with attitude thruster burns. The spacecraft will also manage on-board power consumption, thermal control, and data recording. This will include reserving a memory margin to guarantee that some memory is available for emergency messages from MSEs or from the MINERVA system itself.

6) System Monitoring and Safe Moding

All Autonomy Levels

MINERVA will be able to monitor its own systems. Major anomalies will be predefined on Earth. When any of these anomalies are detected, the occurrence will be recorded as part of the engineering data and sent to Earth at predetermined times or on request. Also, during the check-out period, MINERVA will record data on the functioning of its components for Earth operators to verify. Data on the nominal functioning of all of the instruments will be saved for a set amount of time before being overwritten. The data on the nominal functioning of the instruments will only be sent to Earth on request or when a safe mode is entered.

MINERVA will be able to recognize potential life threatening anomalies and put itself into the proper safe mode. MINERVA will have a given number of safe modes. Some safe modes will still allow parts of the satellite to interact with the others, while other safe modes may completely take the satellite off-line to await instructions from Earth.

Refer also to section 14.2.

7) Operating System

All Autonomy Levels

The operating system will not be affected greatly by the level of autonomy. However, the size of the operating system will depend on the size of the other computer functions.

Table 10.15 summarizes the assumptions for each autonomy level.

Table 10.15: Flight Software Assumptions

	Autonomy Level 1	Autonomy Level 2	Autonomy Level 3
MSE Position Fixing	Determined autonomously on-board the spacecraft; MINERVA continuously tracks all MSE's	Determined on-board the spacecraft with updated satellite position data; MINERVA does not track MSE's continuously	Position fix calculations are done on Earth.
Communications	All Earth/MSE and MSE/MSE communications automatically routed to the desired final destination	Communications routing is pre-planned on Earth and uplinked to Minerva as time-tagged commands; a simple searching pattern is also available to find the final receiver	
Guidance, Navigation, and Control	Satellites autonomously propagate high precision orbits and determines accurate positions from DSN radiometric data	Satellites propagates a medium accuracy orbit; Earth provides accurate position information for each satellite.	
Attitude Determination and Control	Fully autonomous (includes momentum dumping)		
Routine Housekeeping	Power management, thermal control, and data management is autonomous		
System Monitoring and Safe Moding	System monitors self and warns Earth of anomalies		

10.5.1.2 Flight Computer Functions

Several subfunctions are necessary to complete the primary functions listed in Table 10.13. The subfunctions will depend on what each function is to accomplish and how much autonomy is necessary.

The function models that were used to estimate the size of the flight software are described below for each autonomy level. This includes estimates for the size, throughput, memory, I/O device handlers, and data sources for each function. All of the data in the following tables was taken from SMAD Table 16-13.

Note: In the tables below, “Frequency” can be interpreted as “functions per second”.

10.5.1.2.1 MSE Position Fixing

Table 10.16: MSE Position Fixing Software Requirements for Autonomy Level 1

MSE Position Fixing Subfunction	Frequency (Hz)	Required Memory		Required Throughput (KIPS)
		Code (Kwords)	Data (Kwords)	
On-Board Position Fixing (assumed to be computationally similar to orbit propagation)	1	13	4	20
Error Determination	10	1	0.1	12
Complex Autonomy (MSE tracking)	10	15	10	20
Subtotal	**21**	**29**	**14.1**	**52**

Table 10.17: MSE Position Fixing Software Requirements for Autonomy Level 2

MSE Position Fixing Subfunction	Frequency (Hz)	Required Memory		Required Throughput (KIPS)
		Code (Kwords)	Data (Kwords)	
On-Board Position Fixing (assumed to be computationally similar to orbit propagation)	1	13	4	20
Error Determination	10	1	0.1	12
Simple Autonomy (initiated by external user)	1	2	1	1
Subtotal	**12**	**16**	**5.1**	**33**

Table 10.18: MSE Position Fixing Software Requirements for Autonomy Level 3

MSE Position Fixing Subfunction	Frequency (Hz)	Required Memory		Required Throughput (KIPS)
		Code (Kwords)	Data (Kwords)	
On-Board Position Fixing (done on Earth, assume similar to simple autonomy)	1	2	1	1
Error Determination	10	1	0.1	12
Simple Autonomy (initiated by external user)	1	2	1	1
Subtotal	**12**	**5**	**2.1**	**14**

Input/Ouput device handlers control data flow between the computer and external hardware (i.e. rate gyros, attitude sensors, etc.). The number of I/O device handlers is estimated below in Table 10.19.

Table 10.19: MSE Position Fixing I/O Device Handlers

MSE Position Fixing I/O Device Handlers	Actual I/O Device Handlers	I/O Device Handlers to be Developed
Data Bus Connection	1	1
Total	**1**	**1**

The number of data words per second is estimated in Table 10.20. The numbers were taken from page 675 of SMAD.

Table 10.20: MSE Position Fixing Data Words per Second

Data Sources	Data Words Handled per Second
Telemetry (4 kbit telemetry stream)	500
Command (control commands)	50
Total	**550**

10.5.1.2.2 Communications

Table 10.21: Communications Software Requirements for Autonomy Level 1

Communications Subfunction	Frequency (Hz)	Required Memory		Required Throughput (KIPS)
		Code (Kwords)	Data (Kwords)	
Command Processing	10	1	4	7
Telemetry Processing	10	1	2.5	3
Network Processing (assume it is 10x command processing)	100	10	40	70
Error Determination	10	1	0.1	12
Complex Autonomy (MINERVA "remembers" the location of each MSE)	10	15	10	20
Subtotal	**140**	**28**	**56.6**	**112**

Table 10.22: Communications Software Requirements for Autonomy Levels 2 and 3

Communications Subfunction	Frequency (Hz)	Required Memory		Required Throughput (KIPS)
		Code (Kwords)	Data (Kwords)	
Command Processing	10	1	4	7
Telemetry Processing	10	1	2.5	3
Network Processing (All network planning is done by Earth; simple search is also available; assume similar to simple autonomy)	1	2	1	1
Error Determination	10	1	0.1	12
Simple Autonomy (MINERVA does a "dumb" search for desired MSE)	1	2	1	1
Subtotal	**32**	**7**	**8.6**	**24**

The number of I/O device handlers is estimated in Table 10.23.

Table 10.23: Communications I/O Device Handlers

Communications I/O Device Handlers	Actual I/O Device Handlers	I/O Device Handlers to be Developed
Earth-Mars Antenna	1	1
Cross-link Antennas	2	1
Satellite-Mars Antenna	1	1
Omni-directional Antenna	2	1
Data Bus Connection	1	1
Total	**7**	**5**

The number of data words per second is estimated in Table 10.24. The numbers were taken from page 675 of SMAD. In this case, it is assumed that the level of autonomy will affect the number of data words handled.

Table 10.24: Communications Data Words per Second for Autonomy Level 1

Data Sources	Data Words Handled per Second
Telemetry (4 kbit telemetry stream)	500
Command (control commands)	50
Complex Network Processing (assume: 10 x Telemetry)	5000
Total	**5550**

Table 10.25: Communications Data Words per Second for Autonomy Levels 2 and 3

Data Sources	Data Words Handled per Second
Telemetry (4 kbit telemetry stream)	500
Command (control commands)	50
Simple Network Processing (assume: 3 x Telemetry)	1500
Total	**2050**

10.5.1.2.3 Guidance, Navigation, and Control

Table 10.26: GN&C Software Requirements for Autonomy Level 1

Guidance, Navigation, and Control Subfunctions	Frequency (Hz)	Required Memory		Required Throughput (KIPS)
		Code (Kwords)	Data (Kwords)	
Inertial Measuring Units	10	0.8	0.5	9
Main Thruster Control	2	0.6	0.4	1.2
Ephemeris Propagation	1	2	0.3	2
Complex Ephemeris	0.5	3.5	2.5	4
Orbit Propagation	1	13	4	20
Error Determination	10	1	0.1	12
Complex Autonomy (uses DSN data to determine position)	10	15	10	20
Subtotal	**34.5**	**35.9**	**17.8**	**68.2**

Table 10.27: GN&C Software Requirements for Autonomy Levels 2 and 3

Guidance, Navigation, And Control Subfunctions	Frequency (Hz)	Required Memory		Required Throughput (KIPS)
		Code (Kwords)	Data (Kwords)	
Inertial Measuring Units	10	0.8	0.5	9
Main Thruster Control	2	0.6	0.4	1.2
Ephemeris Propagation	1	2	0.3	2
Complex Ephemeris	0.5	3.5	2.5	4
Orbit Propagation (low accuracy; assume it is half of what is listed in Table 16-13 SMAD)	1	6.5	2	10
Error Determination	10	1	0.1	12
Simple Autonomy (Accurate satellite position is determined on Earth)	1	2	1	1
Subtotal	**25.5**	**16.4**	**6.8**	**39.2**

The number of I/O device handlers is estimated in Table 10.28.

Table 10.28: Guidance, Navigation, and Control I/O Device Handlers

Guidance, Navigation, and Control I/O Device Handlers	Actual I/O Device Handlers	I/O Device Handlers to be Developed
Inertial Measuring Units	3	1
Main Thruster	1	1
Data Bus Connection	1	1
Total	**5**	**3**

The number of data words per second is estimated in Table 10.29. The numbers were taken from page 675 of SMAD.

Table 10.29: Guidance, Navigation, and Control Data Words per Second

Data Sources	Data Words Handled per Second
IMU (Assume similar to rate gyros)	48
Thruster Control Data (assume: 10 @ 4 Hz)	40
Telemetry (4 kbit telemetry stream)	500
Command (control commands)	50
Total	**638**

10.5.1.2.4 Attitude Determination and Control

Table 10.30: AD&C Software Requirements for All Autonomy Levels

Attitude Determination and Control Subfunctions	Frequency (Hz)	Required Memory		Required Throughput (KIPS)
		Code (Kwords)	Data (Kwords)	
Reaction Control Wheels	2	1	0.3	5
Thruster Control (for momentum dumping)	2	0.6	0.4	1.2
Rate Gyros	10	0.8	0.5	9
Planet Sensor	10	1.5	0.8	12
Sun Sensor	1	0.5	0.1	1
Kinematic Integration (of attitude)	10	2	0.2	15
Kalman Filter	0.01	8	1	80
Error Determination	10	1	0.1	12
Complex Autonomy (momentum management)	10	15	10	20
Subtotal	**55.01**	**30.4**	**13.4**	**155.2**

The number of I/O device handlers is estimated in Table 10.31.

Table 10.31: Attitude Determination and Control I/O Device Handlers

Attitude Determination and Control I/O Device Handlers	Actual I/O Device Handlers	I/O Device Handlers to be Developed
Reaction Control Wheels	3	1
Thrusters	6	1
Rate Gyros	3	1
Planet Sensor	1	1
Sun Sensor	1	1
Data Bus Connection	1	1
Total	**15**	**6**

The number of data words per second is estimated in Table 10.32. The numbers were taken from page 675 of SMAD.

Table 10.32: Attitude Determination and Control Data Words per Second

Data Sources	Data Words Handled per Second
Reaction Control Wheels (assumed similar to rate gyros)	48
Thrusters (assumed similar to rate gyros)	48
Rate Gyros	48
Planet Sensors	160
Sun Sensors	40
Telemetry (4 kbit telemetry stream)	500
Command (control commands)	50
Total	**894**

10.5.1.2.5 Routine Housekeeping

Table 10.33: Housekeeping Software Requirements for All Autonomy Levels

Routine Housekeeping Subfunctions	Frequency (Hz)	Required Memory		Required Throughput (KIPS)
		Code (Kwords)	Data (Kwords)	
Power Management	1	1.2	0.5	5
Thermal Control	0.1	0.8	1.5	3
Data Recorder Management (Assume similar to Simple Autonomy)	1	2	1	1
Simple Autonomy	1	2	1	1
Subtotal	**3.1**	**6**	**4**	**10**

The number of I/O handlers is estimated in Table 10.34.

Table 10.34: Routine Housekeeping I/O Device Handlers

Routine Housekeeping I/O Device Handlers	Actual I/O Device Handlers	I/O Device Handlers to be Developed
Power System Monitors	10	1
Thermal Monitors	10	1
Data Recorder Monitor	1	1
Data Bus Connection	1	1
Total	**22**	**4**

The number of data words per second is estimated in Table 10.34. The numbers were taken from page 675 of SMAD.

Table 10.35: Routine Housekeeping Data Words per Second

Data Sources	Data Words Handled per Second
Power Management (assume: 10 @ 4 Hz)	40
Thermal Control (assume: 10 @ 4 Hz)	40
Data Recorder (assume: 5 @ 4 Hz)	20
Telemetry (4 kbit telemetry stream)	500
Command (control commands)	50
Total	**650**

10.5.1.2.6 System Monitoring and Safe Moding

Table 10.36: System Monitoring and Safe Moding Software Requirements

System Monitoring and Safe Moding Subfunctions	Frequency (Hz)	Required Memory		Required Throughput (KIPS)
		Code (Kwords)	Data (Kwords)	
Command Processing	10	1	4	7
Telemetry Processing	10	1	2.5	3
Fault Detection Monitors	5	4	1	15
Fault Correction	5	2	10	5
Complex Autonomy	10	15	10	20
Subtotal	**40**	**23**	**27.5**	**50**

(for all autonomy levels)

The number of I/O device handlers is estimated in Table 10.37.

Table 10.37: System Monitoring and Safe Moding I/O Device Handlers

System Monitoring and Safe Moding I/O Device Handlers	Actual I/O Device Handlers	I/O Device Handlers to be Developed
Fault Detection Monitors/Connections	10	1
Data Bus Connection	1	1
Total	**11**	**2**

The number of data words per second is estimated in Table 10.38. The numbers were taken from page 675 of SMAD.

Table 10.38: System Monitoring and Safe Moding Data Words per Second

Data Sources	Data Words Handled per Second
Fault Detection Monitors (assume: 10 @ 5 Hz)	50
Telemetry (4 kbit telemetry stream)	500
Command (control commands)	50
Total	**600**

10.5.1.2.7 Operating System

Once requirements for each of the functions are estimated, the size of the operating system (O/S) can be estimated. The estimated total requirements for each function are summarized in Table 10.39.

Table 10.39: Estimated Flight Software Requirements (not including O/S)

Estimated Flight Software Requirements (not including O/S)	Functions Per Second	Required Memory		Required Throughput (KIPS)
		Code (Kwords)	Data (Kwords)	
Autonomy Level 1	293.61	152.3	133.4	447.4
Autonomy Level 2	167.61	98.8	65.4	311.4
Autonomy Level 3	167.61	87.8	62.4	292.4

There are five main functions of the O/S, as shown in Table 10.40:

Table 10.40: Operating System Functions

1) Executive	4) Built-In Test and Diagnostics
2) Run-Time Kernel	5) Math Utilities
3) I/O Device Handlers	

1) Executive

The executive "manages and schedules the application software and other operating-system functions." [Wertz, 1999] The required memory for the executive is taken from SMAD Table 16-15 and is shown in Table 10.42. The required throughput for the executive is related to the number of tasks scheduled per second.

The number of tasks scheduled per second can be estimated by first finding the total number of functions performed per second. It is then assumed that each function has four tasks (see SMAD, p. 657). The frequency of each function can be interpreted as the number of functions per second.

Thus, the total number of functions per second for each function listed in Table 10.40 can be found by summing the frequencies of the subfunction components, and multiplying by four:

$$\frac{\text{Tasks Scheduled}}{\text{Second}} \approx 4 \sum f_i \qquad \text{where } f = \text{frequency of subfunction } i$$

The total number of functions per second for each autonomy level are given in Table 10.39. The number of tasks scheduled per second is given in Table 10.41:

Table 10.41: Number of Tasks Scheduled per Second

Autonomy Level 1	1174.44
Autonomy Level 2	670.44
Autonomy Level 3	670.44

The required throughput for the executive can now be estimated by SMAD:

$$\text{Required Throughput for O/S Executive} \approx 0.3\left(\frac{\text{Tasks Scheduled}}{\text{Second}}\right)$$

The required throughput for the executive is shown Table 10.42.

2) Run-Time Kernel

The run-time kernel "supports higher-order languages." [Wertz, 1999]. For our purposes, the run-time kernel will be purchased as a commercial-off-the-shelf (COTS) item. This means that money will not need to be spent developing the run-time kernel. While this will save some money, it should be noted that the run-time kernel is a very small portion of the overall flight software. The memory requirements for the run-time kernel are taken from Table 16-15 from SMAD and are shown in Table 10.42. The throughput for the run-time kernel is assumed to be included in the throughput estimate for the other software functions [Wertz, 1999].

3) I/O Device Handlers

The I/O handler "controls data movement to and from the processor" [Wertz, 1999]. The device handler (or device driver) "manages interfaces and data between the processor and any peripheral devices" [Wertz, 1999]. These two related functions are estimated together as the I/O device handlers.

The memory requirements of the I/O device handlers can be estimated from the values in Table 16-15 in SMAD. However, it should be noted that these are the memory requirements for each I/O device handler. It is therefore necessary to estimate the total number of I/O device handlers for the system.

It is assumed that portions of the I/O device handler code can be reused in some cases. For example, if there are three rate gyros, then three I/O handlers are necessary. However, each of these I/O handlers is assumed to be identical. This means that three I/O handlers reside on the computer, but only one piece of code needs to be developed. So, we will need to estimate the actual I/O handler code size to make sure the flight computer can hold it, and the actual code size that needs to be developed. This will be referred to as the "software to be developed".

In order to estimate the throughput for the I/O device handlers, the number of data words handled per second for each function must be estimated. This is a measure of the amount of data handled by the I/O device handlers. These numbers are mostly independent of the level of autonomy in the system.

The total number of I/O device handlers and number of data words handled per second were estimated above for each flight computer function. The required throughput for the I/O device handlers is given by SMAD:

$$\text{Required Throughput for I/O Device Handlers} \approx 0.05\left(\frac{\text{Data Words Handled}}{\text{Second}}\right)$$

The required memory and throughput for the I/O device handlers are shown in Table 10.42.

4) Built-In Test and Diagnostics

Built-in test software "provides testing for computer elements under the control of software" [Wertz, 1999]. Diagnostic software identifies and isolates faults and failures. The memory and throughput requirements are taken from SMAD Table 16-15 and are shown in Table 10.42.

5) Math Utilities

Math utilities are mathematical operations provided by the operating system that can be accessed by several applications. The memory for the math utilities are taken from SMAD Table 16-15 and are shown in Table 10.42.

Table 10.42: Operating System Requirements for Autonomy Level 1

Operating System Subfunction	Actual Required Memory		Software to be Developed		Required Throughput (KIPS)
	Code (Kwords)	Data (Kwords)	Code (Kwords)	Data (Kwords)	
Executive	3.5	2	3.5	2	352.3
Run-Time Kernel (COTS)	8	4	0	0	Included in functions that use the feature
I/O Device Handlers	122	42.7	42	14.7	444.1
Built-In Test and Diagnostics	0.7	0.4	0.7	0.4	0.5
Math Utilities	1.2	0.2	1.2	0.2	Included in estimate of application throughput
Subtotal	**135.4**	**49.3**	**47.4**	**17.3**	**796.9**

Table 10.43: Operating System Requirements for Autonomy Levels 2 and 3

Operating System Subfunction	Actual Required Memory		Software to be Developed		Required Throughput (KIPS)
	Code (Kwords)	Data (Kwords)	Code (Kwords)	Data (Kwords)	
Executive	3.5	2	3.5	2	201.1
Run-Time Kernel (COTS)	8	4	0	0	Included in functions that use the feature
I/O Device Handlers	122	42.7	42	14.7	269.1
Built-In Test and Diagnostics	0.7	0.4	0.7	0.4	0.5
Math Utilities	1.2	0.2	1.2	0.2	Included in estimate of application throughput
Subtotal	**135.4**	**49.3**	**47.4**	**17.3**	**470.7**

The different O/S sizes for each autonomy level from above are shown in Table 10.43. Note that the actual code size and the development code size are both shown.

10.5.1.3 Flight Software Size

The estimated total requirements for each autonomy level are summarized in Table 10.44.

Table 10.44: Flight Software Requirements for Each Autonomy Level

Estimated Flight Software Requirements (including O/S)	Actual Required Memory		Software to be Developed		Required Throughput (KIPS)
	Code (Kwords)	Data (Kwords)	Code (Kwords)	Data (Kwords)	
Autonomy Level 1	287.7	182.7	199.7	150.7	1244.3
Autonomy Level 2	234.2	114.7	146.2	82.7	782.1
Autonomy Level 3	223.2	111.7	135.2	79.7	763.1

Once we have the memory estimates, we can estimate the number of source lines of code (SLOC). The SLOC will depend on the programming language used. For costing purposes, the data words are converted to equivalent code words by using a factor of 0.25. This assumes that data word development takes one quarter of the effort of code word development [Wertz, 1999].

$$\text{Equivalent Code Words} = \text{Code Words} + 0.25\,(\text{Data Words})$$

Dividing the equivalent code words by the number of assembly instructions per SLOC gives the SLOC estimate [Wertz, 1999].

$$\text{SLOC} \approx \frac{\text{Equivalent Code Words}}{\text{Assembly Instructions per SLOC}}$$

The number of assembly instructions per SLOC depends on the programming language used.

Once the SLOC is found, it can be converted into bytes. This conversion factor also depends on the programming language. This formula will be used in the next section to calculate the flight software computer requirements.

$$\text{Bytes of Software} \approx \text{SLOC}\left(\frac{\text{Bytes}}{\text{SLOC}}\right)$$

Table 10.45 shows these factors for Ada and C [Wertz, 1999].

Table 10.45: Software Factors for Programming Languages

Programming Language	Assembly Instructions per SLOC (Words/SLOC)	Bytes per SLOC for a 32-bit Processor
Ada	5	30
C	7	42

Table 10.46 and Figure 10.18 show the actual and development SLOC for each autonomy scenario using Ada and C.

Table 10.46: Flight Software SLOC for Each Autonomy Level

Flight Software Size (kSLOC)	Actual Code (kSLOC)		Code to be Developed (kSLOC)	
	Ada	C	Ada	C
Autonomy Level 1	66.7	47.6	47.5	33.9
Autonomy Level 2	52.6	37.6	33.4	23.8
Autonomy Level 3	50.2	35.9	31.1	22.2

Table 10.47 shows the memory required to hold this amount of SLOC. Note that the memory required is independent of the programming language.

Table 10.47: Memory Required to Hold Estimated Flight Software

Flight Software SLOC	Actual Memory (MB)	
	Ada	C
Autonomy Level 1	2.0	2.0
Autonomy Level 2	1.6	1.6
Autonomy Level 3	1.5	1.5

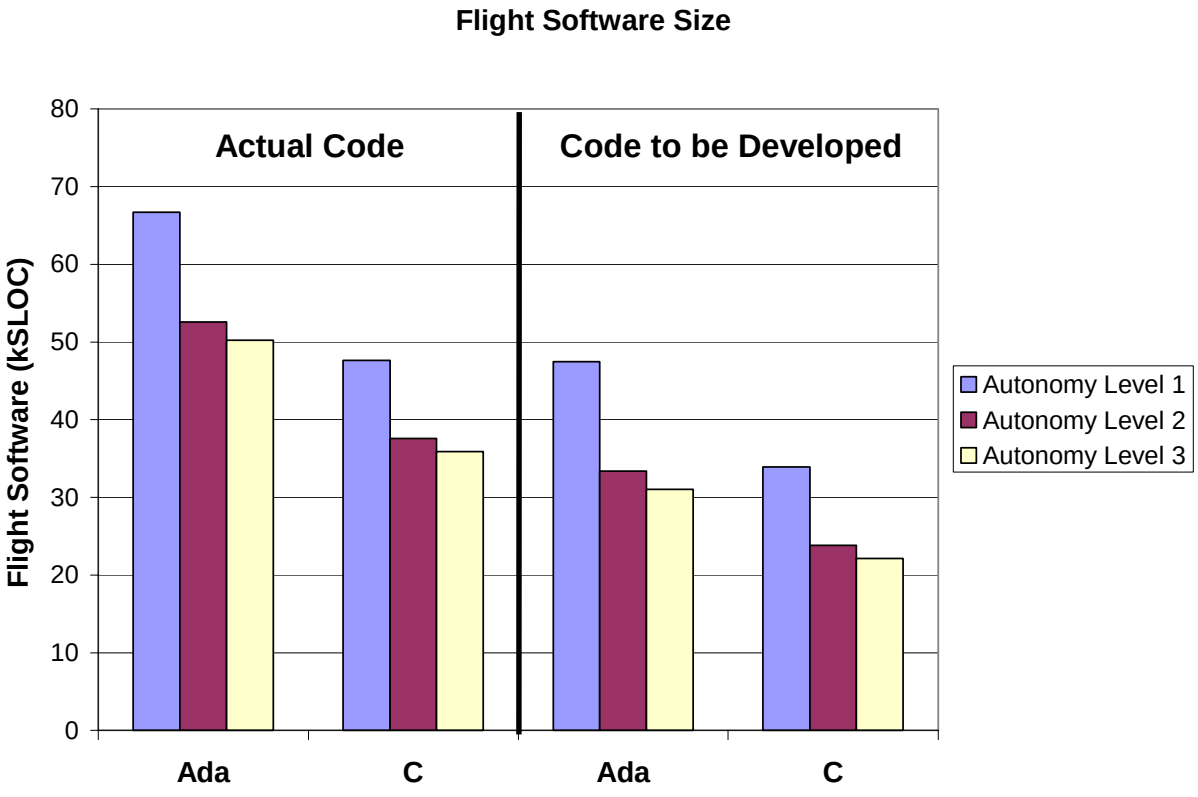

Figure 10.18: Flight Software SLOC for Each Autonomy Level

10.5.2 Flight Software Computer Requirements

The flight computer must be capable of running and storing the actual flight software. It has just been shown that it is possible to estimate the software requirements. However, because changing hardware late in the development phase can increase mission cost, a margin is added to the software requirements. This is done to make sure that the flight computer will have enough speed and memory to run the flight software, even if requirements creep cause the software to grow larger than initially estimated when the computer was chosen. A good estimate on the software requirements ensures that the flight computer will not have to be upgraded or replaced with a more capable unit. Because the requirements of the COTS software are known, no margin is added. For the current software estimate, the only COTS software is the run-time kernel (see previous section). The margin is 100% of the non-COTS estimated software requirements.

To account for on-orbit growth of the flight software, a margin is added for on-orbit spare computer capability. This extra margin allows possible future upgrades to the software after launch. The on-orbit spare is 100% of the initial estimated requirements plus the 100% margin. Essentially, the initial software requirements are multiplied by four to allow for requirements creep and on-orbit growth.

Table 10.48 and Table 10.49 show the sizes of the margin and on-orbit spare. Note that this margin is not used for flight software cost estimation; only to size the flight computer.

Table 10.48: Flight Software Computer Margin

Flight Software Computer Margin (100% of non-COTS software)	Flight Software Memory Margin		Throughput Margin (KIPS)
	Code (Kwords)	Data (Kwords)	
Autonomy Level 1	279.7	178.7	1244.3
Autonomy Level 2	226.2	110.7	782.1
Autonomy Level 3	215.2	107.7	763.1

Table 10.49: Computer Spare for On-Orbit Software Growth

Computer Spare for On-Orbit Software Growth (100% of all software + margin)	Flight Software Memory Spare		Throughput Spare (KIPS)
	Code (Kwords)	Data (Kwords)	
Autonomy Level 1	567.4	361.4	2488.7
Autonomy Level 2	460.4	225.4	1564.3
Autonomy Level 3	438.4	219.4	1526.3

Using the equations from the previous section, the code words and data words can be converted into SLOC. Table 10.50 shows the memory margin and spare memory converted into SLOC.

Table 10.50: Flight Software Spare and Margin for Computer Memory (SLOC)

Flight Software Margin and Spare for Computer Memory	Flight Software Memory Margin (kSLOC)		Flight Software Memory Spare (kSLOC)	
	Ada	C	Ada	C
Autonomy Level 1	64.0	46.3	131.6	94.0
Autonomy Level 2	50.8	36.3	103.3	73.8
Autonomy Level 3	48.4	34.6	98.7	70.5

This can be converted into bytes using the equations from the previous section. Table 10.51 shows the memory margin and spare memory converted into megabytes (MB). Note that this number is independent of the programming language.

Table 10.51: Flight Software Spare and Margin for Computer Memory (MB)

Flight Software Margin and Spare for Computer Memory	Flight Software Memory Margin (MB)		Flight Software Memory Spare (MB)	
	Ada	C	Ada	C
Autonomy Level 1	1.95	1.95	3.95	3.95
Autonomy Level 2	1.5	1.5	3.1	3.1
Autonomy Level 3	1.5	1.5	3.0	3.0

Table 10.52, Figure 10.19, and Figure 10.20 show the total flight software computer requirements on memory and throughput.

Table 10.52: Total Flight Software Computer Requirements

Total Flight Software Computer Requirements	Memory Requirement (MB)	Throughput Requirement (MIPS)
Autonomy Level 1	7.9	4.98
Autonomy Level 2	6.2	3.13
Autonomy Level 3	6.0	3.05

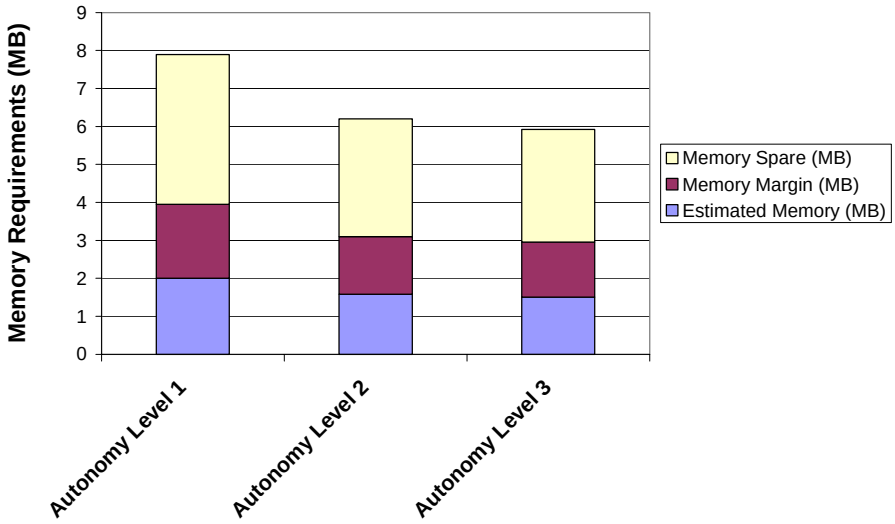

Figure 10.19: Total Flight Software Computer Memory Requirements

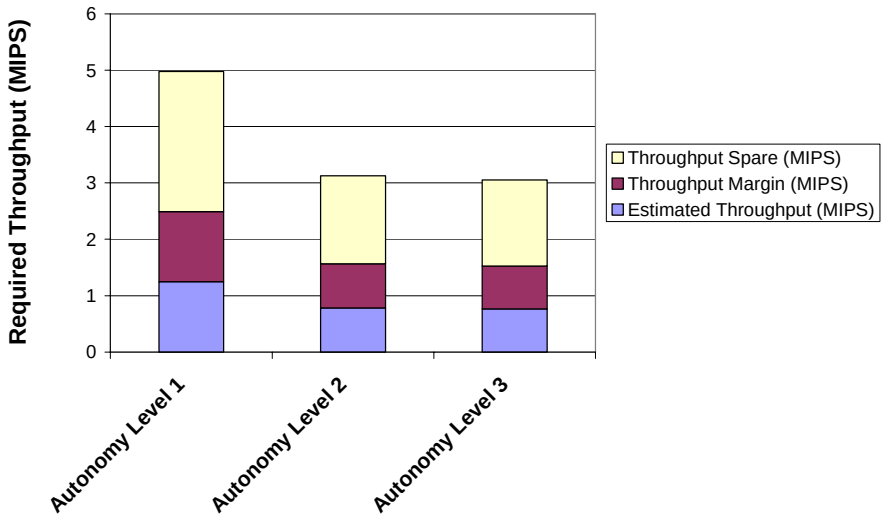

Figure 10.20: Total Flight Software Computer Throughput Requirements

10.5.3 Ground Software Size Estimation

The ground software includes the test, integration, and simulation software and the operations software. Estimation techniques for the ground software were not available for the software design. Therefore, each of the two segments of the ground software was assumed to be four times the size of the flight software. The logic behind this decision is given below.

10.5.3.1 Test, Integration, and Simulation Software

The test, integration, and simulation software is typically between two to four times the size of the flight software [Hansen, 2000]. This size will depend on how much simulation and testing is done to verify the flight software. A reasonable rough order of magnitude estimated can be found by assuming the test, integration, and simulation software is four times the size of the flight software. The following reasoning is quoted from a personal email with L. Jane Hansen of HRP Systems, and co-author of Chapter 16 in SMAD. This information is very useful and is included with the permission Ms. Hansen.

> "To verify on-board algorithms for navigation, orbit control, attitude control, etc. you should have reasonably high fidelity orbit propagator into which the algorithms under development can be inserted. None of this software is flight worthy - it is all prototype software. The orbit propagator can be purchased as COTS from a number of suppliers but inserting your navigation or ACS software modules may be more complex. The propagator should have environmental models that are an order of magnitude better than what the FSW (flight software) is trying to achieve.
>
> "As avionics integration proceeds throughout the program, and especially if there exist a large number of different interfaces and thus different I/O handlers in the FSW, ground software simulating the various subsystems can be used to test the FSW as it resides in the flight computer. This simulation system will need an 'executive' which is similar in complexity and SLOC count as an executive for FSW would be. There needs to be a dynamic model of the 'vehicle' - a 6 DOF representation of the spacecraft which can be as large (in terms of SLOCS) as the basic application software within the FSW count. So we are at approximately 1 time the FSW SLOC count.
>
> "You also need I/O handlers for the external units (like the rate gyros) to send data to the flight computer over the actual network interface. This would be comparable to the size, complexity, and SLOC count for the FSW. However, in addition to the I/O handler you probably want to model (at some level) the functionality behind the external units data output. In the case of the rate gyro you would not need to 're-create' the physical gyro but rather the functions and state transitions the gyro may go through with the associated performance (if performance decreases during high Gs - etc.) You can use the dynamic 6 DOF model of the spacecraft to provide truth about the gyro elements (velocity and acceleration) but then add on errors based on the unit's performance

specifications. This is additional to the SLOC count for the FSW - depending on the number of external devices you are modeling it can be about that same size as the FSW. So now we are at 2 times the FSW SLOC count.

"When testing the FSW in its entirety, you want to continue to simulate the dynamic elements (rate gyros, accelerometers, etc.) and the 'expendable' elements (thrusters, propulsion, etc.) while using real hardware for the static elements (power management, thruster switching mechanisms, communications equipment, etc.) In addition, you may want tot tie the communications equipment into a 'real' base - for example, with the 4 spacecraft you have, and the inter-spacecraft link, you may want to test that link in the 'laboratory' environment (maybe even with all 4 spacecraft!). This can take some special software for configuring the system, for managing the elements that are simulated and real, and for providing 'glue' between what can be real and what cannot (for example driving the thruster selection relays without interfacing to the 'real thrusters'). Worst case this will be another FSW SLOC count. So now we are at 3 times the FSW SLOC, which is what I presented in my charts for ground support software.

"Data collection software for each of the networks involved, as well as internal to the FSW if necessary, and data reduction/analysis tools will easily equal another 1 times the FSW SLOC count. As I said in the presentation, if this software can also be 're-used' to reduce/analysis data from the spacecraft during operations - that's even better!! Which brings us to the 4 time FSW SLOC count."

10.5.3.2 Operations Software

The size of the operations software for the Milstar program was estimated using information from [Keesee, 2000]. It was roughly four times the estimated size of the MINERVA flight software. Milstar is a military communications system that consists of four, cross-linked satellites in geosynchronous orbit. These satellites autonomously route communications between ground users with no input from the Milstar system operators. While there are differences between Milstar and MINERVA, it was reasoned that the Milstar system is similar in complexity to the MINERVA system.

Note that the memory and throughput requirements of the ground software are not as important as for the flight software. This is because the size of the ground computers is not limited by size and mass constraints in the same way as the flight computer. For this reason, only the SLOC sizes are calculated for costing purposes. The test, integration, and simulation software cost is included in a separate cost estimating relationship (CER) used for other components of the MINERVA system. Therefore, only the size of the operations software will be calculated for costing.

Table 10.53 and Figure 10.21 show the ground software size.

Table 10.53: Ground Operations Software Size (SLOC)

Operations Software Size (kSLOC)	Actual Code (kSLOC)		Code to be Developed (kSLOC)	
	Ada	C	Ada	C
Autonomy Level 1	266.7	190.5	189.9	135.643
Autonomy Level 2	210.3	150.214	133.5	95.357
Autonomy Level 3	200.9	143.5	124.1	88.643

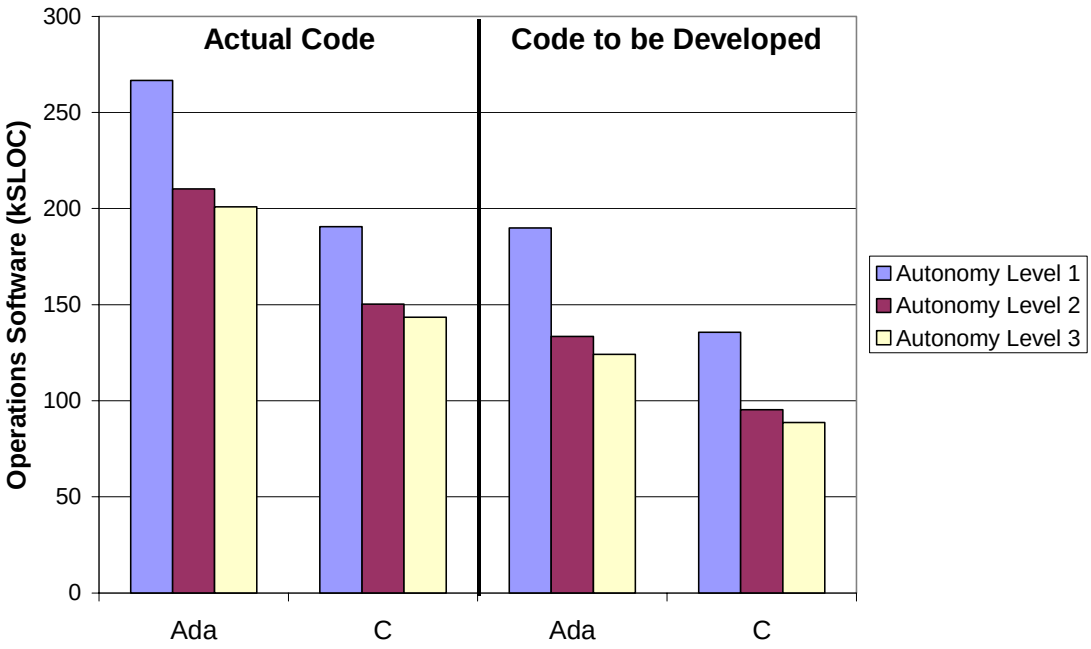

Figure 10.21: Ground Operations Software Size (SLOC)

10.5.4 Software Cost Estimation

The cost of the flight and ground software is estimated from the code size (SLOC) using the cost estimation numbers from SMAD Chapter 20. Table 10.54 shows the numbers used to estimate the software cost. Note that while C costs more than Ada (per line of code), it generally requires less lines of code than Ada to complete the same number of instructions.

Table 10.54: Cost per SLOC

Cost per SLOC	Ada	C
Flight Software	$ 435	$ 726.45
Ground Software	$ 220	$ 220

Table 10.55 and Figure 10.22 show the software costs for the different autonomy levels with Ada or C as the programming language.

Table 10.55: Software Cost

Software Cost (FY00$M)	Ada			C		
	Flight Software	Initial Ground Operations Software	Total Software Cost	Flight Software	Initial Ground Operations Software	Total Software Cost
Autonomy Level 1	20.65	41.78	62.43	24.63	29.84	54.48
Autonomy Level 2	14.52	29.37	43.89	17.32	20.98	38.30
Autonomy Level 3	13.50	27.30	40.80	16.10	19.50	35.60

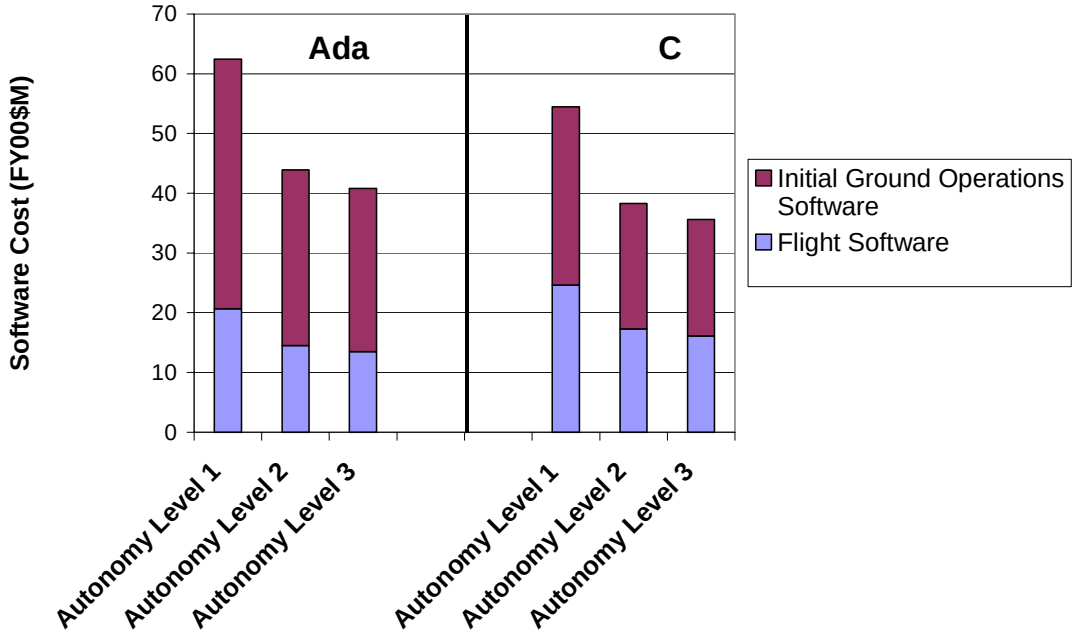

Figure 10.22: Software Cost

We chose autonomy level 2 for the MINERVA system. This allows the system to be more flexible than at autonomy level 3 while not adding much cost (relative to the total program cost). The cost difference between autonomy levels 2 and 3 is roughly $3 million. A small analysis was done to see how this choice affects the operations cost after IOC. This is discussed in the next section.

10.5.5 Level of Spacecraft Autonomy vs. Operations Cost after IOC

Our present goal is to design a system that will cost under $300M by IOC. This forces us to use the cheapest possible solution and thus the least amount of autonomy. However, it is recognized that less autonomy will drive up the operations cost. To get a feel for how the spacecraft autonomy will drive the operations cost of our system, the operations cost for each autonomy level was estimated. We used the operations cost model from [Boden, 1996]. Figure 10.23 shows a comparison between the total software cost (flight software plus operations software) and the estimated yearly operations costs for the different levels of spacecraft autonomy. Only the total software cost with C as the programming language is shown.

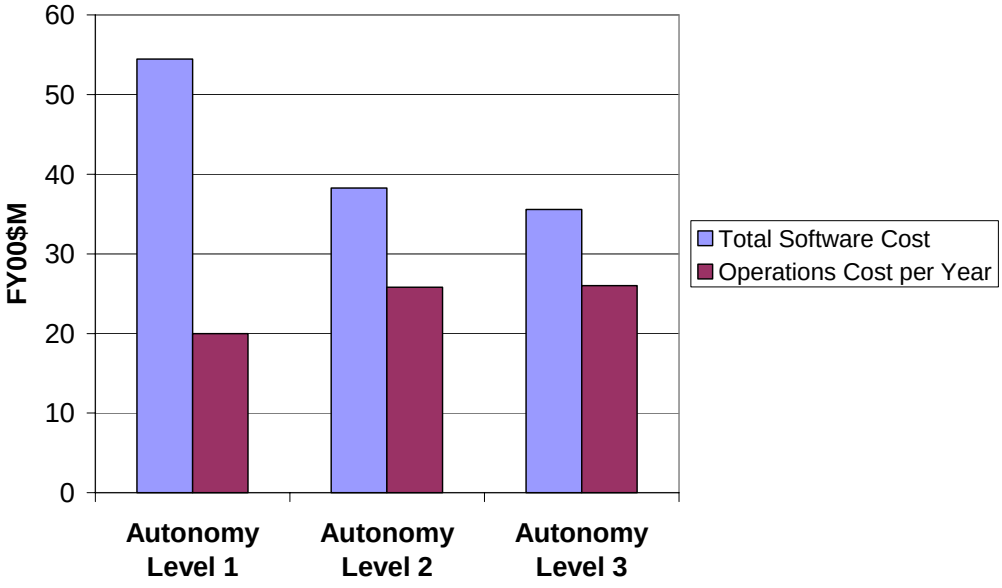

Figure 10.23: Effect of Autonomy on Operations Cost

In order to understand the cost effects over the useful lifetime of our system, the sum of the total software cost and the operations cost was plotted over the first five years after IOC. Inflation was not included in the cost numbers. The result is shown in Figure 10.23.

While less autonomy reduces the cost of the flight software, more autonomy reduces the yearly cost of operations. Initially, the lower autonomy levels lead to a lower amount of money spent. However, the higher autonomy level ends up being cheaper after five years of operations. This implies that high levels of autonomy are desirable for long duration missions, but are less desirable for short duration missions.

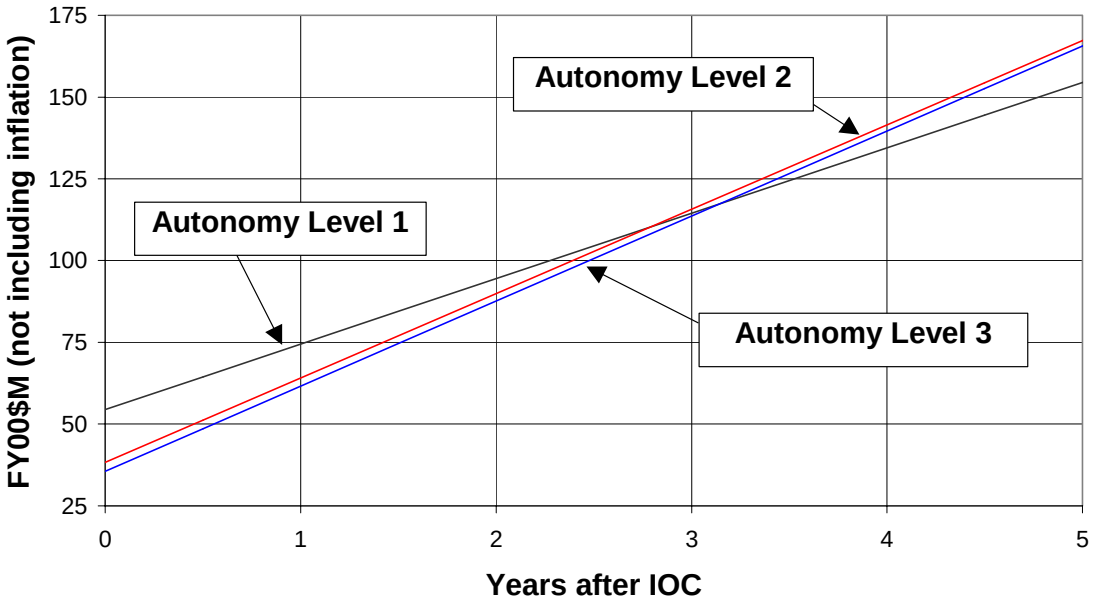

Figure 10.24: Total Software and Operations Cost

10.5.6 Lessons Learned on Software

It is often asked: "Why don't more missions use more autonomy?" During our design process, the reasons for this were learned. We had originally envisioned a fully autonomous system that would allow users transparent communications and position fixing capability. However, we soon found that in order to do this, a lot of money would be needed to develop the flight software. In order to meet our cost cap requirement, we decided to use a low amount of autonomy. Even though it would lead to a more expensive overall mission (including operations), we were limited in the amount of funds available for mission development.

This is a problem facing much of the space industry today. In order to change this, it is important for trade studies to be done in such a way as to show not only the software costs for different levels of autonomy, but also how those autonomy levels will affect operations costs. Only in this way can the money controllers be convinced that paying more money up front for autonomy can actually *reduce* the overall mission cost.

10.6 References

Aharonson, Oded, Zuber, Maria T., Neumann, Gregory A. Mars: Northern Hemisphere Slopes and Slope Distributions. Geophysical Research Letters, Vol 25 No 24, pages 4413-4416, December 15, 1998.

Boden, D. G., Larson, W.J, Cost-Effective Space Mission Operations, McGraw-Hill, 1996.

Daher, John K. Wheeler, Mark L. International Space Station Electric Field Measurement Package (EFMP). Final Technical Report, Report No. A-5508F, Contract No. H-28501D, Submitted To: NASA/MSFC, Submitted By: Sensors and Electromagnetic Applications Laboratory (Georgia Tech Research Institute), 20 January 1998.

Jet Propulsion Laboratory. Mars Global Surveyor Detailed Mission Requirements, Final. November 1995. JPL D-12785.

Levanon, Nadav. Quick Position Determination Using 1 or 2 LEO Satellites.IEEE Transactions on Aerospace and Electronic Systems, Vol 34 No 3, Julu 1998

Lemoine, F.G. & al. Precise Orbit Determination for Mars Global Surveyor during Hiatus and SPO. Advances in the Astronautical Sciences, AAS 99-147.

Dr. C.T.Leondes, editor. Principles and Operational Aspects Precision Position Determination Systems. AGARDograph No.245.

Morgan, Walter L. and Gordon, Gary D. Communication Satellite Handbook. Wiley Interscience, 1989.

Sklar, Bernard. Digital Communication Fundamentals and Applications. Englewood Cliffs, NJ: Prentice Hall, 1988.

Smith, David E. & al. The Global Topography of Mars and Implications for Surface Evolution. Science, Vol 284, 28 May 1999, p1495.

Vijayaraghavan, A, Thurman, Sam W., Kahn, Robert D, and Hastrup, Rolf C. Surface Navigation on Mars Using a Navigation Satellite. Advances in the Astronautical Sciences, 1992. AAS 92-105.

Wertz, J. R. & Larson, W. J. (ed.) Space Mission Analysis and Design. (3rd ed.) Torrance, California: Microcosm, Inc. 1999.

Winton, A., Gerner, J.-L., Michel, P., & Morgan-Owen, R. "The Transponder - A Key Element in ESA Spacecraft TTC Systems." Noordwijk, The Netherlands: RF Systems Division, ESTEC. 1996. http://esapub.esrin.esa.it/bulletin/bullet86/wint86.htm. (April 2000)

Wood, Lincoln J. Orbit Determination Singularities in the Doppler Tracking of a Planetary Orbiter. Journal of Guidance, Vol. 9, No 4, July-August 1986.

AOL Computing's Webopaedia Definition and Links. http://aol.pcwebopedia.com. May 2000.

Mars Pathfinder Frequently Asked Questions. http://mars.sgi.com/mpf/faqs_general.html. May 2000.

Electronic correspondence with L. Jane Hansen, HRP Systems, April 2000.

Electronic correspondence with Dr Chad Edwards, Jet Propulsion Laboratory, February 2000

Electronic correspondence with Dr. Todd Ely, Jet Propulsion Laboratory, April 2000.

Personal conversations with Prof. Thomas Herring, MIT, April 2000.

Personal conversations with Dr. Lorraine Fesq. MIT. April 2000.

Personal correspondence with L. Jane Hansen. HRP Systems. April 2000.

Personal conversations with Col. John Keesee. MIT. April 2000.

Personal conversation with Prof. Staelin, MIT, April 2000.

Personal conversations with Mr. Zack Warfield. Orbital Sciences Corporation, April 2000.

11 Bus

11.1 Introduction to Bus Design[38]

MINERVA consists of a constellation of four satellites in orbit around Mars. The satellite bus includes every physical aspect and component of the spacecraft. The function of the spacecraft bus is to support the communication and position determination payload in its orbit around Mars.

The bus consists of several subsystems. The most important aspect of the bus is the payload itself. The payload consists of the communication and position determination systems that allow the constellation to perform its required tasks. In addition to the payload, the spacecraft bus includes the following subsystems:

- Propulsion
- Power
- Attitude Determination and Control System (ADCS)
- Thermal System
- Structure

These subsystems are described in greater detail below.

11.2 Propulsion Subsystem Design[39]

The propulsion subsystem is primarily responsible for maneuvering the spacecraft. This includes getting the spacecraft into the proper orbit around the proper planet, maintaining that orbit, and maintaining pointing accuracy throughout the lifetime of the mission.

It is important to accurately model the propulsion subsystem since propellant mass makes up the dominant fraction of total launch mass. The propellant mass scales with the dry weight of the spacecraft. For every kilogram added by other subsystems, it takes several more kilograms of propellant to accelerate the new mass. Keeping a close eye on the ever-increasing propellant mass is crucial to meeting launch requirements, as there is a finite mass that can fit on a given launch vehicle.

The following sections detail the general calculations for space propulsion, as well as design trades specific to the Project MINERVA.

---

[38] JMA, DMB

[39] DMB

11.2.1 Basics of Rocket Propulsion

The rocket equation (below), derived by equating the momentum of the vehicle to the momentum of the propellant exhaust, relates the change in mass of the spacecraft to the possible change in velocity.

$$\frac{M_{final}}{M_0} = e^{-\frac{\Delta V}{c}}$$

The goal in designing a propulsion system is to determine what propulsion system is best (pick the characteristic exhaust velocity, *c*), and calculate how much propellant mass is required to complete the mission (ΔV). The difference between initial mass, M_0, and final mass, M_{final}, is the propellant mass. The propellant mass increases as the final mass increases. It is therefore important to understand the component masses that make up the final mass, as they represent the useful elements of the spacecraft used to complete the mission. Some elements of the final spacecraft mass that arrive at the mission destination are dependent on the propellant mass as well.

Figure 11.1 plots the ratio of final mass to initial mass as a function of ΔV/c, where initial mass is equal to final mass plus propellant, and *c* is the exhaust velocity of the propellant gas. The curve shows that as ΔV increases, *c* must also increase in order to prevent a decrease in the mass ratio.

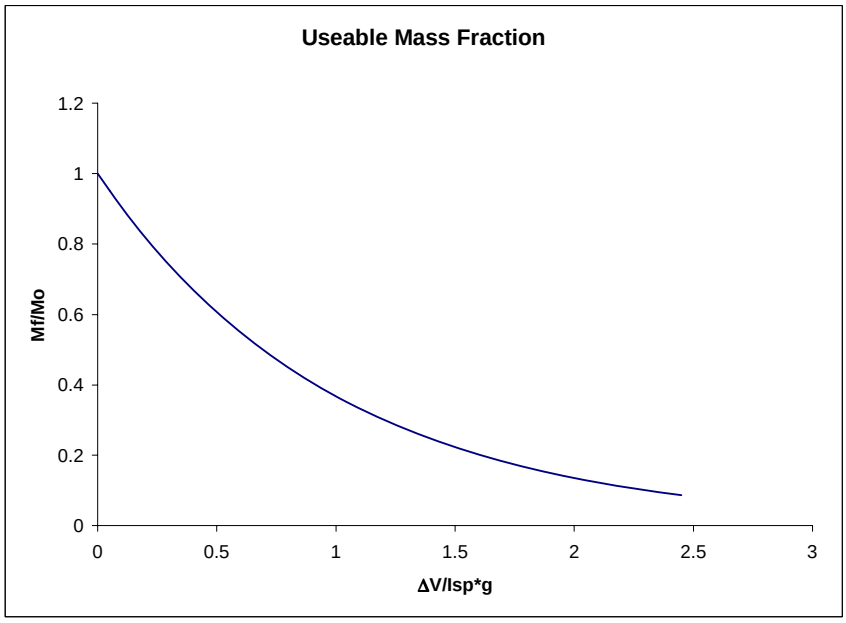

Figure 11.1: Useable Mass Fraction as Function of Propulsion System and Mission Characteristics

11.2.2 Selection of Propulsion Subsystem

For MINERVA, the possibility of electric propulsion was considered due to the high ΔV required to perform deep space missions with long lifetimes. The final mass is separated into power mass and the mass of everything else on board the spacecraft:

$$M_{final} = M^* + M_{power}$$

Some of the major subsystem masses that make up M*:

$$M^* = M_{payload} + M_{structure} + M_{engine} + M_{battery} + M_{ADCS} + \ldots$$

Power mass is important to consider, as power is also a function of propulsion system choice for electric propulsion engines. Rather than extract chemical energy from the reaction of propellant gases, EP adds energy generated separately from the propulsion system to accelerate the propellant. Therefore, the more rapidly you want to accelerate your exhaust (corresponding to an increase in *c*) the more power it takes. For conventional power production means, this requires more mass in the form of solar panels or RTG mass. As will be discussed in section 11.3.2, solar panel mass is less than RTG mass at the Martian solar radius. The choice of *c* which minimizes the total mass, including propellant and power mass was determined, using the following trade equations:

$$\frac{M^* + \alpha \cdot P}{M_0} = e^{-\frac{\Delta V}{c}}$$

$$M_0 = \frac{M^* + \alpha \cdot P}{e^{-\frac{\Delta V}{c}}}$$

$$P_{EP} = \frac{\dot{m}c^2}{2\eta}$$

plots this optimization. Also plotted is the trade for a chemical-only system, highlighting points associated with a hydrazine/nitrogen tetroxide engine, the SSME, and a Hall thruster.

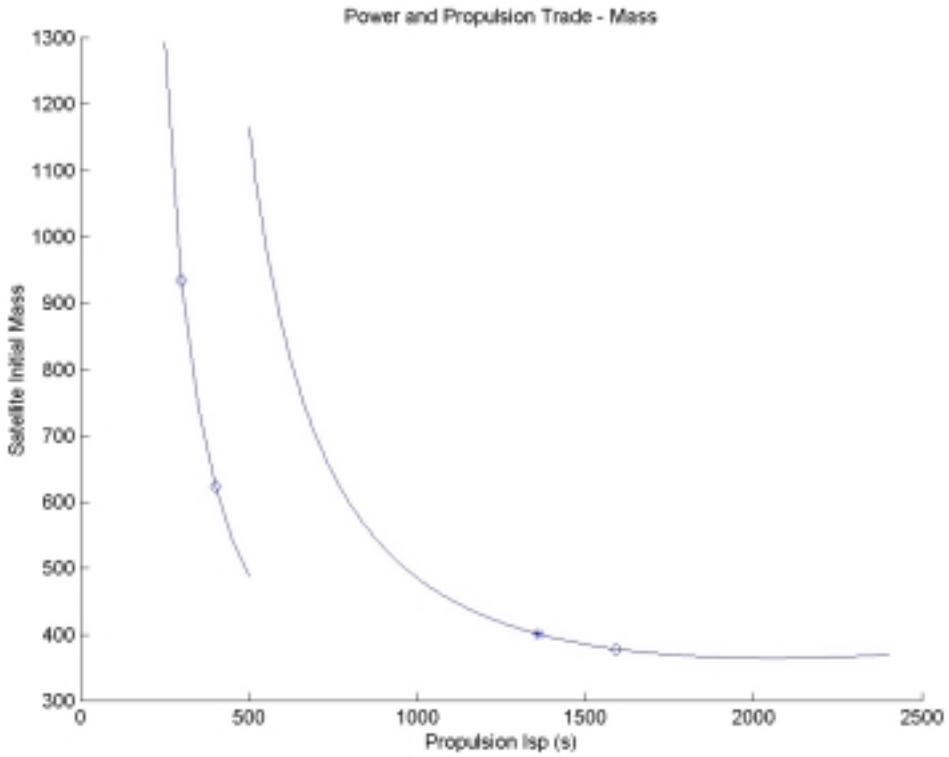

Figure 11.2: Power Propulsion Trade

In this plot, the optimum point is an I_{sp} of 2100 seconds (c = 21000), corresponding to an ion engine. However, mass is not necessarily the figure of merit. In order to meet the cost requirement for MINERVA, and minimize the cost per function of the mission, cost is a more important driving factor.

It turns out that power mass is more expensive than propellant mass. Power mass requires the construction of solar panels, power processing units, and other hardware. Propellant mass is just a chemical that represents weight to be launched. In order to properly perform the trade, the cost of these systems must be considered. For the propellant, it must be launched. For the sake of the optimization, a cost of $10,000 per kg is assumed. The power system must be built and launched. A cost estimating relationship from SMAD is used:

$$Cost = 10000\left(M_0 + 112000 \cdot \left(M_{power\_system}\right)^{0.763}\right)$$

The mass of the power subsystem consists of the mass of solar panels and batteries. The chemical architecture also has batteries and solar panels, although they are smaller than those needed for the EP system. Figure 11.3 shows the cost optimization. There is now a clear optimum for an electric propulsion system. Based on the required mission ΔV, the chemical and electric curves can move relative to one another.

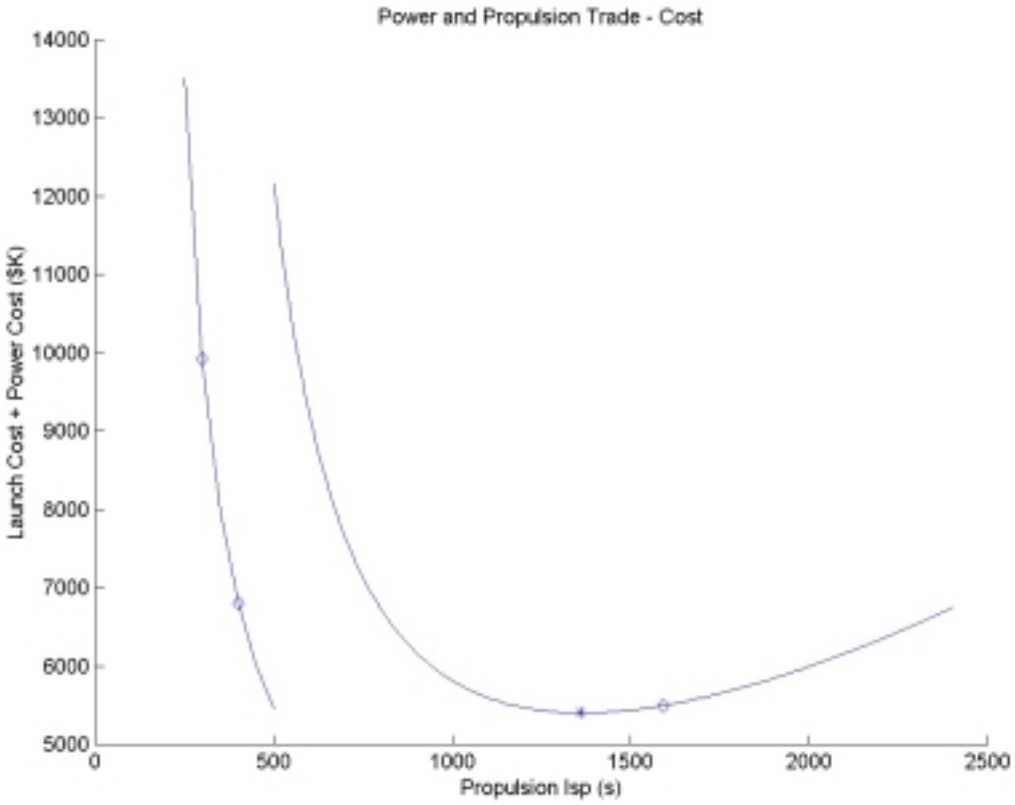

Figure 11.3: Propulsion System Choice

The curves on Figure 11.3 assume a mission where each spacecraft exits the launch vehicle after it escapes from the Earth (effectively on a parabolic orbit) and then maneuvers itself to Mars. The chemical system will follow a Hohmann transfer, capture at Mars and aerobrake into orbit. The electrical system will spiral out in a quasi-circular orbit and "fall" into capture around Mars. The ΔV for these maneuvers was estimated by the orbits group.

However, it may be possible for the chemical system to get enough ΔV from the launch vehicle to ride all the way to Mars, using its own engines for capture only. The electric system cannot benefit from this, as the thrust from the engine is too low to capture at Mars from a hyperbolic entry orbit. In this case, the ΔV for the chemical system is drastically reduced and the optimization changes, as seen in Figure 11.4.

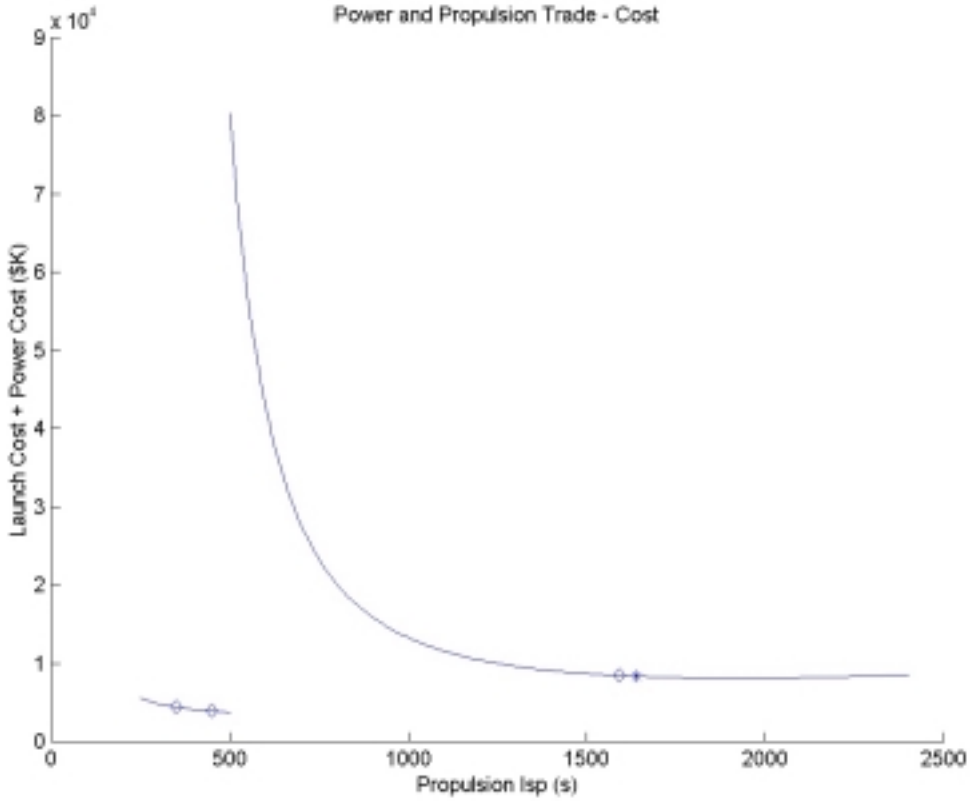

Figure 11.4: Cost vs. I_{sp} for a Chemical System that Rides the Launch to Mars

In the case where a chemical system is used, the best I_{sp} possible is around 320 seconds, corresponding to MMH/NTO liquid bi-propellant. The cryogenic H2-O2 engine used on the Space Shuttle has a higher I_{sp}, but the propellant is not storable for the months of transfer time. Figure 11.5 and Figure 11.6 show the relative size of the masses for the subsystems considered in the optimization for each ΔV case. As I_{sp} increases, the propellant mass shrinks while the power mass grows. For the case where the launch vehicle takes the system to Mars, the chemical system is much less massive than the best electric system.

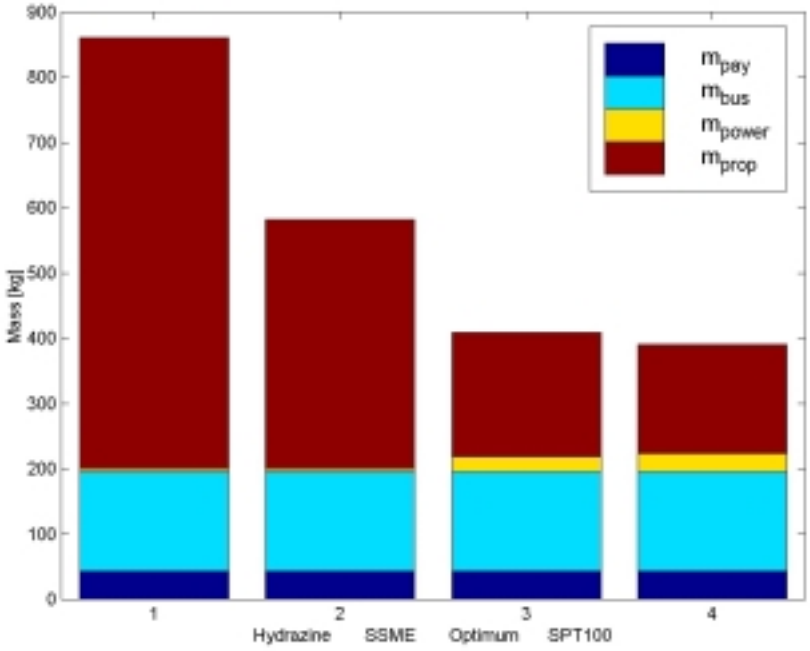

Figure 11.5: Spacecraft Mass for Different Propulsion Choices, Assuming each S/C Completes the Transfer

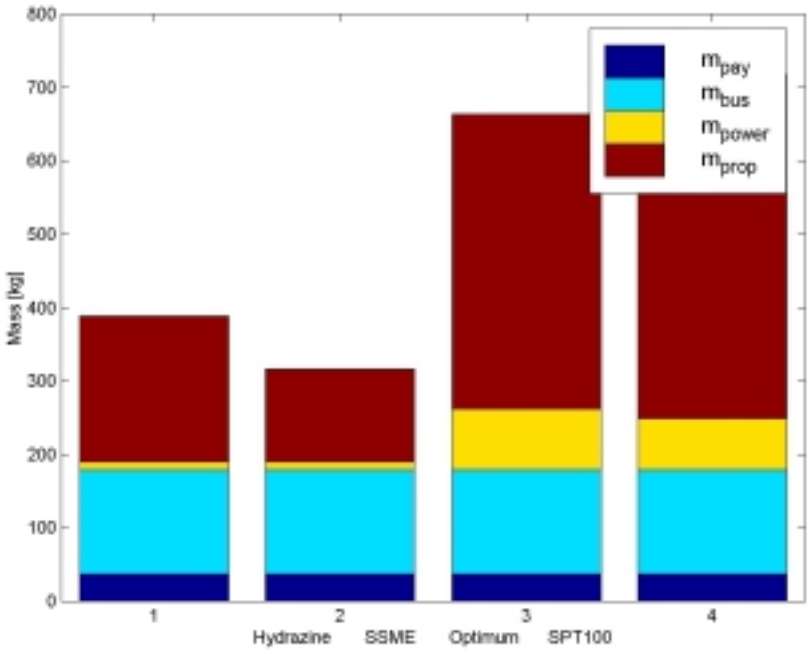

Figure 11.6: Spacecraft Mass for Different Propulsion Choices, Assuming the Chemical S/C Rides the Launch Vehicle.

11.2.3 Propulsion Subsystem Design: Summary of Results

Given the launch considerations, the chemical propulsion system, even without aerobraking, minimized the mission cost. The following section describes the technical details of the chosen propulsion system.

The standard for storable chemical bi-propellant engines is a combination of mono-methyl hydrazine (MMH) for fuel and nitrogen tetra-oxide (NTO) for oxidizer. This propellant offers long-term storability in liquid form, while gaining higher I_{sp} due to the chemical energy released in the reaction. NTO/MMH had an I_{sp} of 320 s, common for space applications. This technology is state of the art for non-cryogenic propulsion systems like the Space Shuttle Main Engines, which can operate at an I_{sp} of 450 s.

For primary propulsion, including capture and orbit repositioning, the Chandra X-Ray Telescope engine provides the necessary impulse for a space vehicle like MINERVA. Manufactured by TRW, the engine has an I_{sp} of 322.5 s, a mass of 4.5 kg, and a 25,000 s operating life, allowing for multiple restarts throughout the life of the spacecraft. The thrust is 4250 N, which is sufficient impulse for a 470 kg spacecraft (about 10 g's).

For attitude control, including de-saturating the momentum wheels, smaller thrusters will be used, but operating with the same propellant system. These thrusters, organized in clusters around the spacecraft, can weigh as little as 0.5 kg and operate at 11 N of thrust. In order to provide total control of the spacecraft, ten of these thrusters are necessary. These small thrusters can be operated in a pulse mode to improve accuracy.

The propellant system includes the oxidizer and fuel tanks, the blow-down tank, and the valve feed system. Figure 11.7 and Figure 11.8 show the schematics for a primary and attitude control NTO/MMH propulsion system. The figures are specific to the Apollo lunar lander, and are therefore larger than the MINERVA counterparts, but the schematic is similar. MINERVA of course only has one main engine, while the Apollo lunar lander had four.

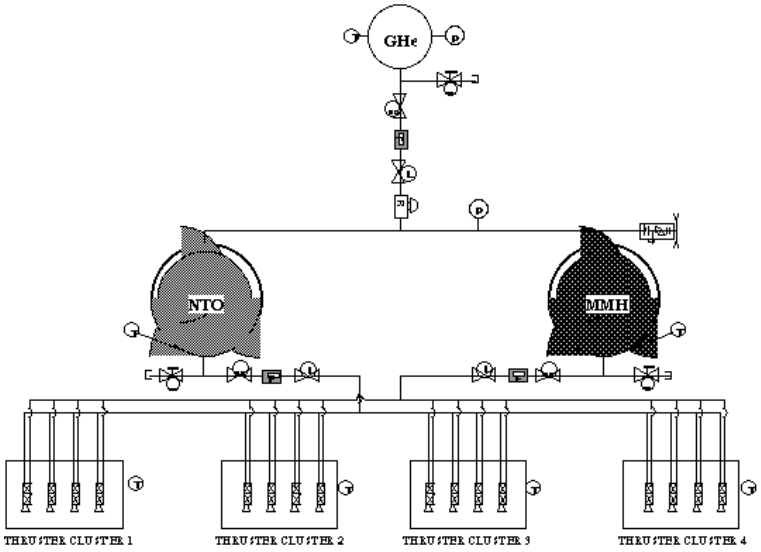

Figure 11.7: Lunar Lander Primary Propulsion Schematic (NTO/MMH)

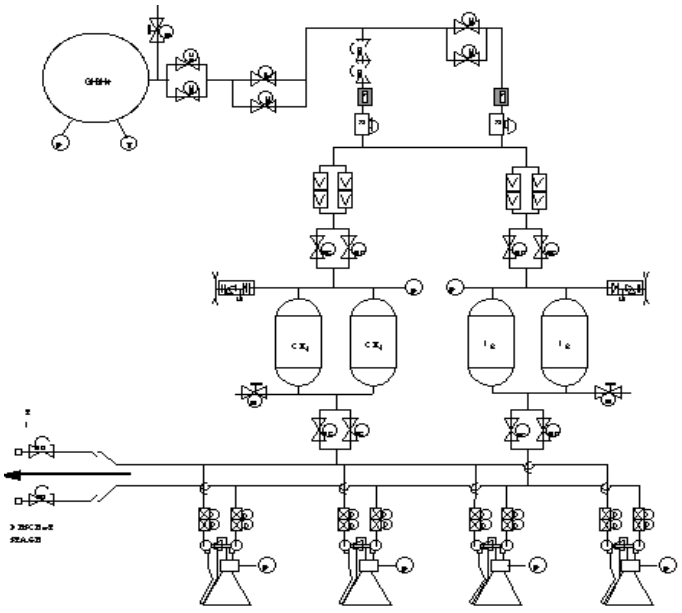

Figure 11.8: Attitude Control Propulsion Schematic (NTO/MMH)

11.3 Power Subsystem Design[40]

11.3.1 Purpose and Overview

The power subsystem supplies the payload and bus with the power necessary to perform all spacecraft functions. The power subsystem performs three major functions:

- Power generation
- Power storage
- Power regulation and control

There are various sources of power for deep space missions, including solar arrays and radio-isotope thermal generators (RTG's). Batteries constitute the power storage system. The batteries store power for use during eclipse and peak power operations of short duration. The power regulation electronics are responsible for converting voltages, conditioning the power, and distributing the power within the spacecraft.

11.3.2 Component Design

The choice of power sources is crucial in determining the size, configuration and cost of a spacecraft. Therefore, the first trade in the power subsystem dealt with the selection between solar arrays and RTG's. The primary trade between the two sources is the ratio of output power to mass. However, many other factors contribute to the final selection of the power source. The other factors include cost, performance, political implications, and environmental effects. RTG's have negative political implications and environmental risks because the technology uses radioactive isotopes as the power source. From a performance perspective, the efficiency of the solar arrays degrades with time, thus limiting the lifetime of the satellite. RTG's provide a constant power output regardless of any environmental conditions. However, solar arrays depend on the solar flux for energy, which is a function of the distance from the sun. Thus, the power per mass of solar arrays is less at Mars than at Earth, while the power to mass of RTG's remains constant. **Error! Reference source not found.** shows the radius from the sun at which RTG's become more efficient than solar arrays. Since Mars is at an average radius of 1.5 AU from the sun, it is advantageous to use solar arrays as the power source.

[40] ZW

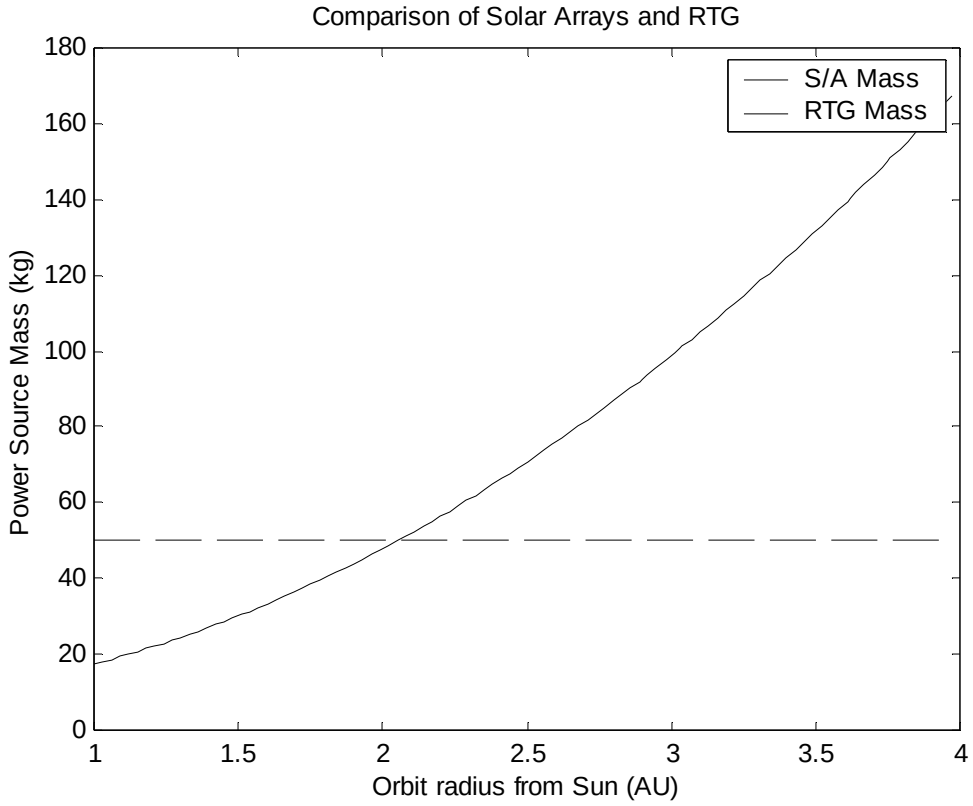

Figure 11.9: Solar Arrays versus RTG

Given the architectural decision to use a combination of solar arrays and batteries as the power source, the power module focused on sizing these components. A MATLAB module determines the area and mass of the solar arrays and the mass of the batteries necessary to meet the power requirements for all phases of the mission. The power module receives power requirements for the payload, ADCS*, thermal subsystem*, and propulsion subsystem*. The (*) subsystems iterate within the bus module to converge upon their final values. The power module uses these power requirements along with the mission timeline and modes of operation to generate the maximum power requirement during daylight and eclipse. The maximum power during daylight is used to size the power generation system (solar arrays). The power requirement during eclipse and time in eclipse are used to size the energy storage system (batteries).

The required area of the solar arrays was determined by sizing for the mission phase with the highest power requirement.

With an electric propulsion (EP) system, the highest power level would have occurred during transfer to Mars while the ion thrusters are active. The power required to enable the EP system during transit would be approximately 1.4 kW. For this configuration the satellite would have to use large solar panels, approximately 13 m^2. For an EP configuration, the transfer power would far exceeds the power required in orbit around Mars (approximately three times).

For a chemical propulsion system the mission phase requiring the highest power is the Mars orbiting phase (nominal operations). This phase involves a circular orbit with a period of approximately 3.4 hours and an eclipse time of approximately 0.7 hours. The maximum continuous power required by the spacecraft during this phase is 280 Watts. Based on these parameters, the following equation is used to determine the total power that the solar arrays must collect.

$$P_{SA} = \frac{\left(\frac{P_E T_E}{X_E} + \frac{P_D T_D}{X_D} \right)}{T_D}$$

After calculating the required solar array output, the MATLAB module determines the performance of the solar cells. Since the satellite must be fully operational throughout the entire design life, the performance characteristics of the solar array must reflect "end of life" properties. The following equation incorporates the yearly degradation (η_D) in determining the power density (W/m^2) of the solar arrays.

$$P_{BOL} = SF \cdot \eta_{SA} \cdot \cos\theta$$
$$P_{EOL} = P_{BOl}\left(1 - \eta_D\right)^{lifetime}$$

The sun incidence angle used to determine the power density is 30°. This is the worst case angle because the solar arrays are free to rotate about the north-south axis. Once the module determines the "end of life" power density of the solar array, dividing the required power by the power density determines the solar array area.

$$A_{SA} = \frac{P_{SA}}{P_{EOL}}$$

Finally, the area density of the solar panel is multiplied by its area to determine the mass.

$$M_{SA} = A_{SA} \cdot \rho_{SA}$$

The second sizing function is to determine the required battery mass to meet the power requirements during eclipse. The batteries must supply the spacecraft with enough power to fully function during eclipse. Sizing batteries involves determining the battery capacity (W-hr) required. Battery capacity (C_R) is a function of the power level, time, depth of discharge (DOD) and transmission efficiency. The depth of discharge is a function of the number of charge/discharge cycles that a battery experiences during its lifetime. Depth of discharge decreases as the number of cycles increases.

$$DOD = 0.84 - 0.30\left[\frac{\ln\left(n_{cycles}\right) - \ln(1000))}{\ln(10)}\right]$$

$$C_R = \frac{P_E T_E}{DOD \cdot \eta_{bat}}$$

The mass of the batteries is simply the required capacity divided by the specific energy density (SED). Table 11.1 lists the values of the power subsystem properties.

$$M_{BAT} = \frac{C_R}{SED}$$

Table 11.1: Power Subsystem Properties

Property	Symbol	Estimated Value
Solar Panel Efficiency	η_{SA}	24.0 %
Degradation per Year	η_D	2.0 %
Panel Area Density	ρ_{SA}	5.04 kg/m^2
Power Conversion Efficiency	X_X	80 %
Battery Transmission Efficiency	η_{BAT}	90 %
Specific Energy Density (Li-Ion)	SED	66 W-hr/kg

Additional components include the power regulation electronics, battery chargers and wiring for the power subsystem. The mass of these components is computed as a fraction of the maximum power level of the system.

$$M_{MPS} = 0.02 \cdot P_{SA}$$

11.3.3 Design Details

The configuration of the spacecraft affects the sizing of the power subsystem. As discussed in section 11.3.2, the first architectural decision within the power subsystem was the choice to use solar panels rather than RTG's. The configuration of the solar panels derives from the architectural decision to use a three-axis stabilized spacecraft configuration rather than spin-stabilized. The three-axis stabilized configuration allows for the most maneuverability of the spacecraft, which is vital in performing the communication and position determination functions. Three-axis stabilized satellites normally use deployable solar panels because they can rotate and position themselves to maximize the incident solar flux. Deployable solar panels, compared to body-mounted panels, significantly reduce the required panel area and mass. Unfortunately, deployable

arrays tend to be more complex (less reliable) and more expensive. The MINERVA satellites use deployable solar arrays as the power generation source because of mass savings and improved thermal management.

The energy storage system for the satellite consists of Lithium-Ion batteries. These batteries are preferred because they have a high specific energy to mass relation. There is some technical risk involved with using Lithium-Ion technology because they have not been proven for space flight. The technology should be qualified for space flight before final assembly of the MINERVA satellites. Alternatively, existing battery technologies such as Ni-H_2 could be used, this would require increased battery mass. To increase the reliability of the energy storage system, the total battery mass is a factor of 1.5 times the required mass. Therefore, there is a redundant battery for every two required batteries.

11.4 Thermal Subsystem Design[41]

11.4.1 Purpose and Overview

The motivation for thermal control of the spacecraft derives from the need to satisfy the operating temperature requirements for the various satellite components. The components sensitive to the thermal environment include the electronics, batteries, transponders, and solar arrays. Table 11.2 lists the operating temperature ranges for these various components. The thermal environment at Mars is colder than Earth due to the increased distance form the sun. Thermal control devices heat or cool the critical components as required, thereby maintaining the temperature in the operating range.

Table 11.2: Operating Temperature Ranges

Component	Range (°C)
Batteries	- 5 to 30
Computers	-10 to 50
Propellant Tanks / Thrusters	7 to 55
Solar Arrays	-105 to 110
Mechanisms	-35 to 60

11.4.2 Thermal Modeling

The thermal model determines the temperature profile of the satellite while it orbits Mars.

[41] ZW

11.4.2.1 Thermal Environment

While in orbit around Mars the satellite experiences the harshest thermal environment. Temperatures are highly transient, varying from 180K to 280K. The transience is due to a portion of the orbit being in eclipse, while the average low temperature is due to the extreme distance from the sun (compared to Earth orbiting satellites). Since the orbital period is short (~three hours), the spacecraft temperature oscillates and does not have sufficient time to reach a steady state.

Other external sources of heat include the albedo and irradiance from Mars. Radiation is the only mode of heat transfer from the spacecraft.

11.4.2.2 Heat Transfer

In order to simplify modeling the heat transfer through the satellite, a spherical model of constant surface properties is used to represent the body of the satellite, and thin planes for the solar arrays. For surface temperature calculations, both the solar arrays and the satellite body model assume lumped thermal capacitance. The equilibrium equations used for determining the satellite surface and solar array temperatures are:

$$A_{SA} \cdot \sigma \cdot \varepsilon \cdot T_{SA}^4 + m \cdot C_P \frac{\partial T_{SA}}{\partial t} = A_{SA} \cdot \alpha \cdot Q_{surface} - P$$

$$A \cdot \sigma \cdot \varepsilon \cdot T_{surface}^4 + m \cdot C_P \frac{\partial T}{\partial t} = A_C \cdot \alpha \cdot Q_{surface} + Q_{core}$$

where,

$$Q_{surface} = Q_{sun} + Q_{albedo} + Q_{IR}$$

and

A_{SA}	Solar array area
σ	Stefan-Boltzman constant
α	Absorptivity
ε	Emissivity
T_{SA}	Solar array temperature
$T_{surface}$	Satellite surface temperature
m	Satellite/array mass
C_P	Thermal capacitance
P	Power of the solar array
$Q_{surface}$	Total incident heat flux on the satellite
Q_{sun}	Incident heat flux from the sun
Q_{albedo}	Incident heat flux from the Mars albedo
Q_{IR}	Incident heat flux from Mars irradiance

Q_{core} Heat dissipated in the core components

To determine the transient profile, the equations are discretized and the temperatures are calculated at incremented time steps.

Once the surface temperature for a time increment is known, the core temperature is determined. The core temperature represents the average temperature inside the satellite.

Modes of heat transfer within a satellite include conduction through the structure and radiation between internal surfaces. An average thermal resistance (R_{core}) approximates the thermal relationship between the core and surface temperature. The following equation captures the relationship between the surface and core temperatures. Notice that this equation includes the thermal capacitance of the core, thus the core temperature is transient.

$$T_{core} + m \cdot C_P \cdot R_{core} \frac{\partial T_{core}}{\partial t} = T_{surface} + Q_{core} R_{core}$$

11.4.2.3 Thermal Control Modeling

The average core temperature of the spacecraft is determined by integrating the transient temperature profile over three orbit periods. By comparing the average core temperature to the operating temperature ranges of the thermally critical components, the thermal subsystem requirements can be determined. For example, if the average core temperature is less than the nominal operating temperature (as in our case), the required thermal subsystem power increases by $\Delta T/R_{core}$.

Figure 11.10 illustrates the transient temperature profile for the spacecraft core, spacecraft surface and solar arrays.

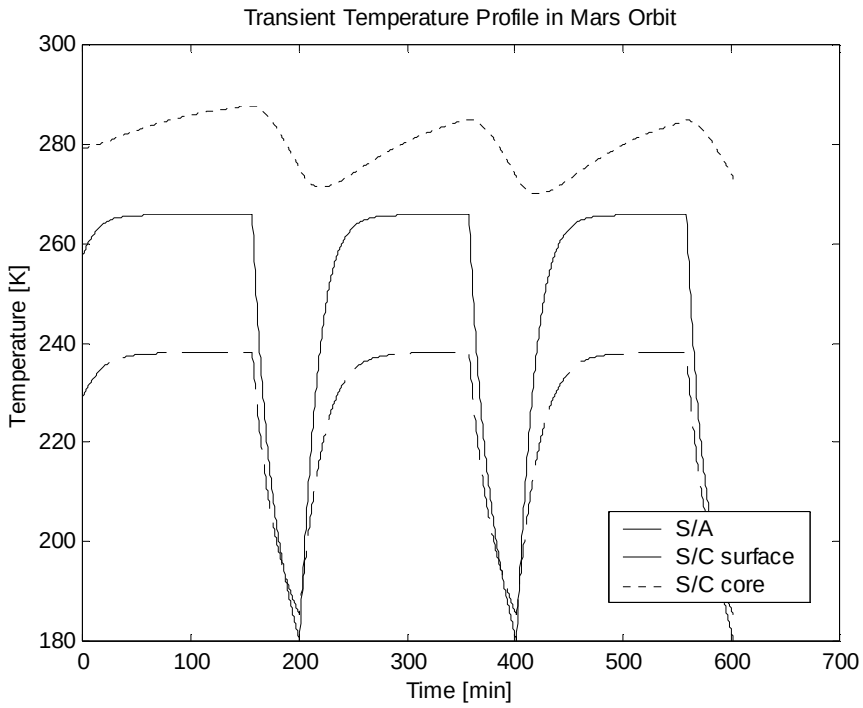

Figure 11.10: Temperature Profile for Satellite Orbiting Mars

The required core temperature is 280 K (~ 7°C), which is the median of the operating temperature ranges of the thermally critical components. The core temperature fluctuates between 270 and 286 K. The power necessary to maintain the spacecraft core in this temperature range is approximately 25W. The solar array temperature ranges from approximately 190 to 265 K. This range for the solar array is low but not unreasonable.

The total mass of the thermal control subsystem is approximated as a fraction (4%) of the dry mass of the satellite. This is the allotted percentage specified in SMAD.

11.4.3 Thermal Design Details

The thermal control subsystem consists of both active and passive control devices. The active control devices include heaters, heat pipes and louvers (if necessary). The passive devices include paints, radiators, and thermal blankets. Using passive control devices to adjust the absorption and emittance rates helps achieve a desirable heat transfer rate into and out of the satellite. Changing the ratio of absorptivity (α) to emissivity (ε) effectively increases or decreases the average spacecraft temperature. Since MINERVA is a deep space mission, thus operating in a colder environment, surface materials having a (α/ε) ratio near unity will be selected.

Radiators will dissipate excess heat, while heaters will help maintain the required temperature ranges of the batteries, tanks and electronics.

Unlike the Mars orbiting phase, the temperature during the transfer phase is quasi-steady. During transfer the distance between the sun and the spacecraft increases, thus reducing the solar-flux incident to the spacecraft. As a result, the temperature of the spacecraft slowly decreases during the nearly 300-day journey to Mars. The average surface temperature of the spacecraft during transfer ranges from 280 K (near Earth) to 220 K (near Mars).

11.5 Attitude Determination and Control Subsystem Design[42]

The Attitude Determination and Control Subsystem (ADCS) is responsible for keeping the satellite pointed in the appropriate direction for performing a given mission objective.

Attitude control for each satellite in the MINERVA constellation is achieved through the use of torquers that are driven by the outputs of the on-board attitude sensors. The sensors and actuators chosen for each satellite in this mission are dual horizon sensors, two-axis digital sun sensors, redundant coarse sun sensors; and rate gyros, momentum/reaction wheels and thrusters.

It was determined that three-axis control is necessary for the mission because of the pointing accuracy requirement, the sun-oriented solar array requirement, and the nadir-pointed payload requirement. The two latter requirements require at least two axes of control, and the last needs a third axis of control to point in the direction of flight. Full active control (using propulsion thrusters and wheels) was preferred over passive control because of the pointing accuracy requirement of 0.1°. This accuracy is needed to point the Ka-band parabolic antenna at the Earth because its half-power beamwidth is only 0.3°.

Attitude determination is accomplished by measuring the orientation of the satellite in two reference vectors fixed in inertial space. The dual horizon sensors provide information in the pitch and roll axes, and the two-axis sun sensors in the yaw and pitch axes. Thus, the horizon sensor establishes the local vertical reference (two axes) and the sun sensor supplies the third-axis reference (as well as a redundant measurement). (See Figure 11.11)

[42] JJM

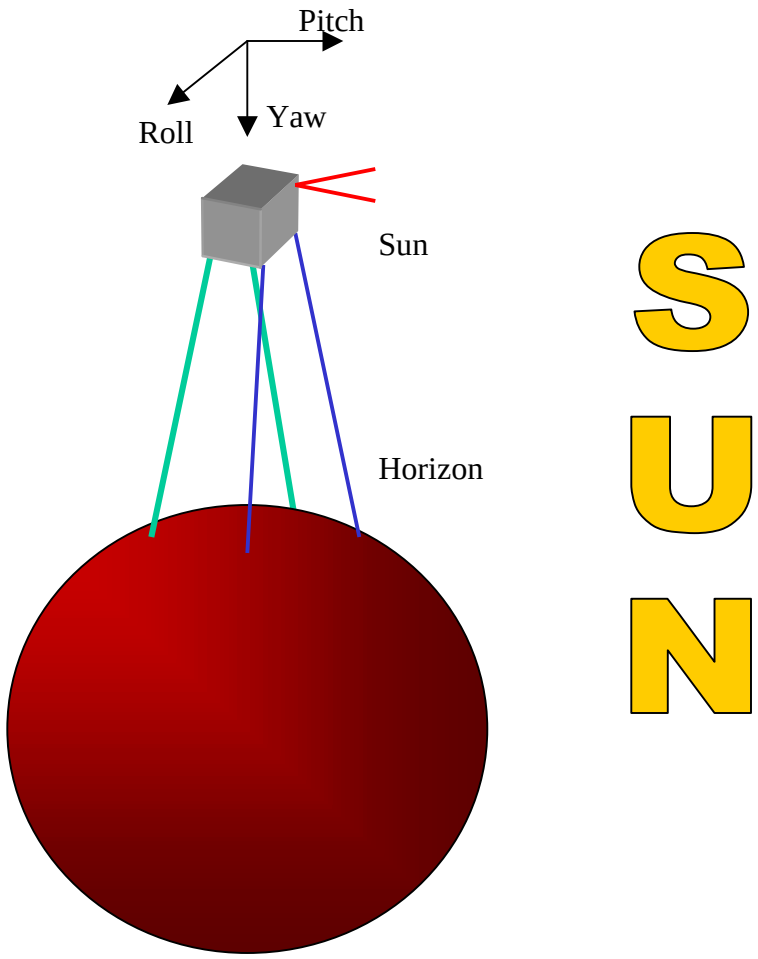

Figure 11.11: Attitude Determination Schematic

The attitude for each satellite is determined through the use of sun and horizon sensors. There is allocation within the satellite for two two-axis sun sensors and four dual horizon sensors. These instruments output the orientation of the spacecraft with respect to the sun or the planet's (Mars in this case) horizon, respectively. Both types of sensors provide high pointing accuracy, exceeding the 0.1° pointing accuracy requirement. The selected fine sun sensors have a field of view (FOV) of 64 x 64° and 0.02° accuracy. The selected horizon sensors have an accuracy of 0.05° and a 1.65 x 1.65° FOV (for the dual sensor assembly).

A three-axis gyro is to be used when the satellite cannot rely on its main sensors for attitude determination. The gyro measures the spacecraft's angular rates and, coupled with the four redundant coarse sun sensors, is part of the satellite's attitude stabilization system during safe mode. The selected gyro has three axes outputs and has a range of 1000°/second. A second on-board gyro is added for redundancy.

There is space allocated for the two accelerometers that the payload needs to determine orbit propagation. The second on-board accelerometer is added for redundancy.

Due to weight and size constraints, small momentum/reaction wheels were chosen for the actuators in each satellite. There is space allocated for three wheels, one for each body principal axis, and a redundant fourth wheel. The set of three wheels fulfils the pointing accuracy requirement also. The selected wheels have an output torque of 0.35 N-m and a momentum output range of 5-10 N-m-s. The selected wheels have an output torque greater than the maximum calculated disturbance torque of 0.15 N-m.

Torque requirements were estimated from the various disturbance torques, namely orbit insertion torque, aerodynamic torque, gravity gradient torque, and solar radiation torque. Estimation of orbit insertion torque is calculated with

$$T = \frac{1}{2}\omega_t^2 \left(I_s / \theta_{\max}\right)$$

where ω_t is the tip-off rate (angular velocity in radians/second imparted to satellite at orbit insertion), I_s is the spacecraft's moment of inertia, and θ_{max} is the maximum attitude excursion (in radians). Disturbances due to gravity are estimated using the following formula

$$T_g = \frac{3\mu}{2R^3}\left|I_z - I_y\right|\sin(2\theta)$$

where μ is Mars' gravity constant, R is the orbit radius, θ is the maximum deviation of the Z-axis from local vertical in radians (corresponding to 0.1°) and I_z and I_y are the moments of inertia about the z and y axes of the spacecraft. Solar radiation torque is calculated to be

$$T_{sp} = \frac{F_s}{c} A_s (1+q)\cos\left(i\left(c_{ps} - c_g\right)\right)$$

where F_s is the solar flux at Mars, c is the speed of light, A_s is the surface area, c_{ps} is the location of the center of solar pressure, c_g is the center of gravity, q is the reflectance factor (estimated 0.6) and i is the angle of solar incidence.

Finally, the aerodynamic torque is assessed to be:

$$T_a = 0.5\left[\rho \cdot C_d \cdot A \cdot V^2\right] \cdot \left(c_{pa} - c_g\right)$$

where ρ is the atmospheric density, C_d is the drag coefficient (estimated 2), A is the surface area, V is the spacecraft velocity, and c_{pa} is the center of aerodynamic pressure. Each estimated torque is compared and the greatest is selected to be the maximum torque requirement. In this case, orbit insertion was the largest torque requirement of 0.15 N-m.

Image removed due to copyright restrictions.

Figure 11.12: Horizon Sensor

Image removed due to copyright restrictions.

Figure 11.13: Reaction Wheel

Image removed due to copyright restrictions.

Figure 11.14: Sun Sensor

11.6 Structural Design[43]

The spacecraft structure mechanically supports all other spacecraft subsystems. Spacecraft structure includes primary structure that carries the spacecraft's major loads and secondary structure that supports wire bundles, propellant lines, and other components. The bus group modeled the spacecraft structure to determine the mass and volume of the spacecraft bus. By summing the individual mass components of the subsystems, the total spacecraft bus mass was computed. A pie chart depicting the subsystems and component mass percentages is shown in Figure 11.15 and Figure 11.16.

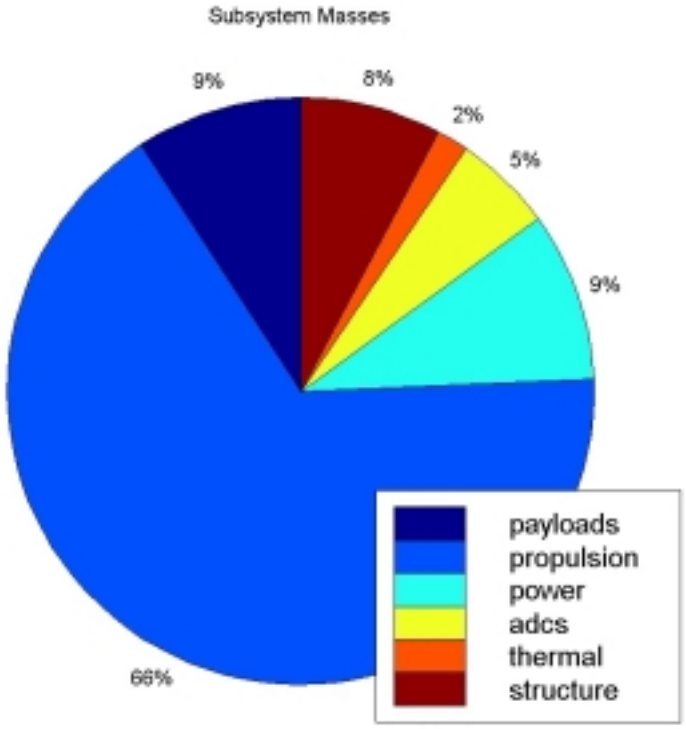

Figure 11.15: MINERVA System Mass Breakdown

[43] JMA

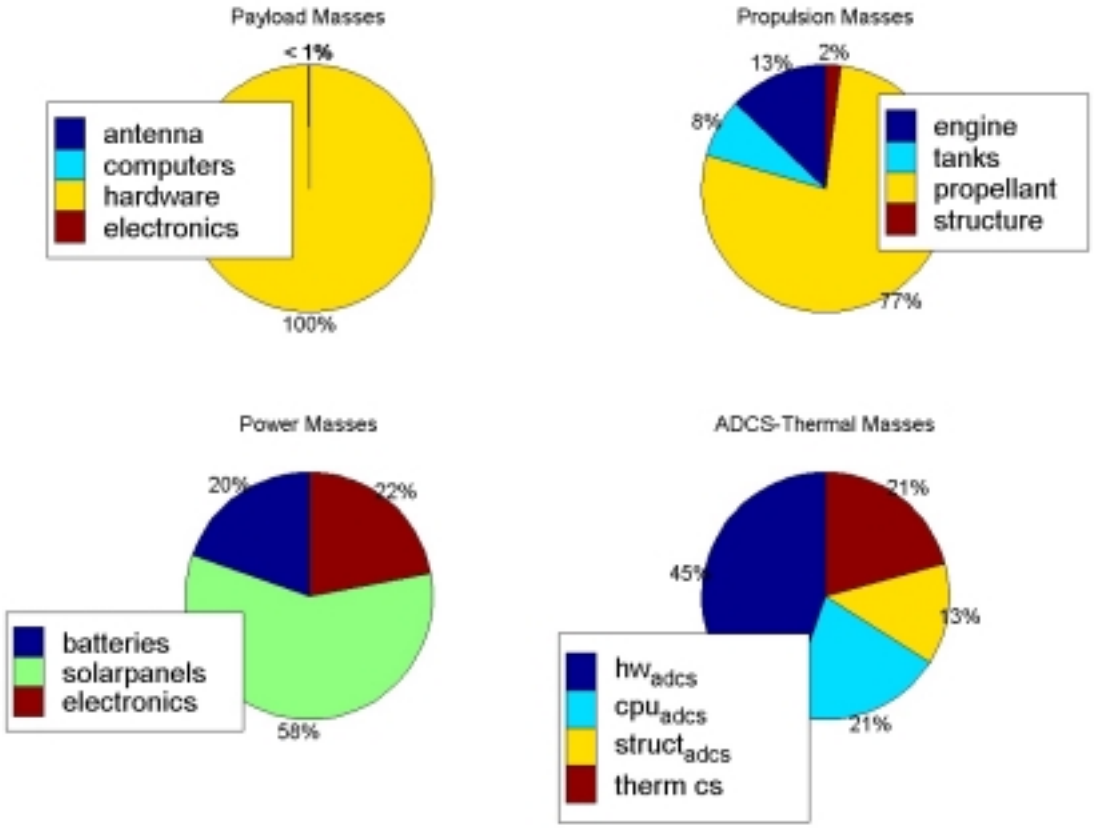

Figure 11.16: MINERVA Subsystem Mass Breakdown

In order to determine the feasibility of the design, the bus group calculated a rough estimate of the volume of each spacecraft. SMAD indicates that the average density of spacecraft built between 1978 and 1984 was 79 kg/m^2. This density was used to compute a rough estimate of spacecraft volume.

The spacecraft structure serves another role in that it interfaces with the launch vehicle. To assure that the spacecraft would fit into the launch vehicle fairing, Pro-Engineer was used to model the spacecraft in both deployed and stowed configurations.

Various spacecraft models are shown in Appendix C.

11.7 Bus Cost Modeling[44]

In addition to mass, power, and size, the bus group modeled the cost of the subsystems in an effort to estimate the total mission cost from the ground up. This activity served two main purposes. First, in order to compare different architectures in a common way, the performance of each was normalized by its cost. Thus, a most "cost-efficient" design could be chosen. Second, the mission had an overall budget requirement of $300 million. Relatively accurate modeling of spacecraft cost is an important scaling factor for the total mission cost.

To estimate the costs of the subsystems, Cost Estimating Relationships (CERs) from SMAD Section 20.3 were used. CERs are generated using statistical regression of data from historical space missions. The relationships used in the bus cost model calculate Research, Development, Testing & Evaluation (RDT&E) costs separately from the Theoretical First Unit (TFU) costs. Each relationship scales the cost with some design parameter pertinent to the system. Typically, this is scaled with the subsystem dry weight, but may include relationships based on power or size dimension.

The accuracy of these models is not very good – typically between 25 and 50 % of the cost. For purposes of calculating a cost per function for architectural comparisons, this inaccuracy is not very relevant, as all proposed designs will benefit or suffer equally. Choosing the better of two options is still possible. However, when calculating the total spacecraft cost in order to meet the cost requirement, the inaccuracy can put the mission drastically over budget. Therefore, in a separate cost model designed to estimate mission cost, a 25% accuracy margin was applied. Figure 11.17 and Figure 11.18 show the cost breakdown for a single MINERVA spacecraft. TFU cost is used in a learning curve in calculating the total hardware costs for the spacecraft.

[44] DMB

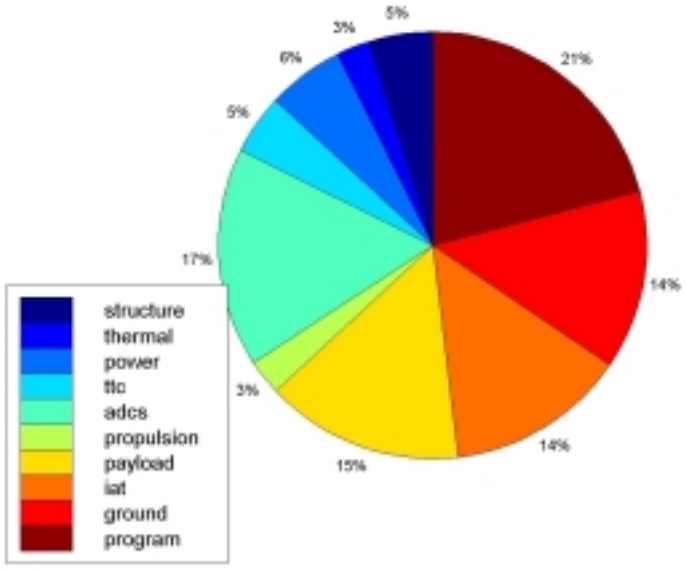

Figure 11.17: RDT&E Costs for MINERVA

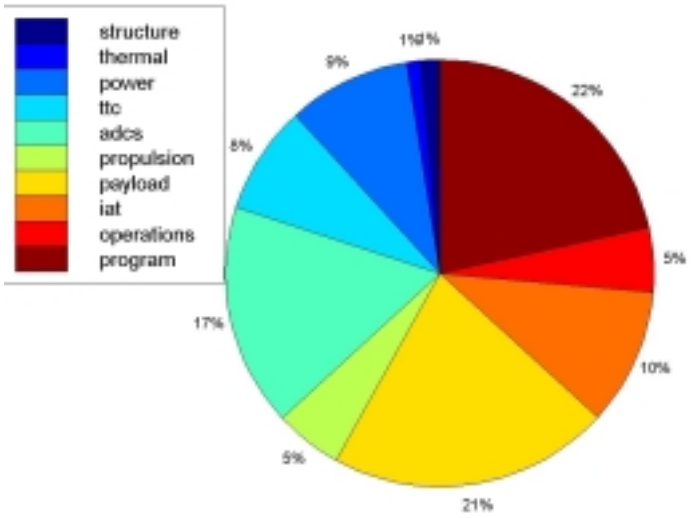

Figure 11.18: TFU Costs for MINERVA

11.8 Detailed Satellite Design[45]

The bus module estimates overall mission cost and spacecraft budgets based on models of subsystem elements. Table 11.3 shows the list of components modeled on a MINERVA spacecraft, along with the number, mass, and power of each subsystem. For those components that drive the size of the spacecraft, critical dimensions are also listed. For example, the antenna diameter, propellant tank diameters, and solar array areas are drivers of spacecraft size and are included in the design.

The solar array power is the end-of-life power the arrays can produce at Mars. While in transit closer to the sun, the power density is higher. Throughout the spacecraft lifetime, the performance will slowly degrade, ending at 418 Watts after 6 years.

Reliability is increased at the subsystem level through redundancy. There are extra batteries, sensors, and an extra reaction wheel. In safe mode, other subsystems are used to accomplish similar functions. For example, the solar panels can be used as sun sensors, the thrusters are used for attitude control, and gyros are used in place of horizon sensors.

The launch structure refers to the docking rings on the top and bottom of each spacecraft. As seen in the drawings of the stowed spacecraft (Appendix C), the main antenna hangs over the interface, so a standard belt could not be used for attachment. The docking rings must remain attached to the spacecraft, rather than separating, to avoid damaging the antenna. Therefore, the mass of the docking rings must be included in the vehicle mass that undergoes thrust maneuvers.

The spacecraft maintains contact with the sun, Mars, and Earth through Sun-Nadir steering. Every 180º of orbit, the spacecraft flips about the Nadir pointing axis, reversing the north-south solar array directions. The solar arrays need only rotate through 180º, and then rotate back. This avoids wrapping of any cables, and allows the Earth antenna to always point in the proper direction.

[45] DMB

System Component		Number	Mass	Total Mass	Total Power	Critical Dim
Payload		**1**	37	**37**	**190**	Ant Diam = 2m
ADCS				**30.72**	**39**	
	Sun sensor	6	1.17	7	0.8	
	Horizon Sensor	4	0.7	2.8	5	
	Gyroscope	2	0.65	1.3	10	
	Accelerometer	2	0.1	0.2	1.2	
	Reaction Wheel	4	3.75	15	22	
	Structure	-	4.42	4.42	-	
Propulsion				**273.82**	**25**	
	Propellant	-	177.4	211.84	-	
	Main Engine	1	4.5	4.5	15	
	ACS Engine	12	0.5	6	-	
	Propellant Tank	2	10.59	21.18	-	Diameter = 0.6m
	Blowdown System	1	20	20	-	
	Feed System	-	5	5	10	
	Structure	-	4.43	5.3	-	
Thermal				**6.98**	**11.56**	
	Heater	-	2.33	2.33	11.56	
	Radiator	-	2.33	2.33	-	
	Insulator	-	2.33	2.33	-	
Power				**50.089**	**418**	
	Solar Arrays	2	10.99	21.98	418	Area = 4.00 m^2
	Electronics	-	8.34	8.34	-	
	Batteries	6	1.2415	7.449	393 W-hrs	
	Wiring	-	1	1	-	
	Structure	-	11.32	11.32	-	
Launch Structure		-	10.52	**10.52**	-	
			Total Mass:	409.129		
			w/ margin	**470.49835**		

Table 11.3: MINERVA Bus System Design, Including Sub-System Mass and Power

11.9 References

Wertz, J. R. & Larson, W. J. (ed.) Space Mission Analysis and Design. (3rd ed.) Torrance, California: Microcosm, Inc. 1999.

Wertz, James, ed. Spacecraft Attitude Determination and Control. Kluwer Academic Publishers: Dordrecht, The Netherlands. 1978.

12 Earth Ground Segment

The Earth Ground Station will consist, in part, of a dedicated area within the facilities controlled by the Jet Propulsion Laboratory.

This station will serve a central processing function for both MINERVA and MSEs operators, and MSEs principal investigators. It will collect, process and disseminate all the information from and to MINERVA, which is communicated through DSN.

The staff will consist of dedicated engineers and technicians, to be supplemented by crisis action team members as necessary.

13 Cost Analysis[46]

13.1 Overall Philosophy

One of the specific minimum requirements levied on the MINERVA system was a cost cap. The class program plan states:

"The cost to IOC (Initial Operational Capability) is not to exceed $300 Million."

We have interpreted this cost figure to be in constant fiscal year (FY) 2000 dollars. All cost figures in the following analyses are calculated consistent with this assumption. Program costs include launch, spacecraft development and ground station development. Operations costs, including those incurred in transit to Mars, are not included. On-orbit checkout activities are included.

Treatment of costs was divided into three distinct phases, reflecting the nature of the ongoing activity. During the first phase, preparation for the Trade Analysis and Requirements Review (TARR), cost was not a major driver because of the intent to define competing families of architectures and down-select to a single architecture. Cost was assessed at the TARR to give a sense of how big a constraint it would be in the preliminary design phase. As indicated below, this early assessment clearly indicated that cost would be a major consideration and constraint for system design.

The second phase, preparation for the Preliminary Design Review (PDR), included cost analysis as an integral part of the design process. Due to the lack of specific design details, we used mass-based Cost Estimating Relationships (CERs) to approximate total system costs. This approach led to the flow down of an allowable spacecraft mass to the bus and payload groups, which constrained the design. Cost constraints, along with requirements assessment, led to the selection of a four spacecraft constellation.

In the final phase, the definition of design specifics for the Critical Design Review (CDR) allowed a more sophisticated approach for estimating costs. We maximized use of non-mass-based CERs in order to let specific design details (such as antenna size, lines of software code, etc.) determine our calculated costs. This approach had a more significant implication for design trades, since the cost implications of each trade were more readily apparent.

In the last two phases, we applied two elements of conservatism to the cost estimation process. We retained a 25% cost margin at PDR, relaxing this margin to a 15% level at CDR. The margin represented risk management for cost, since it protected against anticipated cost growth associated with the ongoing design process. Retaining 15% margin at CDR protects against cost growth that has historically taken place during the production, integration and test phases of a program.

---

[46] RED

We also applied a cost factor to the spacecraft development and ground system cost estimates to account for limitations in the CER-based methodology. In the pre-PDR phase, the cost factor was based on comparison to six deep space missions, which provided some validation for the assumed cost levels. During the pre-CDR phase, a lower cost factor was used on the assumption that non-mass-based CERs would provide greater accuracy than was possible with mass-based CERs. However, due to the complex selection of CERs for this phase, it was not possible to do a validation through comparison to other deep space programs. Cost elements were generally of the same magnitude as had been observed in the previous phase. Because of this lack of validation, these cost estimates should be treated as approximate. In a real program, it would be essential to perform a thorough bottom-up cost estimate for comparison to the CER methodology in order to ensure cost realism in the estimation process.

13.2 TARR Cost Estimation

The “architecture family” approach used during this phase makes cost estimates highly speculative. We looked at a large range of possible architectures, whose costs would have varied widely. Each architecture was assessed subjectively to see if it contained substantive cost drivers that might have proved problematic.

At the TARR, the MINERVA team selected a single family of architectures (based on a Mars orbiting solution), allowing generation of a single point estimate to give rough order of magnitude (ROM) cost. This estimate was chosen to be in the mid-range of candidate design solutions for that family of architectures.

The representative sample chosen for cost estimating purposes was twelve satellites (with 90% learning curve) and 4 Delta II launches. The elements of cost for this ROM estimate, along with their source, are listed in Table 13.1. The payload line includes elements for communication, position determination and observation (C+N+O). This ROM calculation was not a true cost estimate in the normal sense. Rather this was an attempt to see where in the total cost spectrum a sample architecture might fall. The sample architecture is from the Architecture 3 “family” (Mars orbiting), but it does not necessarily represent the number of satellites or launch costs that would actually result from the next phase of design.

The implications of this cost estimate were that we would need to be at the lower end of cost spectrum for this type of architecture. Since total number of spacecraft in the constellation was assumed to be a major cost driver, the estimate implied that the eventual design would probably be in the four to six spacecraft regime rather than twelve spacecraft.

Table 13.1: TARR ROM Cost

Cost Component	RDT&E (R)	1st Unit	Prod (12)* (P)	Total $ (R+P)	Source
Payload	37.1	15.1	124.2	161.3	CER
S/C Bus	15.1	7.4	60.9	76.0	SMAD
Integration Assembly Test	20.0	1.0	8.2	28.2	
Program Level	25	10	82.3	107.3	
Ground Support Equipment	11			11	
Launch/On Orbit Support		0.7	5.8	5.8	
Flight S/W	12			12	
CR Cost	120.2	34.2	281.3	401.5	
Fee (10%)	12.02	3.42	28.13	40.15	
Government Cost	132.22	37.62	309.4	441.65	
Launch				200	
Total Program Cost (to IOC)				**$641.7M**	

* Using 90% learning curve

One option raised at the TARR to accommodate the possible difficulty with doing the mission within the cost cap was to consider international financial partnerships. This option was not pursued due to the fact that further system analyses (post TARR) showed a four spacecraft configuration could meet performance requirements without exceeding the cost cap.

The last resort option briefed at the TARR was the possibility of relaxing some technical requirements to reduce costs. While minimum requirements were met in the next phase, it proved necessary to delay implementation of the observation mission to a future phase.

13.3 PDR Cost Estimation

The PDR cost estimation was done from the top down, starting with the $300 million cost cap, subtracting launch cost, and using a mass-based CER approach to calculate an allowable (i.e. affordable) mass for the spacecraft, given a certain number of spacecraft. The mass allowable was allocated to the bus group, and a sub-tier allocation of mass was passed to the payload group. This methodology ensured that, as long as the total spacecraft dry mass stayed within the established limits, total system costs would stay below the cost cap.

The cost methodology used looked first at potential launch vehicles. The Delta II and Athena II were chosen because of their low cost per kilogram to orbit. Foreign launch vehicles were not considered because foreign launchers might add an undesirable element of political risk to the program. We selected a 12-hour parking orbit (GPS orbit) for purposes of estimating the necessary launch vehicle performance. The baseline design at this point included electronic propulsion for transfer from the parking orbit to Mars. In the last design iteration prior to PDR, the Delta II was chosen due to insufficient performance from two Athena II launchers.

Spacecraft development costs were calculated based on the number of spacecraft in the constellation, a learning curve (95%), a 25% cost margin, and a cost factor to account for limitations in the mass-based CER methodology. Note: the CER methodology used is described in more detail in the cost modeling portion of the bus description (section 12.7).

To validate the cost levels calculated by the CER methodology, outputs of the cost model were compared to data from six deep space missions. These missions were: Mars Climate Observer, Mars Polar Lander, Stardust, Deep Space 1, NEAR and Lunar Prospector. This comparison showed the CER model was under-stating the probable costs, which indicated the need for a cost factor to scale costs to a more realistic level. Table 13.2 presents cost and mass information on the six deep space missions.

Table 13.2: Deep Space Missions (Cost/kg)

Deep Space Missions	Cost/kg (normalized 0 –1)	Comments
Mars Climate Observer	.571	Heavy, out of family
Lunar Prospector	.255	Simpler mission
Mars Polar Lander	.215	
Stardust	.427	Similar complexity, size
Deep Space 1	.247	
NEAR	.251	
Average	.316	
Cost Model	.240	Assumes 400 kg spacecraft

Given the large dispersion of cost/kg values, we compared the cost model result (.240) to one of the missions that was above average cost/kg. Stardust (.427) was a mission of similar size and equal or greater complexity. Taking the ratio of the Stardust cost/kg to the value from the model (for a 400 kg spacecraft mass) yielded a cost factor of 1.78.

Given the need for design iterations, the output of the cost model was expressed as spacecraft dry mass allowable for a range of possible numbers of spacecraft. This output is reflected in Figure 13.1.

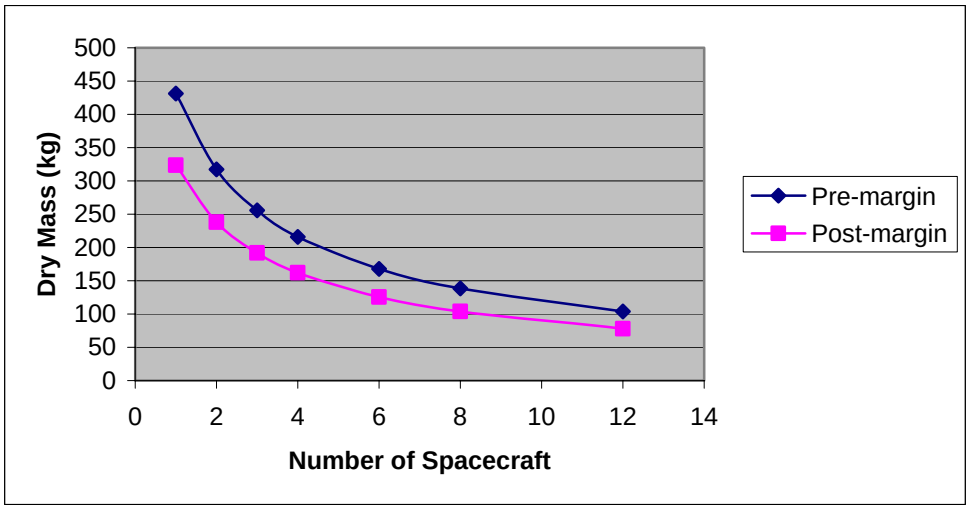

Figure 13.1: Allowable Spacecraft Dry Mass

13.4 CDR Cost Estimation

Due to the increasing availability of design detail during this phase, it was possible to use design-based CERs to drive the cost estimate. The payload group and the bus group each used CERs from SMAD section 12.7.

Design trades and assessments in this phase took place in a concurrent engineering mode in the design lab. The payload group module provided payload costs as an input to the bus group module, which added bus costs and provided two cost figures to the systems MATLAB module. These figures were the research, development, test and evaluation (RDT&E) costs and the theoretical first unit (TFU) costs associated with the design under evaluation. The launch module evaluated the spacecraft mass associated with the design and provided the systems module with a launch cost. Total ground software cost was constant in the systems module, based on information from the payloads group (see section 11.2.4.) The concurrent engineering cost scheme is presented in Figure 13.2.

The systems module used these inputs to generate total systems costs, which were made up of launch, spacecraft development and ground station development costs. Within the systems module, spacecraft development costs included a 10% profit, a 15% cost margin and a 1.25 cost factor to reflect potential inaccuracy in the CER methodology. Even with the cost factor, it should be noted that cost estimates using this methodology cannot be considered as reliable as bottom-up cost estimates. In a typical program, such a bottom-up cost estimate would be developed concurrently with detailed design, providing a sanity check for CER-based estimates.

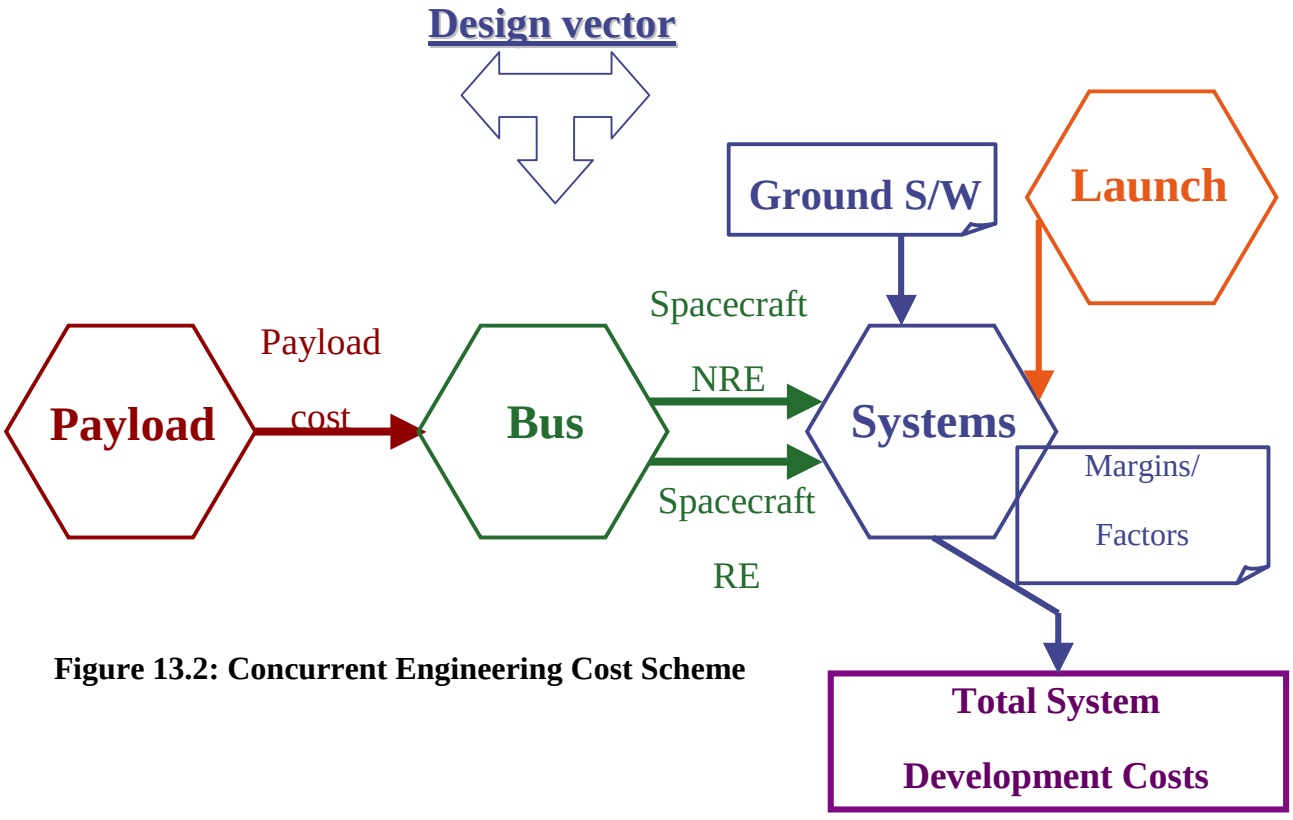

Figure 13.2: Concurrent Engineering Cost Scheme

Ground station development also included a 10% profit and a 15% cost margin, although no cost factor was applied. Ground station costs were modeled as 1.5 times the value of ground software (see section 10.5 for a software cost description.) This factor encompassed anticipated costs for equipment, management, etc. We assumed JPL would provide space and equipment to minimize costs because of their dependence on the MINERVA system to support JPL Mars missions.

The launch vehicle selected in this phase of design was the Delta III. We assumed a reduction in Delta III costs would come about because of EELV-related efficiencies and market pressures, resulting in a launch cost of $56.25 million (25% reduction from today's $75 million cost.)

Finally, the cost estimation specifically excludes all operations costs, both for transit to Mars and for on-orbit operations at Mars. The class elected to perform an official design freeze approximately two weeks before CDR. Table 13.3 presents the four options considered for the down-select, which looked at three versus four spacecraft and electrical versus chemical propulsion. Option 2 was selected because it came in under the cost cap (at a CDR margin level) and met all requirements. Options 3 and 4, with three spacecraft, did not meet all technical requirements.

Table 13.3: Design Freeze Down-Select

	# of S/C	Propulsion	Launch	Cost	Margin	Total
Option 1	4	EP	Delta 3	291.4	54.0/32.4	345.4 323.8
Option 2	4	Chemical	Delta 2	253.8	51.0/30.6	304.8 284.4
Option 3*	3	EP	Delta 3	267.1	48.0/28.8	315.1 295.9
Option 4*	3	Chemical	Delta 2	231.6	45.4/27.2	277.0 258.8

*Does not meet all requirements (coverage, Gb/sol)

By the time of final preparations for CDR, some minimal design changes and modifications to cost estimations resulted in slightly different final cost figures. Margin was available to add a payload capability for on-orbit position determination fix, which improved timeliness of the position determination capability.

Figure 13.3 shows the major elements of cost that contributed to the final MINERVA system cost of $297.9M. Note that margin is indicated as 11% because the launch costs did not include any margin.

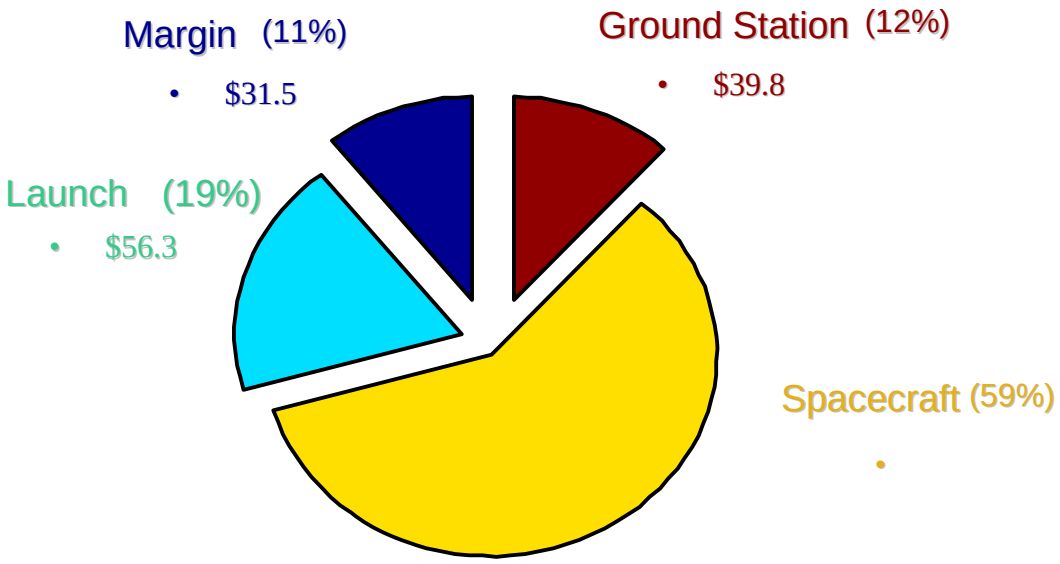

Figure 13.3: Major Elements of Cost for MINERVA

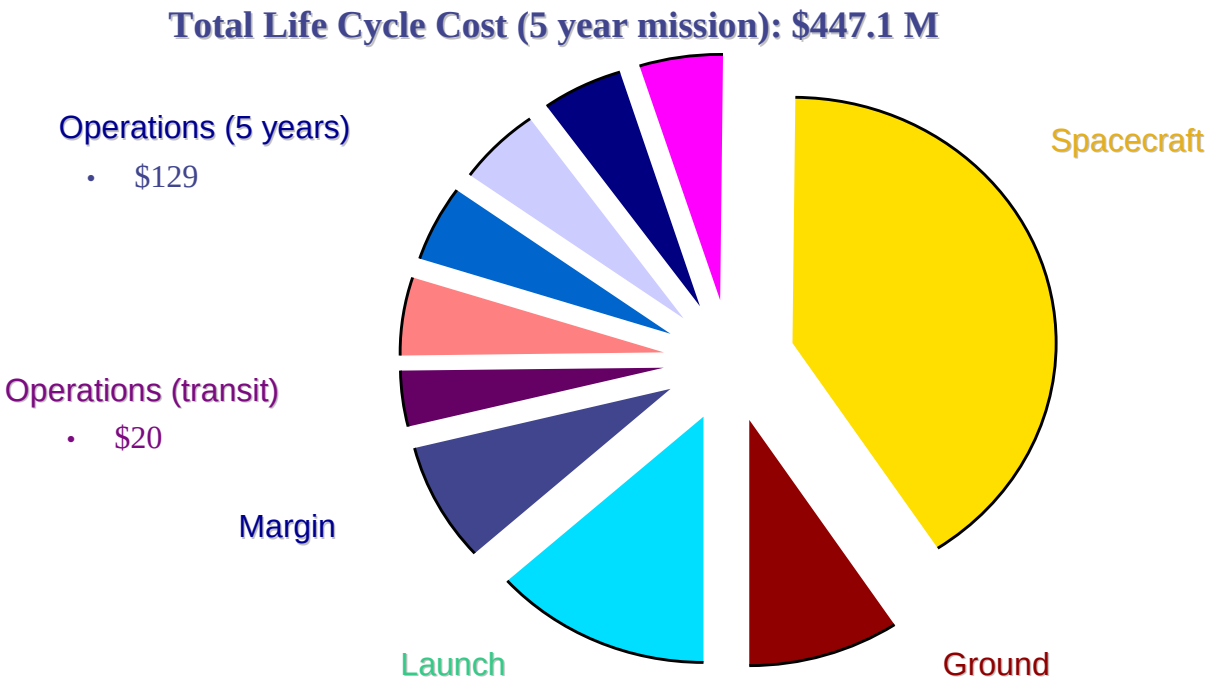

Figure 13.4: Life Cycle Cost for MINERVA

The payload group calculated operations costs for the MINERVA system.

Figure 13.4 captures the total life cycle costs for MINERVA, given the requirement for a five-year life on orbit and the 286 days of transit time. As indicated in the figure, the total life cycle cost (5 year mission) would be $447.1 million.

Figure 13.5 shows the final funding profile for the mission. This profile was derived using the spreading formula from SMAD.

Total Program Cost: $297.9 M*

(CY00 $M)

Program Yr	1	2	3	4	5	6	7	8
Calendar Yr	2001	2002	2003	2004	2005	2006	2007	2008
Funding	4.8	26.1	51.1	67.0	67.0	51.1	26.1	4.8

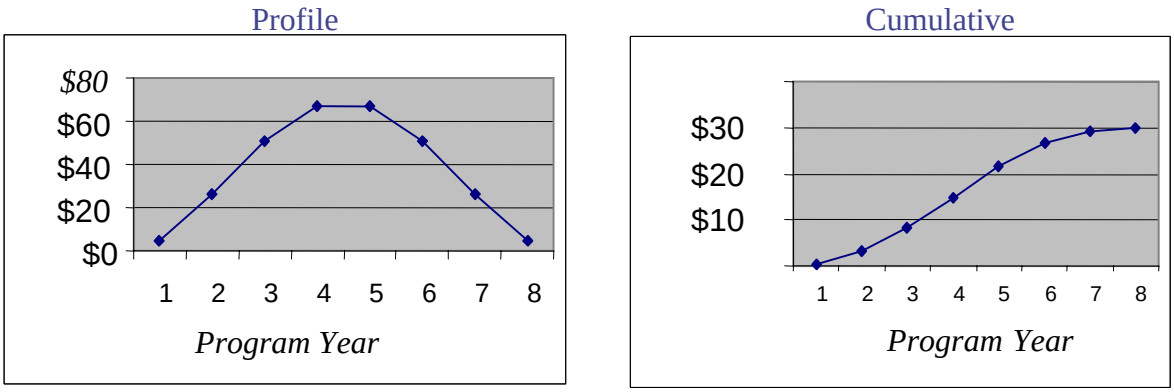

Figure 13.5: Funding Profile

13.5 Conclusions

The total program cost estimated at CDR ($297.9 M) contained a 15% cost margin below the $300M cost cap for spacecraft and ground station development. This margin protects the program from potential cost growth during the production, integration and test phases of the program. However, due to the lack of available means to validate the 1.25 cost factor (which was used to account for inaccuracies in the CER methodology), these cost figures cannot be regarded with high confidence. Cost risk for the program would be greatest in the areas of flight and ground software, integration and test, and launch (if EELV-related cost savings are less than 25%).

14 System Reliability

The MINERVA system reliability analysis was accomplished mainly through the use of three tools: failure tree analysis, safe modes analysis, and event reliability analysis. Much of this analysis was accomplished and carried through implicitly throughout the design, often with different reliability concepts used within different subgroups. A more established and explicit manner of executing the reliability analysis earlier in the design would have aided in the optimization and clarification of functions and components.

14.1 Failure Tree Analysis[47]

This analysis included an examination of the critical failures that could occur within the MINERVA system, rather than the common fault tree analysis method that examines more closely the individual faults and how they propagate. It is recognized, however, that each of the critical failures in MINERVA would likely result from a lower level fault. Taking this into account, much of the reliability and redundancy analysis held to the philosophy that utilized multi-path subsystems as much as possible, rather than completely redundant components. Some completely redundant components were necessary, however, to prevent subsystems from the possibility for a single-point failure. For the sake of clarifying and simplifying the problem, this analysis attends to the setup portion of the MINERVA lifetime separately from the nominal lifetime operations.

The setup portion of the system includes launch, separation, detachment of the individual spacecraft, transfer from the parking orbit to the Mars sphere of influence, capture into the Martian orbits, and deployment of necessary spacecraft mechanisms. Launch, separation, and transfer exhibit binary reliability; either they successfully occur or they fail, due to the united nature of the spacecraft during these phases. Detachment, Capture, and Deployment may involve partial success, to where only some of the spacecraft meet success in these phases. Figure 14.1 diagrams the MINERVA Setup failure tree with critical subsystem or activities listed under the “success” of each phase.

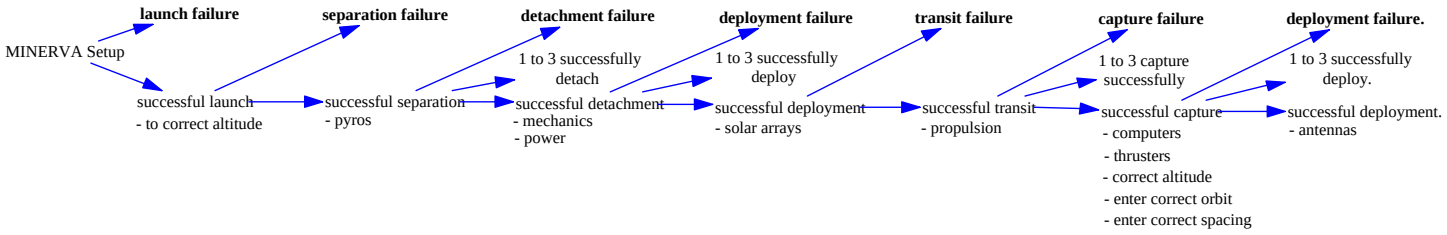

Figure 14.1: MINERVA Setup Failure Tree

[47] RM

The failure tree analysis for the nominal lifetime operations segment includes the possibility of no failures, externally-caused failures, and internally-caused failures. External sources of failure account for interactions with external interfaces, as well as environmental factors. Internal sources of failure include system operators, software, and hardware. Due to the highly coupled nature of subsystems within each of the spacecraft, the analysis examined critical failures within components rather than subsystems. Figure 14.2 diagrams the MINERVA nominal operations failure tree.

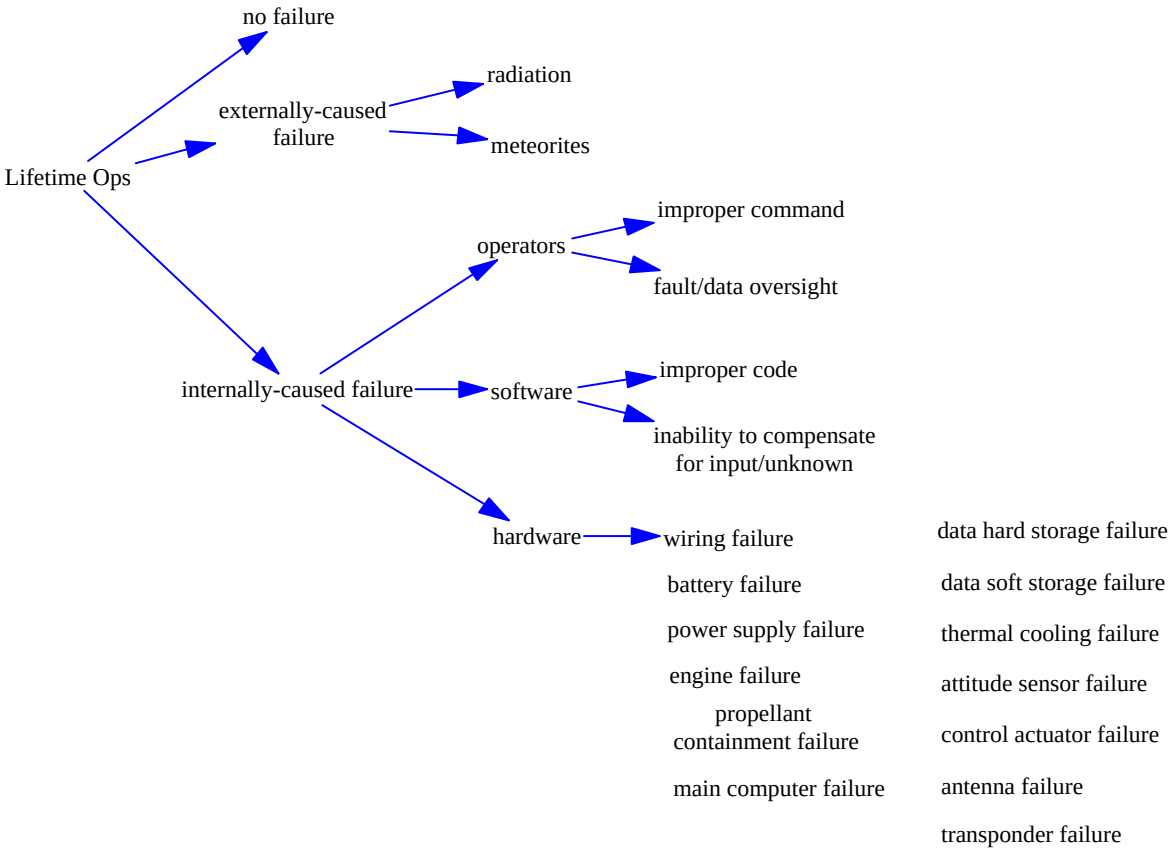

Figure 14.2: MINERVA Nominal Operations Failure Tree

14.2 Safe Modes[48]

Each MINERVA satellite is capable of entering three levels of Safe Mode, which exhibit progressive levels of operations reduction or shutdown. The advantages of this anomaly resolution scheme lie with a graceful implementation of recovery methods, and by the same notion, graceful degradation of system functions. This method also maintains a high level of availability to the users rather than a scheme by which the satellite goes directly to system shutdown each time an anomaly occurs. This method uses autonomy to compensate for the high time latency in communication compared to that experienced by Earth-orbiting satellites. As the MINERVA system will see about a twenty-minute time lag between origination and receipt of a satellite status transmission, the satellite must have the ability to take autonomous action to prevent spacecraft loss within those twenty minutes. The disadvantage of this level of autonomy results from additional complexity within the system as well as increased cost and time in the development and testing of the Safe Mode software.

14.2.1 Safe Mode 1

Should a satellite's regular subsystem checkout identify a problem, or a subsystem send an anomaly flag, the spacecraft will enter Safe Mode 1. This mode is the first level of anomaly/fault resolution. All anomaly/fault resolution efforts begin in this stage to determine the nature and severity of the anomaly.

Anomalies include irregularities in system functions, such as incorrect power levels or unexpected signals. Faults include non-performance of system functions, such as loss of power or absence of required signals.

In the specific occurrence that the main processor resets, an identical backup processor runs operations while the main computer reinitializes. The backup processor maintains and then reloads the primary processor with all recent satellite navigation and user positioning information, which is in non-volatile storage for this reason.

If at all possible, the satellite "flies through" problems in this mode, and uses autonomous resolution schemes to either correct or reroute around the anomaly or fault. Satellites use self-checking and cross-checking with other MINERVA satellites in order to pinpoint the source and effects of the anomaly. For example, antenna anomalies first receive scrutiny through self-diagnostic procedures, and then through cross-link testing with other MINERVA satellites.

In this mode, the satellite holds primary analysis responsibility, and will only notify the Earth Ground Station (EGS) of Safe Mode 1 activity within the regular transmission cycles. Should the severity of the anomaly exceed Mode 1 definitions and abilities of the satellites to correct the problem, the satellite enters either Safe Mode 2 or 3, and transmits a notification and status signal to the EGS for assistance.

---

[48] RLM

14.2.2 Safe Mode 2

This mode includes non-critical power or mechanical failures. The satellite cannot fix the problem autonomously but complete operational shutdown is not necessary. This mode will attempt to maintain the highest level of availability possible with degraded system health. The intermediate level of operations reduction may include the decision by the EGS to shut down individual satellite components or subsystems.

14.2.3 Safe Mode 3

This mode involves the highest level of system shutdown, to where availability is not of concern, but rather saving the spacecraft for future utility. This mode is entered as a result of a spacecraft critical control failure such as a loss of control software, ADCS sensors, actuators, and thrusters. It is essential that each satellite maintain the ability to account for these critical failures and their propagation, since there may be up to fourteen hours between the time of failure and contact with the EGS.

Safe Mode 3 software accounts for the criticality of circumstances and length of communication latency by autonomously shutting down all non-essential subsystems, turning nadir to Mars, and pointing the solar arrays normal to the sun until instructions are received from the EGS.

14.3 Event Reliability Analysis[49]

Like the failure tree analysis, this analysis was broken down into set-up and nominal operations segments. Much of the set-up design was driven by cost rather than by reliability due to the limited number of options available within the MINERVA budget. For this reason, a single point failure exists at the launch phase, with a single booster rather than distributed launches. Table 14.1 details the reliabilities used in this analysis for each phase.

[49] RLM, ZW

Table 14.1: MINERVA Reliabilities by Phase

Phase	Reliability	Comment
Launch	0.997 (or 0.90)	Paper estimation (or infant mortality likelihood)
Separation	0.99	Separation from the booster/fairing
Detachment	0.99	Detachment of individual spacecraft
Transfer	(0.005 failures/year)	Individual transfer from Earth to Mars
Capture	0.99	Using conventional chemical burns
Deployment	0.99	Deployment of solar arrays and one antenna

The Normal Lifetime Operations analysis included closer examination of which components or functions should be interlaid with redundancy and rerouting ability. Table 14.2 details the failure rates used in this analysis.

Table 14.2: MINERVA Subsystem Failure Rates

Subsystem	Failure Rate (number of failures/year)	Comment
ADCS	0.001	
Payload	0.00201	Includes all electronics, plus steering devices
Propulsion	0.005	Includes tanks, thrusters, plumbing
Power	0.00045	Includes batteries, solar arrays
Thermal	0.002	
Computer	0.005	

The MINERVA system reliability plot Figure 14.3 combines the Setup and Lifetime Operations segments and depicts the distribution of reliability throughout the mission phases. The plot shows six years, to include almost a year for system setup plus the five-year operational lifetime requirement. At the end of the six years, the MINERVA system exhibits approximately 79% probability of success with four operational spacecraft, and 83% with three spacecraft. This point is a major factor of reliability and risk reduction for the MINERVA system. The minimum requirements can be met with only three spacecraft, but four give increased performance and reduced risk. In effect, the whole system can account for four-for-three redundancy in terms of functioning spacecraft.

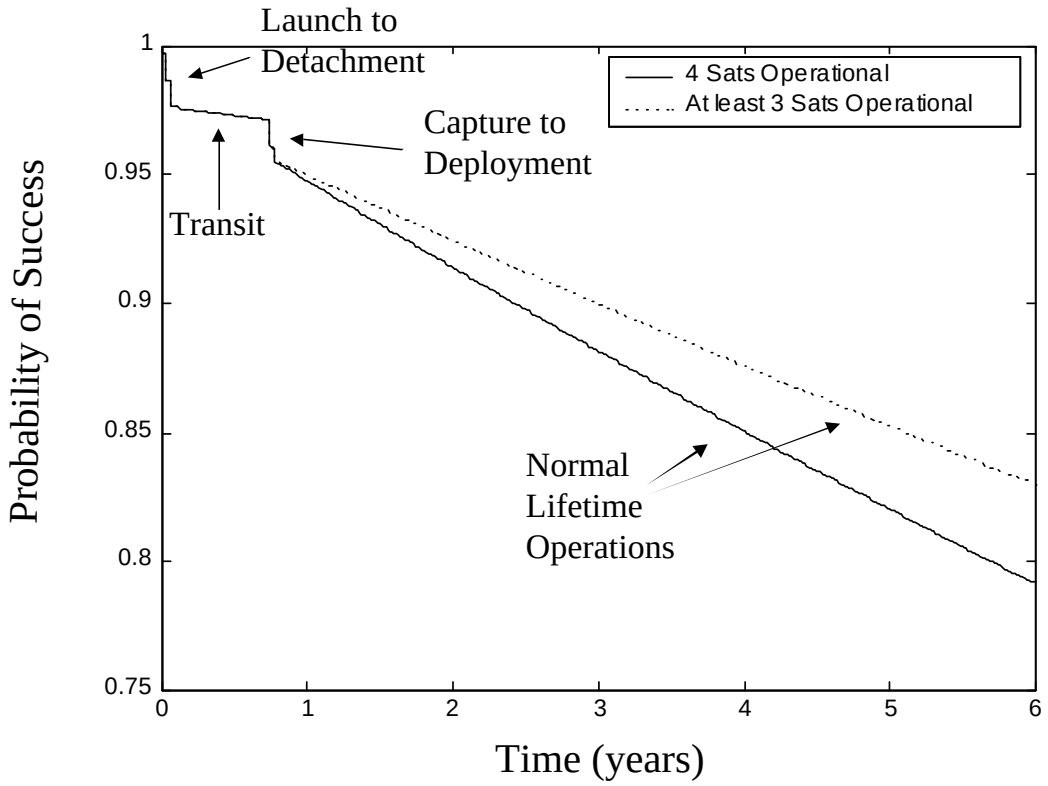

Figure 14.3: MINERVA Mission Probability of Success

15 Conclusions

15.1 MINERVA Architecture

MINERVA represents a feasible architecture for a communication and position determination infrastructure around Mars. The detailed design meets all of the technical requirements specified in Appendix A. Our cost estimate of $297.9 M satisfies the cost cap requirement, although limitations inherent in the Cost Estimating Relationship (CER) methodology would make a bottom up cost estimate highly desirable to ensure realistic cost figures. Performance of the MINERVA system significantly exceeds requirements for maximum revisit time, and provides partial coverage up to 65 degrees north and south of the equator. Selection of a four-spacecraft architecture leads to robustness in the event that one spacecraft fails, since both the communication and positioning missions can continue at a slightly reduced level of performance.

The class consensus was that a Mars-orbiting infrastructure system like MINERVA would be a significant advantage for future Mars robotic exploration missions, and it is our hope that NASA planning that is already underway will lead to development and deployment of such a system.

15.2 Lessons Learned

The biggest challenge faced by the class was maintaining communication between the different groups. The class learned several methods for improving communication and minimizing errors. In particular, frequent integration meetings of the systems group with representatives from each of the other groups helped uncover disconnects and mistakes earlier than would otherwise have been possible. Also, communication was expedited during concurrent engineering sessions due to the real-time interactions of the group and the ability to share input and output parameters with ICEMAKER software. All of the groups reported finding mistakes in their module codes as a result of evaluating the results of concurrent engineering runs. These sessions therefore led directly to rapid improvement in sophistication and accuracy of modeling the various systems in MATLAB code.

Over the course of the semester, the class experienced two significant transition points. Our efforts to retain design flexibility allowed innovative thinking, but the team reached a point after the TARR when a significant reduction of the trade space was essential in order to meet design review milestones. Completion of the TARR led to the reorganization of the class into different teams developing the various aspects of the design. Once the class was able to make this transition, the groups were able to complete their preliminary design activities. Based on this experience, the systems group encouraged a rapid transition to detailed design activities and concurrent engineering sessions after completion of the PDR. The class was successful in maintaining momentum during this second transition, which led to a detailed design campaign that culminated in CDR and generation of this design document.

The class found concurrent engineering to be a useful practice for rapid characterization of a multitude of design options. Each group continued their detailed design analysis work in between sessions to clarify which options should be evaluated in concurrent engineering. ICEMAKER was a useful tool for exchanging input and output values through its subscribe and publish capabilities.

Most of all, the class learned about the challenges of doing systems engineering for a major design project in a large group setting. Tools, theory, and methodology were important, but so was the dynamic of human interaction. In the end, we have discovered that people determine the level of project success.

15.3 Recommendations and Future Work

Some interesting studies were left undone due to the time span of the class. A first area of additional work would address further details within the existing design. The details of heat exchangers, plumbing, and electrical wiring in the bus design, and the payload multiple access scheme and protocols in the payload design are some areas of potential improvement. With further design details, a bottom up cost estimate would be made possible. Such an estimate is very time-consuming to perform, but it is the only means of establishing a highly reliable cost estimate.

Evaluating the performance of the current design for accomplishing secondary objectives would also be an interesting study. A good example is MINERVA's potential capabilities for communication with and orbit determination of, spacecraft orbiting or approaching Mars.

A second area of work would address the expandability of the system's performance. Future work might study the best way to improve the performance of the system if more money was available. Planning for a human presence on Mars would require additional research. Possible areas of mission expansion include additional satellites for continuous coverage, reduced time to accuracy and improved reliability, improved autonomy through the uploading of replacement software, and in-situ orbit determination measurement coupled with highly autonomous software for on-board orbit propagation and MSE position determination. Future spacecraft could also perform additional missions such as remote sensing and continuous Mars weather forecasting.

MINERVA represents a plausible architecture, designed to meet the cost and performance requirements placed on the 16.89 class. The MARSNET, proposed by JPL, represents another possible architecture, meeting a different set of user requirements. With less stringent cost or data return constraints, an interesting area of future work would be to compare a wide range of such architectures on the basis of a cost per function. Feasible point designs such as MINERVA serve as a strong basis for this research.

Due to the time constraints of the semester, some design details could not be accommodated. Future work could address design of radiators, plumbing and electrical wiring, and other details of the bus and payload configurations.

Another beneficial future activity would be a bottom up cost estimate, which would be possible after completion of the design details described above. Such an estimate is very time-consuming to perform, but it is the only means of establishing a highly reliable cost estimate.

While the communications and positioning missions are described in the current design, another future task could include a more detailed description of how these missions are performed by the software, both on the ground on onboard the multiple spacecraft.

Several options for expansion of the network could also be designed. These options include improved autonomy through upload of replacement software, positioning and communications services for other spacecraft, relay between MSEs without Earth interaction, automated ground operations, and additional spacecraft in the constellation to improve coverage, availability and reliability. Future spacecraft could also provide more advanced capabilities such as remote sensing if the funds were available for development and integration of the required hardware and software.

Improvement in the approach to concurrent engineering would be possible through integration of MATLAB modules or re-coding in EXCEL to interface directly with ICEMAKER.

16 Authors

Jason Andringa	JMA
Marshall Brenizer	DMB
Robert Dare	RED
Jay M Falker III	JMF
David Ferris	DLF
Elisabeth Lamassoure	EL
Alexander Manka	AKM
Karen Marais	KM
Jessica Márquez	JJM
Richard Millard	RLM
Simon Nolet	SN
Alexander Omelchenko	AO
Jeremy Rea	JRR
Joseph Saleh	JS
Samuel Schweighart	SAS
Alexis Stanke	AKS
Zachary Warfield	ZW
Julie Wilhelmi	JLW